







GRADUATE EDUCATION

UNIFORMED SERVICES UNIVERSITY OF THE HEALTH SCIENCES  
F. EDWARD HÉBERT SCHOOL OF MEDICINE  
4301 JONES BRIDGE ROAD  
BETHESDA, MARYLAND 20814-4799



APPROVAL SHEET

TEACHING HOSPITALS  
WALTER REED ARMY MEDICAL CENTER  
NAVAL HOSPITAL, BETHESDA  
MALCOLM GROW AIR FORCE MEDICAL CENTER  
WILFORD HALL AIR FORCE MEDICAL CENTER

Title of Dissertation: "Identification of Aminopeptidase N  
as a Cellular Receptor for Human  
Coronavirus-229E"

Name of Candidate: CPT Curtis Yeager  
Doctor of Philosophy Degree  
May 12, 1992

Dissertation and Abstract Approved:

Stephanie N. Vogel  
Committee Chairperson

5/12/92  
Date

Tracy J. Beebe  
Committee Member

5/12/92  
Date

Alison D. O'Brien  
Committee Member

5/12/92  
Date

Frank J. King  
Committee Member

5/12/92  
Date

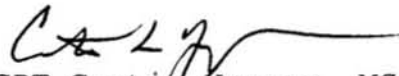
Kathryn V. Holmes  
Committee Member

12-10-92  
Date

The author hereby certifies that the use of any copyrighted material in the thesis manuscript entitled:

"Identification of Aminopeptidase N as a Cellular Receptor for Human Coronavirus-229E"

beyond brief excerpts is with the permission of the copyright owner, and will save and hold harmless the Uniformed Services University of the Health Sciences from any damage which may arise from such copyright violations.

A handwritten signature in black ink, appearing to read 'C. Yeager', with a long horizontal flourish extending to the right.

CPT Curtis Yeager, MS, USA  
Department of Microbiology  
Uniformed Services University  
of the Health Sciences

## ABSTRACT

Title of Dissertation: Identification of Aminopeptidase N  
as a Cellular Receptor for Human Coronavirus 229E

Curtis L. Yeager, CPT, MS, US Army, Doctor of Philosophy,  
1992

Dissertation directed by : Kathryn V. Holmes, Ph.D.  
Professor

Human coronaviruses (HCV) are the cause of 25 percent of common colds. Difficulty in isolation of clinical pathogens has limited the characterization of these viruses and their interaction with host cells. The purpose of this research project was to characterize and identify the cellular receptor(s) for HCV-229E.

Assays to detect virus binding demonstrated that HCV-229E would bind to membranes from human respiratory and intestinal epithelium and from several susceptible human cell lines. HCV-229E binding and infection of human cells could be blocked by antiserum from mice immunized with human cell membranes. Using splenocytes from these mice, we developed an anti-receptor monoclonal antibody, MAb-RBS, which would block HCV-229E binding and infection.

Concurrently with MAb-RBS development, others reported that a porcine coronavirus, TGEV, could utilize



aminopeptidase N (APN), a cell surface metalloprotease, as a receptor on swine testicular cells. Because of the relatedness of TGEV and HCV-229E and the similar chromosomal assignments of the genes for human aminopeptidase N (hAPN) and HCV-229E sensitivity, hAPN was tested as a receptor for HCV-229E. HCV-229E and MAb-RBS bound competitively to membranes from mouse cells transfected with hAPN, but not to the untransfected parental mouse cells. MAb-RBS also immunoprecipitated the hAPN from these transfected mouse cells. Immunofluorescence assays for intracytoplasmic HCV-229E antigens demonstrated that both mouse and hamster cells would permit HCV-229E entry and replication only after the cells were transfected with an hAPN expression vector. When the same parental mouse cell line was engineered to express a deletion mutant of hAPN, MAb-RBS failed to recognize this form of hAPN and these cells were not susceptible to HCV-229E infection. MAb-RBS and other anti-hAPN antibodies inhibited both HCV-229E infection and hAPN protease activity.  $Zn^{++}$ -chelating enzyme inhibitors, but not competitive inhibitors of hAPN enzyme activity, also protected human cells from HCV-229E infection. These results demonstrate that HCV-229E can utilize human aminopeptidase N as a cellular receptor and that the site of HCV-229E binding may be near the region of hAPN enzyme activity. The identification of this well-characterized molecule as an HCV-229E receptor should result in improved

methods for isolation of additional HCV strains. It should also serve as the molecular and genetic basis for virus- and receptor-targeted drugs against HCV-229E infection and for development of a transgenic animal model in which to study the pathogenesis, prevention and treatment of natural HCV-229E infections.



IDENTIFICATION OF AMINOPEPTIDASE N AS A CELLULAR RECEPTOR  
FOR HUMAN CORONAVIRUS 229E

by

CURTIS L. YEAGER, CPT, MS, US ARMY

Dissertation submitted to the Faculty of the  
Department of Microbiology Graduate Program of the  
Uniformed Services University of the Health  
Sciences in partial fulfillment of the  
requirements for the degree of  
Doctor of Philosophy  
1992

## ACKNOWLEDGEMENTS

The completion of this Ph. D. program and the work described herein was made possible by many concerned and supportive individuals.

I would first like to thank the U S Army and the Medical Service Corps for allowing me to participate in this training. I would also like to thank the members of my dissertation committee and the Department of Microbiology for their patience and guidance throughout the program.

In the laboratory, I would like to thank: my major advisor, Dr. Kathryn Holmes, for her constant advice and guidance; my friend and mentor, Dr. Rick Williams, for his untiring technical, professional, and personal support; my teachers and friends, Dr. Mark Frana, Dr. Dave Snyder, Dr. Gabriela Dveksler, Christy Cardellichio, Hanh Nguyen, and Pat Elia; my collaborators, Dr. Tom Look and Dr. Dick Ashmun, for their cells and reagents; and the other members of the labs of Dr. Holmes, Dr. Frank Jenkins, Dr. Iain Hay and Dr. Carl Dieffenbach for their help and friendship.

Finally, and most important, I would to thank and to dedicate this work to my wife, Laura, my sons, Robert, Benjamin, and Steven (RBS), and my whole family, both natural and acquired, for their steadfast love, understanding and support throughout this and all my other undertakings.



## TABLE OF CONTENTS

	<u>PAGE</u>
INTRODUCTION.....	1
Coronaviruses.....	1
History of isolation and classification.....	1
Tropism and diseases.....	4
Structure and replication.....	7
Virus receptors.....	16
The virus-receptor interaction.....	16
Discovery, diversity and similarities of virus receptors.....	17
Coronavirus receptors and species specificity..	23
Human coronaviruses.....	25
Clinical significance and epidemiology.....	25
Isolation and growth of human respiratory coronaviruses.....	31
Human coronavirus 229E.....	35
MATERIALS AND METHODS.....	38
Virus and cell propagation, virus purification.....	38
Plaque assay.....	40
Parental and transfected mouse and hamster cells.....	41
Tissue sources.....	41
Brush border membrane preparation.....	42
Cell membrane preparations.....	43
Antisera, antibodies.....	43

Monoclonal antibody development and characterization.....	44
Monoclonal antibody ascites.....	47
Solid phase virus binding assay.....	48
Virus overlay protein blot assay.....	49
<u>In vitro</u> virus challenge and blocking assays.....	49
Immunofluorescence assays.....	51
Enzyme-linked immunosorbant and virus binding assays.....	52
Immunoprecipitation of hAPN.....	53
Enzyme activity and enzyme inhibition assays.....	55
RESULTS.....	57
Growth of HCV-229E in WI38 cells and detection of HCV-229E antigens.....	57
Growth and cytopathic effects of HCV-229E in cell culture.....	58
Species and tissue specificities of HCV-229E binding.....	66
Binding of HCV-229E to human and animal intestinal brush border membranes.....	66
Binding of HCV-229E to human respiratory epithelium.....	69
Binding of HCV-229E to membranes of human and animal cell lines.....	72
Characterization of the HCV-229E-receptor interaction.....	78
Sensitivity of HCV-229E binding activity to SDS-PAGE.....	78
Effects of detergents on the HCV-229E receptor.....	79
Effects of heat and reduction on the HCV-229E receptor.....	85



Alternative approaches to characterization of the HCV-229E-receptor interaction.....	86
Development of an enzyme-linked virus binding assay.....	90
Development of an anti-receptor monoclonal antibody.....	95
Identification of a monoclonal antibody that blocked HCV-229E infection of WI38 cells.....	98
Generation of MAb-RBS mouse ascites.....	99
Testing of carcinoembryonic antigen family members as HCV-229E receptor candidates.....	100
Identification of human aminopeptidase N as a cellular receptor for HCV-229E.....	106
Correlation of the genetic mapping of HCV-229E sensitivity with the discovery of a porcine coronavirus receptor.....	106
Binding of MAb-RBS to hAPN in hAPN-transfected mouse cell membranes.....	112
Immunoprecipitation of hAPN from hAPN- transfected mouse cells by MAb-RBS.....	115
Binding of HCV-229E to hAPN-transfected mouse cell membranes and blocking of virus binding by MAb-RBS.....	115
HCV-229E infection of hAPN-transfected mouse cell and hamster cells.....	124
MAb-RBS inhibition of hAPN enzyme activity in hAPN-transfected mouse cells and HL60 cells...	135
Specific anti-hAPN antibodies and some hAPN enzyme activity inhibitors protected WI38 cells from HCV-229E challenge.....	139
DISCUSSION.....	148
BIBLIOGRAPHY.....	175

## LIST OF TABLES

<u>Table</u>	<u>Page</u>
1. Coronavirus Diseases.....	3
2. Virus Receptors.....	20
3. Viruses Which Cause Common Colds.....	28
4. HCV-229E Binding Activity of Membranes From Cell Cultures and Tissues.....	89
5. Comparison of Solid Phase and Enzyme-linked Virus Binding Assays.....	92
6. Screening of Hybridoma Supernatants for Antibody to the HCV-229E Receptor.....	97
7. Anti-CEA Antibodies Tested for Binding Inhibition of HCV-229E.....	104
8. CEA Glycoprotein-expressing Rodent Cells Challenged by HCV-229E.....	105
9. Characteristics of Human Aminopeptidase N/CD13.....	111
10. Properties of Anti-APN Monoclonal Antibodies and Inhibitors.....	143



## LIST OF FIGURES

<u>Figure</u>	<u>Page</u>
1. Coronavirus structure.....	9
2. Coronavirus replication.....	12
3. Electron micrograph of negatively-stained human coronavirus particles.....	34
4. HCV-229E growth and cytopathic effects in WI38 cells.....	60
5. HCV-229E growth and cytopathic effects in HL60 cells.....	63
6. HCV-229E growth and cytopathic effects in RD cells..	65
7. HCV-229E binding to the intestinal brush border membranes of humans and animals.....	68
8. HCV-229E binding to human adult intestinal membranes from different individuals.....	71
9. HCV-229E binding to membranes from human intestinal and respiratory epithelium and from a human cell line.....	74
10. HCV-229E binding to human and animal tissue and cell membrane preparations with and without detergent extraction.....	77
11. Virus overlay protein blot assay (VOPBA) of HCV-229E and TGEV binding to partially renatured human intestinal membranes (HAI).....	81
12. Detergent and trypsin sensitivity of HCV-229E binding.....	84
13. HCV-229E binding after treatment of membranes with heat and reduction.....	88
14. Enzyme-linked virus binding assay of HCV-229E binding to human and mouse cells.....	94
15. Protection of WI38 cell from challenge with HCV-229E by MAb-RBS.....	102
16. HCV-229E and TGEV binding to membranes of human and pig intestinal epithelium.....	110

17.	MAB-RBS binding to hAPN-transfected mouse cell membranes.....	114
18.	Immunoprecipitation of hAPN by MAb-RBS and MAb-MY7.....	117
19.	HCV-229E binding to hAPN-transfected mouse cell membranes.....	120
20.	Concentration-dependent competition between HCV-229E and MAb-RBS for binding to parental and hAPN-transfected mouse cell membranes.....	123
21.	Growth and cytopathic effects of HCV-229E in hAPN-transfected mouse cells.....	126
22.	Intracellular virus antigens in hAPN-transfected mouse cells after HCV-229E challenge.....	129
23.	Intracellular virus antigens in hAPN-transfected BHK cells after HCV-229E challenge.....	131
24.	Native hAPN and hAPN <sub>mut</sub> molecules.....	134
25.	APN enzyme activity assay of control APN and membranes of parental and hAPN-transfected mouse cells and HL60 cells.....	138
26.	hAPN enzyme activity inhibition by MAb-RBS.....	141
27.	Predicted APN amino acid sequences.....	160
28.	Homology of human, rabbit, rat and pig APNs.....	164

# LIST OF ABBREVIATIONS

<u>Abbreviation</u>	<u>Full form</u>
Ala-PNA	alanine-p-nitroanilide
APN	aminopeptidase N
ATCC	American Type Culture Collection
bAAPN	bovine alanine aminopeptidase N
BAI	BALB/c (mouse) adult intestine
BBM	brush border membranes
BCV	bovine coronavirus
BGP	biliary glycoprotein
BHK	baby hamster kidney
BME	beta-mercaptoethanol
BSA	bovine serum albumin
BUF	buffer only
CAI	chicken adult intestine
CCL	certified cell line
CD13del	CD13 (hAPN) with 39 amino acid deletion mutation (also referred to as hAPN <sub>mut</sub> )
CEA	carcinoembryonic antigen
CCV	canine coronavirus
cDNA	complementary DNA
CHO	Chinese hamster ovary
CMP	cell membrane preparation
CPE	cytopathic effect
cpm	counts per minute
CVLP	coronavirus-like particle
Det. Extract.	detergent-extracted
DMEM	Dulbecco's modified eagle medium
DTT	dithiothreitol
DVIM	demyelinating virus of infant mice
EDTA	ethylenediaminetetraacetic acid
ELISA	enzyme-linked immunosorbant assay
ELVIRA	enzyme-linked virus receptor assay
FACS	fluorescein-activated cell sorting
FBS	fetal bovine serum
FECV	feline enteric coronavirus
FIPV	feline infectious peritonitis virus
HAI	human adult intestine
hAPN	human aminopeptidase N
hAPN <sub>mut</sub>	human aminopeptidase with 39 amino acid deletion mutation
HCV	human coronavirus
HE	hemagglutinin esterase
HEV	hemagglutinating encephalomyelitis virus
HIV	human immunodeficiency virus
HRE	human respiratory epithelium
HRT	human rectal tumor
IBV	infectious bronchitis virus

Ig	immunoglobulin
IP	intraperitoneal
kb	kilobase
kDa	kiloDalton
MAb	monoclonal antibody
MHC	major histocompatibility complex
MHV	mouse hepatitis virus
MHVR	mouse hepatitis virus receptor
mRNA	messenger RNA
NCA	normal cross-reacting antigen, non-specific cross-reacting antigen, or normal colonic antigen
NGS	normal goat serum
NMA	normal mouse ascites
OC	organ culture
ORF	open reading frame
PAGE	polyacrylamide gel electrophoresis
PBS	phosphate-buffered saline
PFU	plaque-forming unit
PMSF	phenylmethylsulfonyl fluoride
Pro-PNA	proline-p-nitroanalide
PSF	penicillin-streptomycin-fungizone
PSG	pregnancy specific glycoprotein
RAI	rat adult intestine
RbCV	rabbit coronavirus
RCV	rat coronavirus
RER	rough endoplasmic reticulum
RD	rhabdomyosarcoma
RGD	amino acid sequence: arginine-glycine-aspartic acid
SDAV	sialodacryoadenitis virus
SDS	sodium dodecyl sulfate
SPA	Staphylococcal protein A
TCID	tissue culture infectious dose
TCV	turkey coronavirus
TGEV	transmissible gastroenteritis virus
Tk-	thymidine kinase -
TMB	3,3',5,5'-tetramethylbenzidine (peroxidase substrate)
VAP	virus attachment protein
VOPBA	virus overlay protein blot assay



## INTRODUCTION

### Coronaviruses

History of Isolation and Classification: The first coronavirus was isolated in 1937 and was identified as the causative agent of a previously described respiratory illness of chickens (Schalk and Hawn, 1931; Beaudette and Hudson, 1937). The virus was designated infectious bronchitis virus (IBV). Transmissible gastroenteritis virus (TGEV) of swine was isolated in 1946 and the first of the murine hepatitis viruses (MHV), in 1949 and 1951 (Doyle and Hutchings, 1946; Cheever et al., 1949; Gledhill and Andrewes, 1951). In 1965, the structure of IBV was described by the use of an improved negative staining technique in electron microscopy which allowed enhanced visualization of crude virus suspensions (Berry et al., 1964; Brenner and Horne, 1959). The relationship of these viruses was not recognized until a human common cold virus (HCV-B814) was isolated and characterized in 1965 (Tyrrell and Bynoe, 1965). When viewed by the same electron microscopic technique, it was found that IBV and HCV-B814 shared a similar, distinctive morphology which included the presence of large, petal-shaped envelope proteins which gave a "corona"-like appearance, reminiscent of the solar corona or a halo, to the virions (Almeida and Tyrrell, 1967). The eventual isolation of several other morphologically similar appearing animal viruses including feline infectious

peritonitis virus (FIPV), canine coronavirus (CCV), bovine coronavirus (BCV), turkey coronavirus (TCV), rat coronavirus (RCV), the rat sialodacryoadenitis virus (SDAV), and the porcine hemagglutinating encephalomyelitis virus (HEV) resulted in the classification of these viruses as the Coronaviridae family by the International Committee on the Taxonomy of Viruses in 1975 (Tyrrell et al., 1975). During this period, additional human coronaviruses were isolated from common cold patients as a product of the medical interest in finding the cause and the cure for the common cold in the 1960's. One strain, HCV-229E, was isolated in 1964 (Hamre and Procknow, 1966) and found to be identical in morphology to HCV-B814 (Almeida and Tyrrell, 1967), while several other strains isolated in 1967, including HCV-OC38 and HCV-OC43, were also found to be IBV-like in morphology (McIntosh et al., 1967). Coronavirus-like virus particles (CVLP) have also been found in the stools of patients with intestinal illnesses as well as in those of healthy individuals (Macnaughton and Davies, 1981; Resta et al., 1985) and from the brains of multiple sclerosis patients (Gerdes et al., 1981). Coronaviruses have been grouped serologically into 4 groups based on antigenic cross-reactivity as seen in Table 1 (McIntosh et al., 1969). Other methods can now be used to classify new coronaviruses which are based on the better understanding of their individual virion components and unique replication

**TABLE 1**

**Coronavirus Diseases**

Antigenic group	Virus <sup>a</sup>	Host	Respiratory infection	Enteric infection	Hepatitis	Neurologic infection	Other <sup>b</sup>
I	HCV-229E	Human	X				
	TGEV	Pig	X	X			X
	CCV	Dog		X			
	FECV	Cat		X			
	FIPV	Cat	X	X	X	X	X
II	HCV-OC43	Human	X	?			
	MHV	Mouse	X	X	X	X	
	SDAV	Rat	X				X
	HEV	Pig	X	X		X	
	BCV	Cow		X			
	RbCV	Rabbit		X			X
III	IBV	Chicken	X				X
IV	TCV	Turkey	X	X			

<sup>a</sup> Abbreviations: HCV-229E, human respiratory coronavirus; TGEV, porcine transmissible gastroenteritis virus; CCV, canine coronavirus; FECV, feline enteric coronavirus; FIPV, feline infectious peritonitis virus; HCV-OC43, human respiratory coronavirus; MHV, mouse hepatitis virus; SDAV, sialodacryadentis virus; HEV, porcine hemagglutinating encephalomyelitis virus; BCV, bovine coronavirus; RbCV, rabbit coronavirus; IBV, avian infectious bronchitis virus; TCV, turkey coronavirus (turkey bluecomb disease).

<sup>b</sup> Other diseases caused by coronaviruses include infectious peritonitis, runting, nephritis, pancreatitis, parotitis, and adenitis.

Adapted from Holmes, 1989

strategy, including the properties of their structural proteins and genomic RNA and mRNAs, and by their nucleic acid homology (Holmes et al., 1984; Siddell et al., 1983; Spaan et al., 1988b; Sturman and Holmes, 1983). Thus, the coronaviridae represent a family of viruses which share a common, distinctive morphology and have been isolated from a variety of economically important domestic animal hosts as well as humans.

Tropism and diseases: Tropism is a term used to denote the material or entity for which an organism or substance shows a special affinity. For viruses, tropism may be thought of as the virus's affinity for and ability to replicate in certain cell types. The coronaviruses are strongly species and tissue specific and most coronaviruses are able to infect only one species or several closely related species (McIntosh, 1974; Wege et al., 1982).

For MHV-A59, this tropism has been further defined within mouse species by the differential expression of its particular receptor among mouse strains. In susceptible BALB/c mice, the MHV-A59 receptor has been identified as a 110kDa member of the CEA family of glycoproteins (Williams et al., 1991). A homologous, yet nonfunctional form of this molecule is expressed in SJL/J mice which lacks the specific epitope recognized by MHV-A59, rendering the same cells in this strain of mouse resistant to MHV-A59 infection (Williams et al., 1990). The various host and tissue



tropisms for many coronaviruses are listed in Table 1.

Coronaviruses are able to infect several tissue types resulting in a variety of diseases (Table 1). The majority of these infections are found in the mucosal epithelium of the respiratory and intestinal tracts, but other infections include the liver, pancreas, kidney, lacrimal and salivary glands and central nervous system. While most of these viruses infect only one host, they may cause pathology in several organs of that host (McIntosh, 1974; Wege et al., 1982). The diseases caused by the human coronaviruses will be described in another section of the Introduction. Many of the non-human diseases caused by coronaviruses are among domestic and laboratory animals important to some aspect of human use, such as livestock or research and these diseases cause significant economic losses by both of these industries (Wege et al., 1982).

Coronavirus infections of the respiratory epithelium are caused by the chicken IBV, turkey coronavirus (TCV), rat coronavirus (RCV), cat feline infectious peritonitis virus (FIPV), and the human coronaviruses. These include the slow, patchy destruction of ciliated epithelial cells with the loss of beating cilia necessary for the proper function of respiratory mucosa (Tyrrell and Bynoe, 1965). The respiratory infection by IBV is more severe and prolonged than the other respiratory infections with the virus able to spread to the reproductive organs and kidneys of the chicken

(McIntosh, 1974). The RCV respiratory infection is characterized by rhinotracheitis with mild interstitial pneumonitis and a mixed cellular interstitial infiltrate (Bhatt and Jacoby, 1977).

Enteric infections are caused by the cow BCV, pig TGEV and hemagglutinating encephalomyelitis virus (HEV), canine coronavirus (CCV), cat FIPV and feline enteric coronavirus (FECV), human CVLPs, mouse hepatitis viruses, rabbit coronavirus (RbCV), and turkey coronavirus. Enteric coronavirus pathology may include the loss of epithelial cells and absorptive function (Doughri and Storz, 1977), abnormalities in electrolyte transport (Mishra et al., 1973), and necrotizing enterocolitis (Chany et al., 1982). Some of these infections, especially those of cow and swine, can infect all ages, but most are especially severe in young animals (Mebus et al., 1973; Doyle and Hutchings, 1946).

Hepatitis has been described in cat FIPV infections as well as in the mouse diseases. In mice, some form of hepatitis is caused by MHV1, MHV2, MHV3, MHV-JHM, MHV-A59, and MHV-D and -S (reviewed by Compton, 1988). The pathology of these liver infections usually involves hepatocyte destruction ranging from focal to massive necrosis and can result in death.

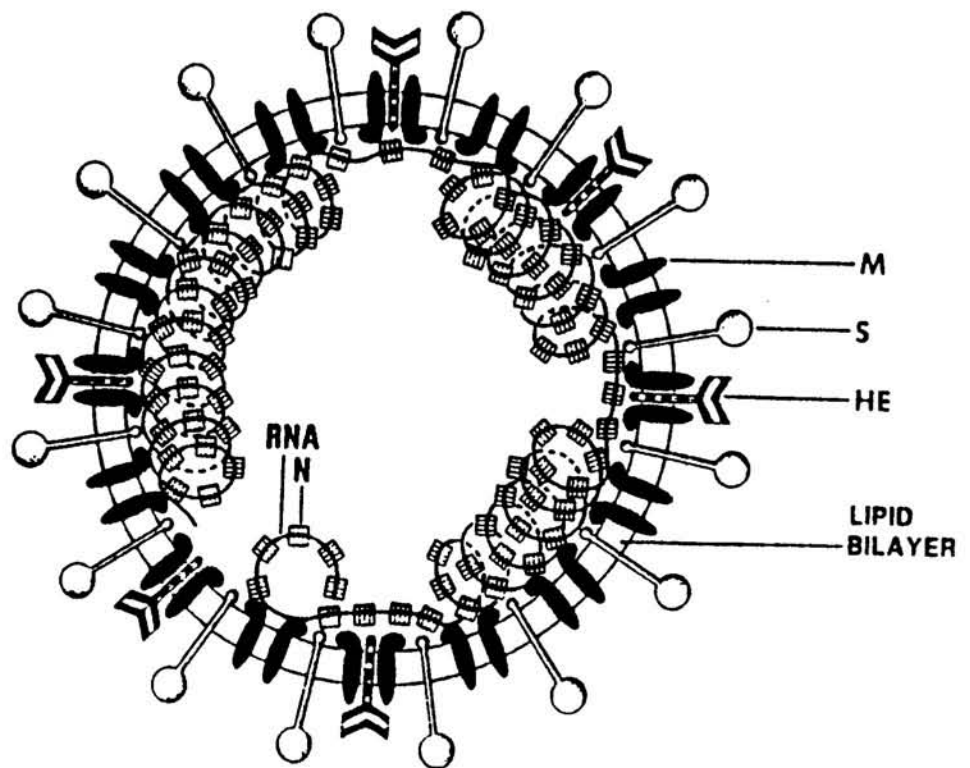
Infections of the central nervous system have been described for FIPV (Montali and Strandberg, 1972), most MHV strains (Compton, 1988), and the porcine HEV (Greig et al.,

1971). The pathology seen in these infections include granulomatous lesions in the meninges and ependyma of the spinal cord and brain as seen in FIPV infection, encephalomyelitis in HEV infection, and necrotic lesions and demyelination in the spinal cord and brains of MHV-infected mice. As mentioned, several coronaviruses cause pathology in more than one tissue or organ of the host. Notably, HEV, FIPV, and MHV can infect other organs causing tonsillitis in HEV-infected pigs, peritonitis, nephritis, or pleuritis in FIPV-infected cats and lesions of various lymph organs in mice with some strains of MHV (reviewed by Compton, 1988). Rat coronavirus SDAV causes infection of the parotid and submaxillary salivary glands in addition to the respiratory epithelium (Jacoby et al., 1975). Overall, coronavirus evolution has resulted in their ability to infect a diversity of tissues and hosts. This tropism may eventually be shown to be partially, if not mostly, dependent on the presence of a functional receptor in the host tissues as has been shown for MHV-A59 (Guadagni et al., 1990).

Structure and replication: Coronaviruses are large, enveloped, pleomorphic viruses with a positive sense genomic RNA in a helical nucleocapsid. The overall structural organization of a typical coronavirus virion is shown in Figure 1. I will briefly describe each viral component and its role in coronavirus replication. All coronaviruses possess at least 3 structural proteins: a nucleocapsid

Figure 1. Coronavirus structure. The helical viral nucleocapsid is composed of the positive-stranded RNA genome organized into a helical arrangement by nucleocapsid (N) proteins. The nucleocapsid is associated with the integral membrane (M) glycoproteins of the lipid bilayer envelope. Also part of the envelope are the spike glycoprotein (S) and the hemagglutinin esterase (HE). These glycoproteins are used by the virus for attachment to host cell receptors and for cell fusing activity. The HE is not found in all coronaviruses and, when present, has acetylcysteine aminopeptidase activity. Adapted from Holmes, 1989.



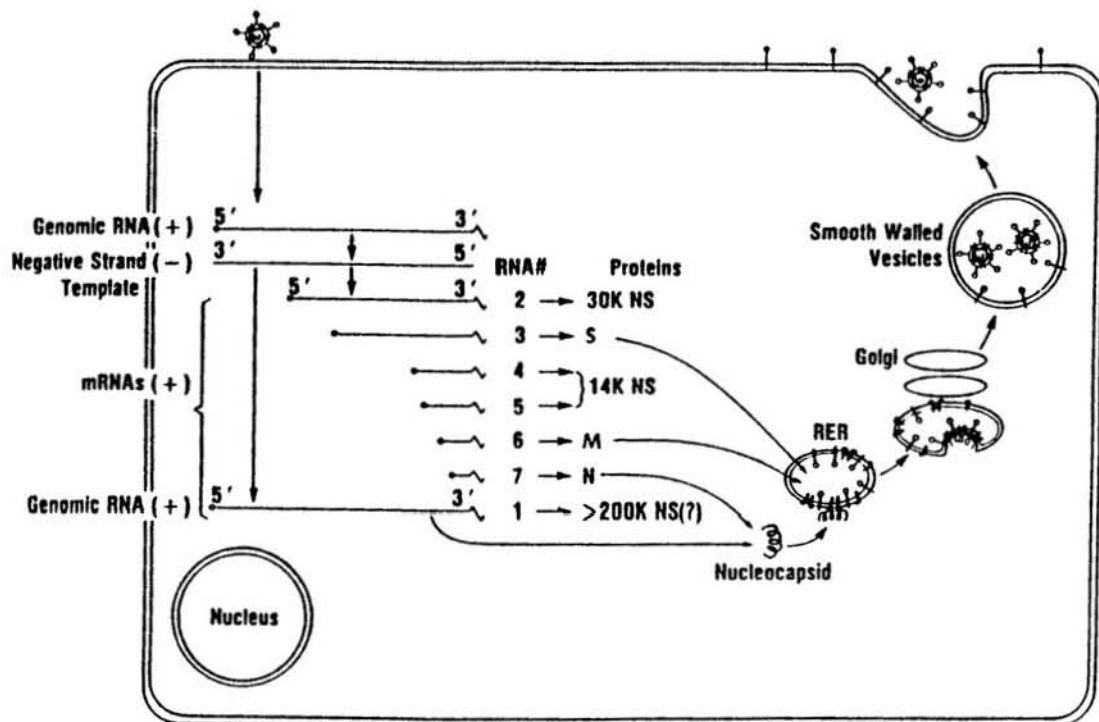


phosphoprotein (N) (50-60kDa), a small integral membrane glycoprotein (M) (20-30kDa), and an integral spike glycoprotein (S) (180-200kDa) (reviewed in Holmes, 1991). Several coronaviruses also possess an additional spike glycoprotein with hemagglutinin activity (HE) (65kDa) which is expressed as a dimer (Callebaut and Pensaert, 1980; Dea and Tijssen, 1988; Deregt *et al.*, 1987; Hogue and Brian, 1986). Additional non-structural proteins encoded by the coronavirus RNA include the large polymerase protein and smaller proteins with varying molecular weights of approximately 30kDa, 14kDa, 13kDa and 10kDa whose functions have not yet been described (Denison and Perlman, 1987; Leibowitz *et al.*, 1982; Siddell *et al.*, 1980; Raabe and Siddell, 1989).

Although the replication cycles of several coronaviruses have been studied, the best understood is that of the MHVs which has been thoroughly described elsewhere and will be briefly described here (reviewed in Spaan *et al.*, 1988b; Holmes, 1989). Reference should be made to Figure 2 for the cellular location of the various steps discussed.

Like other viruses, coronaviruses bind to receptors on the host cell membrane. This initial attachment is mediated by the structural spike glycoproteins (S and/or HE) on the viral envelope (Boyle *et al.*, 1987; Schultze and Herrler, 1992). The spike (S) glycoprotein of MHV-A59 binds

Figure 2. Coronavirus replication. This model is based on mouse hepatitis virus (MHV) replication. The coronavirus particle binds to host cell receptors on the plasma membrane and enters either by fusion with the plasma membrane or by receptor-mediated endocytosis. Replication is thought to occur exclusively in the cytoplasm. Translation of the positive-stranded genomic RNA by host ribosomes results in the synthesis of the viral RNA-dependent RNA polymerase. The viral polymerase transcribes a negative-stranded template RNA and from there a nested set of overlapping subgenomic MRNAS. The subgenomic MRNAS are translated by host cytoplasmic or rough endoplasmic reticulum (RER)-associated polysomes to yield the various structural and nonstructural proteins. The S, HE, and M glycoproteins are inserted co-translationally into the RER and modified by RER and Golgi enzymes. The nucleocapsid (N) phosphoprotein is translated by cytoplasmic ribosomes and associates with genomic mRNAs to form helical nucleocapsids. The nucleocapsids interact with the M proteins and bud into membranes of the RER and Golgi in regions containing the S and HE glycoproteins (when present) resulting in the assembly of whole virions. The structural proteins of the virion are further modified during migration of the virion through the Golgi. Virus particles are released either by the budding of Golgi vesicles with the plasma membrane or by lysis of the cell. Adapted from Holmes, 1989.



to a specific 110kDa receptor present only in certain mouse strains and tissues (Boyle et al., 1987; Compton et al., 1992). Binding by the HE glycoprotein is probably less specific since it recognizes the 9-0-acetylated neuraminic acid residues found in various glycolipids and glycoproteins with complex glycosylation found on the cell surface (Boyle et al., 1987; Compton et al., 1992; Schultze and Herrler, 1992). The envelope of the virion consists of the viral glycoproteins and is a lipid bilayer membrane derived from the Golgi or the rough endoplasmic reticulum (RER) of the host cell. The penetration of bound coronavirus genomic RNA into the cell is not completely understood. Fusion of the viral envelope with a membrane of the host cell is required and may occur at the plasma membrane or within an endoplasmic vesicle (reviewed in Holmes, 1989).

The genome of coronaviruses is a large, plus-stranded RNA of 27 to 32 kb which can act as messenger RNA (mRNA) and bind directly to host ribosomes (Bournsnell et al., 1987; Spaan et al., 1988a; Strauss and Strauss, 1983; Lomniczi, 1977). The genomic RNA of coronaviruses represents a unique linear organization of 6 or 7 regions with one or more open reading frames (ORF) per region (reviewed in Spaan et al., 1988a). The complete sequencing of several coronaviruses has revealed the presence of transcriptional initiation signals between these ORFs from which subgenomic RNAs are transcribed. The linear organization of the genome



can be seen in Figure 2. The overall replication strategy of coronaviruses is unique and involves the generation of a nested set of overlapping subgenomic mRNAs with common 3' ends from the negative strand template of the genomic RNA. These smaller mRNAs encode the various viral proteins and may also be found in double stranded replication intermediates, possibly serving to amplify protein synthesis through the generation of additional subgenomic messages (reviewed in Holmes, 1989; Sawicki and Sawicki, 1990).

Once released into the host cell cytoplasm, primary translation of the first open reading frame of the genomic mRNA yields the putative RNA-dependent RNA polymerase protein necessary for the transcription of the negative-stranded RNA replication template (Strauss and Strauss, 1983). The polymerase is one of two cleavage products from a larger polypeptide, the other being a 28kDa nonstructural protein with unknown function. The various subgenomic messages are transcribed to yield the structural and nonstructural viral proteins and will be discussed in their linear order within the genome. mRNA 2 is the largest of the subgenomic RNAs with 2 ORFs which encode a 30kDa nonstructural protein in all coronaviruses and the 65kDa HE glycoprotein in certain coronaviruses where a proper initiation site precedes the second ORF. mRNA 3 encodes the S glycoprotein, which is always expressed, and both the HE and S proteins are synthesized on RER-associated polysomes

and are inserted co-translationally and glycosylated at the RER. Both glycoproteins are integral membrane proteins and are transported through the RER and Golgi, modified by complex glycosylation and/or acylation and assembled into their multimeric spike glycoprotein forms. At the Golgi, the remainder of the virion components eventually assemble and bud to form enveloped particles within Golgi vesicles (reviewed in Holmes, 1989 and Spaan et al., 1988b).

The 2 to 3 proteins encoded by mRNAs 4 and 5 are nonstructural proteins of various molecular weights among different coronaviruses ranging from 10.2 to 15.3kDa. The functions of these proteins are not known. mRNA 6 encodes the 20 to 30kDa M glycoprotein which is also synthesized on RER-associated polysomes. This glycoprotein has 3 membrane-spanning regions and the presence of several internal insertion sequences suggests that it is inserted and processed differently from that of the S and HE glycoproteins. It, too, is transported to the Golgi for final virion assembly where it probably functions like the matrix proteins of other viruses by associating with genomic RNA in nucleocapsids and the envelope. The smallest subgenomic species, mRNA 7, encodes the phosphorylated 50 to 60kDa nucleocapsid protein (N). The N protein, like the nonstructural proteins, is synthesized on cytoplasmic ribosomes and interacts with genomic RNA, both specifically and non-specifically. It has also been shown to interact

with the M protein, an association which probably results in the incorporation of nucleocapsids into Golgi vesicles.

The assembly of the virus particles begins with the formation of the helical nucleocapsids by association of genomic length mRNAs with N proteins in the cytoplasm. The ability of the N protein to interact with the M protein in the membranes between the RER and the Golgi probably results in the orderly alignment of nucleocapsids with regions of these organelles containing the other structural proteins of the virion. Eventually, these complexes bud into the lumen of these organelles where whole virions can be seen. The virions migrate through the Golgi, where structural proteins are modified, and are eventually transported by Golgi vesicles to the cell surface where they are released either by fusion of the vesicles with the plasma membrane or by lysis of the cell (reviewed in Holmes, 1989).

### **Virus Receptors**

The virus-receptor interaction: The ability of a virus to replicate within a cell requires the presence of many compatible cellular components starting with the binding site on the cell surface and including the various cellular processes necessary for virus component synthesis, assembly and egress. While many eucaryotic cells possess homologous constituents for basic cellular processes, the array of molecules expressed on the cell surface can be very

specialized and defined by the cell's function within the organism.

A necessary first step in the replication cycle of any virus is the attachment of the virus to the host cell membrane (Dales, 1973; Longerg-Holm and Philipson, 1974; Dimmock, 1982; Tardieu et al., 1982; Paulson, 1985; Marsh and Helenius, 1989). Viruses, whether naked or enveloped, possess attachment proteins (VAP) that have evolved for the purpose of recognizing and binding to a membrane component on the host cell. This membrane component can be lipid, carbohydrate, or protein. The diversity and identification of various known receptors will be discussed in the next section. This virus attachment process may be modeled after that of a typical ligand-receptor interaction where an extracellular ligand binds to its cell surface receptor. Here, the virus represents the extracellular ligand and its interaction with the cell surface receptor is essential to the replication of the virus. It should be remembered that virus receptors are cellular components which have only been adopted for use as a receptor by the virus.

Discovery, diversity and similarities of virus receptors: Various methods have been used to study and identify virus receptors. The methods chosen to study particular receptors have depended upon the type of virus-receptor interaction being investigated and on the methods available at the time of study. Earlier studies, such as

those which identified the carbohydrate moieties to which orthomyxoviruses bind through their hemagglutinin (HA) protein relied on observations that removal of sialic acid residues from the receptors by neuraminidase resulted in the loss of viral hemagglutination. Eventually, sialoglycosides were discovered as the specific receptor components for influenza viruses by the in vitro restoration of missing sialic residues to erythrocytes by using purified sialyltransferases (Paulson et al., 1979).

The development of monoclonal antibody (MAb) technology has greatly facilitated the characterization of several virus receptors. Specific monoclonal antibodies to cell membrane components have been used to characterize distinct receptors on different cell types by the same group B Coxsackievirus (Hsu et al., 1988). One receptor for this particular virus was later purified and identified as a 49.5kDa protein by a method involving detergent extraction and SDS-PAGE analysis of <sup>125</sup>I-labeled virus-receptor complexes (Mapoles et al., 1985). Another use for MAbs is the production of anti-receptor antibodies which block virus infection. The MAbs can be used to immuno-purify the receptor from tissues or cells known to be susceptible to the virus. The MHV-A59 receptor was purified and identified as a 110kDa glycoprotein by using MAb-CC1 to extract receptor material from large scale preparations of receptor-bearing mouse liver membranes (Williams et al., 1990). MAbs

were similarly used to identify the HIV receptor as the CD4 molecule by blocking the binding, syncytium formation and infection of lymphocytes with specific anti-CD4 MAbs (Dalgeish et al., 1984; Klatzmann et al., 1984; McDougal et al., 1986b).

It is now possible to confirm the biological relevancy of a virus receptor as demonstrated by the development of a transgenic mouse engineered to express the cloned human poliovirus receptor and with acquired susceptibility to poliovirus (Ren et al., 1990). This innovation, adapted to research on other viruses, should allow for the development of animal models of natural human infections and a system for testing anti-viral reagents and vaccines.

Viruses utilize a diverse assortment of host cell surface molecules as receptors and a list is provided in Table 2 of those receptors for which substantial evidence has accumulated. In some cases, molecules which act as receptors for cellular functions also serve as virus receptors. Included are the  $\beta$  adrenergic receptor for reovirus type 3 (Co et al., 1985) and the epidermal growth factor receptor for vaccinia virus (Eppstein et al., 1985). Integrin molecules, which serve as adhesion proteins on the cell surface and many of which recognize the arginine-glycine-aspartic acid (RGD) sequence on extracellular ligands, are the target of binding for foot and mouth virus



TABLE 2

Table of Putative Host Cell Receptors for Viruses

Virus Family	Virus	Host Cell Receptor
Papovaviridae	Polyomavirus	Sialyloligosaccharides
Adenoviridae	Human Adenovirus	Class I HLA MHC Molecule
Herpesviridae	Human Cytomegalovirus	Class I HLA MHC molecule via $\beta_2$ -microglobulin
	Epstein-Barr virus	C3d receptor CR2 (CD21) of B lymphocyte
Poxviridae	Vaccinia virus	Epidermal growth factor receptor
Hepadnaviridae	Hepatitis B virus	Hepatocyte receptor for polymerized serum albumin via albumin
		Hepatocyte receptor for polymeric IgA
		Sialoglycoprotein
Picornaviridae	Poliovirus	Member of immunoglobulin superfamily
	Human rhinovirus	Intercellular adhesion molecule-1 (ICAM-1)
	Encephalomyocarditis virus	Sialoglycoproteins
	Mengo Virus	
	Foot-and-mouth disease virus	Integrins (adhesion proteins)
Reoviridae	Reovirus 3	$\beta$ Adrenergic receptor
		Sialoglycoproteins
Togaviridae	Semliki Forest virus	Class I HLA and H-2 MHC molecules
	Lactate dehydrogenase- elevating virus	Class II Ia MHC molecule macrophage

Virus Family	Virus	Host Cell Receptor
Orthomyxoviridae	Influenza virus	Sialyloligosaccharides
Paramyxoviridae	Sendai virus	Sialyloligosaccharides
	Newcastle disease virus	Sialyloligosaccharides
Rhabdoviridae	Vesicular stomatitis virus	Phosphatidylserine Phosphatidylinositol GM3 ganglioside
	Rabies virus	Acetylcholine receptor Sialylated gangliosides
Retroviridae	Oncovirinae Human T cell leukaemia virus (HTLV-1)	Class I HLA MHC molecule Interleukin 2 receptor
	Murine leukaemia virus	Lymphoma cell surface IgM 622 amino acid, hydrophobic protein of unknown function
	Radiation leukaemia virus	T cell receptor-L3T4 molecule complex
Lentivirinae	HIV-1	CD4 molecule of T lymphocyte CD4 molecule interacting with class II HLA-DR MHC molecule
	HIV-2 Simian Immunodeficiency virus	CD4 molecule CD4 molecule

Adapted from Lentz, 1990

(Fox et al., 1989). Several hemagglutinating viruses bind to host membrane components bearing 9-O-acetylated neuraminic acid (sialic acid) residues. Molecules containing this carbohydrate moiety have also been shown to mediate virus entry for the orthomyxoviruses, polyomavirus (Fried et al., 1981), hepatitis B virus (Komai et al., 1988), encephalomyocarditis virus (Burness and Pardoe, 1981), reovirus type 3 (Paul and Lee, 1987), rabies virus (Superti and Donelli, 1991), and for the paramyxoviruses, Sendai virus, and Newcastle disease virus (Paulson et al., 1979). Finally, lipids are also utilized by viruses for binding and the plasma membrane constituents, phosphatidylserine and phosphatidylinositol of erythrocytes, are used by vesicular stomatitis virus for attachment and fusion (Mastromarino et al., 1987).

While viruses may use a variety of different cell surface molecules, several different members of the same molecule superfamily can serve as a virus receptors. Members of the immunoglobulin superfamily in their various roles on the surface of cells have proven to be common vehicles for virus binding and entry and are reviewed by Lentz (1990). Some lines of evidence supporting these findings are much stronger than others, but studies show that the following Ig superfamily members have been implicated as the putative receptors for the following viruses: the major histocompatibility complex (MHC)

molecules by adenovirus (Chatterjee and Maizel, 1984), cytomegalovirus (Grundy et al., 1987), Semliki Forest Virus (Helenius et al., 1980), lactate dehydrogenase-elevating virus (Inada and Mims, 1984), and human T cell leukemia virus-1 (Clarke et al., 1983); Intercellular adhesion molecule-1 (ICAM-1) by rhinoviruses (Greve et al., 1989; Staunton et al., 1989; Tomassini et al., 1989); the CD4 molecule by HIV-1 (Dalglish et al., 1984; Klatzmann et al., 1984; McDougal et al., 1986a), HIV-2 (Guyander et al., 1987), and simian immunodeficiency virus (Hoxie et al., 1988); and an Ig member of undescribed function by poliovirus (Mendelsohn et al., 1989).

#### Coronavirus receptors and species specificity:

Naturally occurring coronavirus infections are highly species specific and usually only infect one host species. Within the species, coronaviruses may infect more than one strain as with mouse hepatitis virus strain A59 (MHV-A59), which can infect several mouse strains including the BALB/c and C3H strains (reviewed in Holmes, 1989). The strain specificity of MHV-A59 correlates with virus binding and is limited, at least in part, by the absence of a specific receptor epitope from an otherwise homologous molecule found in the resistant SJL/J mouse strain (Boyle et al., 1987; Williams, 1990). MHV can also infect suckling rats if a highly neurotropic strain, such as MHV-JHM, is inoculated intracerebrally (Hirano et al., 1980; Sorensen and Dales,

1985).

Studies on the characterization and identification of the cellular receptor for MHV-A59 have been a major focus of our laboratory. Initially, MHV-A59 was shown to bind to 2 proteins of 55 and 110kDa when mouse intestinal membranes were separated by SDS-PAGE, transferred to nitrocellulose and blotted with the virus. A significant advance was the development of an anti-receptor MAb, CC1, which blocked the infection of susceptible cells by MHV-A59 (Williams, 1990). This MAb was subsequently used to purify a 110kDa molecule for further characterization (Williams, 1990).

Previous studies by our laboratory on the specificity of coronavirus binding were performed using solid phase virus binding assays (Compton, 1988). These studies indicated that the binding of some coronaviruses may not be as species specific as the natural infections. Results showed that some coronaviruses would bind to the intestinal brush border membranes of host species outside the natural host. This occurred especially among the coronaviruses in group 1 (Table 1). Human coronavirus 229E, porcine TGEV, cat FIPV and dog CCV all bound to the intestinal membranes of pigs, dogs, cats, and humans, suggesting that these serologically related viruses might recognize some common component found on the intestinal epithelium of these species. While the expression of the hemagglutinin (HE) glycoprotein by bovine coronavirus (BCV),

hemagglutinating encephalomyelitis virus (HEV) of swine, human coronavirus strain OC43 and some strains of avian infectious bronchitis virus (IBV) and MHV (MHV-JHM and MHV-DVIM) could lead to nonspecific binding of common sialic acid residues, none of the group 1 coronaviruses express HE. The nature of this inter-species binding by group 1 coronaviruses is of great interest since no animal models currently exist for the study of human coronavirus infections.

#### **Human Coronaviruses**

Clinical significance and epidemiology: Human coronaviruses of both antigenic groups I (HCV-229E) and II (HCV-OC43) were isolated from patients suffering from acute upper respiratory illnesses which have been referred to historically as the common cold (Table 1) (Hamre and Procknow, 1966; McIntosh et al., 1967). A survey of the usually mild patient symptoms in a human volunteer study included varying degrees of malaise, headache, fever and chills, sore throat, mucopurulent nasal discharge, and cough (Bradburne et al., 1967). Direct correlation of the human coronaviruses with this respiratory syndrome is based on the isolation of these viruses from patients displaying these symptoms (Bradburne et al., 1967; McIntosh et al., 1967a), the inoculation of human volunteers with the virus (Bradburne et al., 1967), acute and convalescent serological



studies on common cold patients (Macnaughton et al., , 1981) and on the immunofluorescent detection of replicating HCVs in the cells shed from the nasopharynx of patients (McIntosh et al., 1973).

The prevalence of HCV seroconversion and HCV-induced common colds has been studied serologically by using enzyme-linked immunosorbant assays (ELISA) (Kraaijeveld et al., 1980) to detect specific anti-HCV antibodies in the blood of several populations. Specific antibodies to HCV-229E and HCV-OC43 were detected in healthy adults in two different surveys demonstrating seroconversion to HCV-229E in 94% and 86% of individuals and to HCV-OC43 in 100% and 87% of individuals in England and Iraq, respectively (Hasony and Macnaughton, 1982). Another survey demonstrated that seroconversion to these two viruses normally occurs early in childhood and increases in prevalence rapidly with age (McIntosh et al., 1970). Studies on the percentage of common colds caused by HCVs have yielded variable rates of incidence among different populations and from season to season and year to year. Colds due to HCV-229E in 3 separate surveys revealed incidences varying from 15% to 34%, with an overall average of 24.3%. Other surveys of colds due to HCV-OC43 resulted in incidences of 25%, 27%, and 5%, with an average of 19% (Hamre and Beem, 1972; Monto, 1974; Kapikian et al., 1969). Infections due to both of these viruses show epidemic and seasonal occurrences mainly

in the winter and spring (Monto and Lim, 1974). Thus, the human respiratory coronaviruses cause a significant proportion of total common colds and they and other agents of the common cold are listed in Table 3.

The natural transmission of upper respiratory HCVs is not well described, but human volunteer studies have used intranasal inoculation of liquid HCV suspensions and resulted in a 50 to 62% infection rate (Bradburne et al., 1967; Bende et al., 1989). The natural site of infection and the epidemic nature of HCV infections among individuals within a population suggest that these viruses may be spread by direct contact and transfer of nasal discharge containing the virus or by inhalation of respiratory droplets. Models for rhinovirus transmission based on experimental infections has shown these analogous upper respiratory tract viruses to be spread mainly by direct hand to hand contact between individuals (Gwaltney et al., 1978) or via contaminated surfaces (Gwaltney, 1982). Due to similarities between the pathology of HCV and rhinovirus infections, rhinovirus infections may be an appropriate model for HCV infection. A possible difference in the transmission of these two types of viruses could result from different survival characteristics for the two viruses outside of the host. Rhinoviruses are stable, non-enveloped viruses and can survive for hours to days at room temperature on contaminated surfaces (Hendley et al., 1973). On the other

**TABLE 3****Viruses Which Cause Common Colds**

<b>COMMON</b>	<b>LESS COMMON</b>
<b>Rhinoviruses, &gt; 100 types</b>	<b>Adenoviruses 1-7, 14, 21</b>
<b>Coronaviruses</b>	<b>Coxsackie A21, 24; B2-5, etc/</b>
<b>Parainfluenza 1-3</b>	<b>Echovirus 11, 20, etc.</b>
<b>Respiratory syncytial virus</b>	<b>Parainfluenza 4</b>
<b>Influenza A, B</b>	

Adapted from White and Fenner, 1986

hand, the half-life of HCV-229E decreases significantly (from 5 days to less than 3 hours) with a reduction in relative humidity (50% to 20%) after aerosolization at room temperature (Ijaz et al., 1985). These data suggest that HCVs are susceptible to drying and that their survivability may depend on rapid transmission from one host to another with minimal exposure to external conditions.

HCVs have also been observed in association with other human diseases including more severe pulmonary diseases, enteric infections, and multiple sclerosis. The more severe respiratory diseases include pneumonia (Wenzel et al., 1974; McIntosh et al., 1974) and chronic pulmonary disease (Buscho et al., 1978; Gump et al., 1976; Smith et al., 1980) in adults and asthma in children (Dea et al., 1989). Though not proven to be a causative agent of these diseases, HCVs may at least exacerbate the symptoms of the underlying conditions. To date, opportunistic respiratory infections caused by HCVs in patients with HIV infection have not been described, but some of these immunocompromised individuals do shed coronavirus-like particles in their stools (Kern et al., 1985). Since the first observation of coronavirus-like particles in the stools of healthy individuals in 1975 (Mathan et al., 1975), the possible role of HCVs in enteric infections has been studied with increasing interest. Several surveys have shown the presence of these CVLPs in stools of healthy individuals

(Marshall et al., 1982; Puel et al., 1982) and in the stools or biopsied enterocytes of individuals with gastroenteric disorders of varying severity (Vaucher et al., 1982; Baker et al., 1982; Chany et al., 1982; Gerna et al., 1985; Mortensen et al., 1985). The symptoms of those disorders thought to be caused by the CVLPs ranged from mild watery stools to necrotizing enterocolitis and even death (Rettig and Altshuler, 1985). To date, several enteric HCVs have been isolated and cultivated from patients with intestinal disorders (Resta et al., 1985; Caul and Egglestone, 1977; Caul et al., 1979). One thorough study proved that the CVLP isolate had typical coronavirus morphology by electron microscopy and had induced appropriate acute and convalescent titers of antibody in the patients to specific viral antigens so as to fully implicate the isolate as the cause of the disease (Resta et al., 1985).

Finally, HCVs have also been associated with human neurological disease by their observation in thin sections of human brain (Tanaka et al., 1976) and by their isolation from the brains of patients with multiple sclerosis (Burks et al., 1980). The isolated viruses possessed serological cross-reactivity and nucleic acid homology with MHV and HCV-OC43, but their isolation and propagation in mice and mouse tissues causes uncertainty as to their actual origin. While HCVs are best recognized as the causative agents of common colds, the full spectrum of their ability to cause disease

in humans is still unknown. The combined morbidities of these HCV infections and their economical impact on manpower resources renders the human coronaviruses worthy of intense study.

#### Isolation and growth of human respiratory

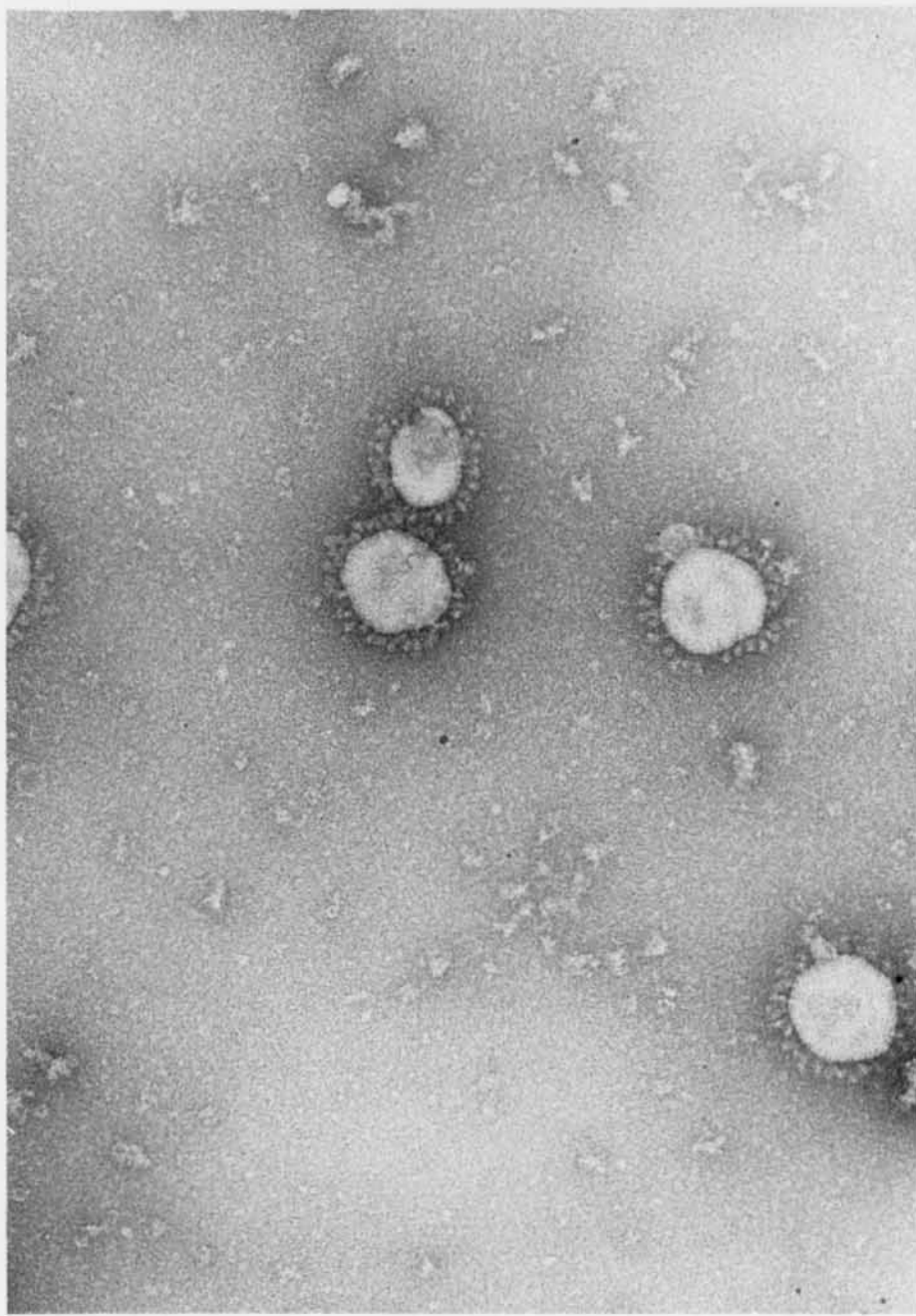
coronaviruses: The first human coronavirus described was known as strain B814 and was isolated from a schoolboy with a cold in 1965 by passage through human embryonic tracheal organ cultures (Tyrrell and Bynoe, 1965). HCV-229E was isolated by another group from a medical student with a cold by passing the clinical specimen through secondary human kidney cells (Hamre and Procknow, 1966). When HCV-B814 and HCV-229E were later viewed by electron microscopy in negatively stained preparations, they were morphologically identical to each other and to the previously isolated IBV of chickens (Almeida and Tyrrell, 1967). The propagation of HCV-229E after the 2 blind passages in human kidney cultures was accomplished in WI38 human lung diploid fibroblast cells. An attempt to re-isolate this virus from a frozen aliquot of the original specimen on WI38 cells failed to produce any viral cytopathic effects and suggested a need for organ cultures in rescuing these viruses from clinical samples (Hamre and Procknow, 1966). Human tracheal organ cultures were again used to isolate several more common cold viruses in 1967, including another prototypical strain, HCV-OC43, which was found to be morphologically identical to the



previously described mouse hepatitis virus (McIntosh et al., 1967) as well as to the other human isolates. Although other HCV strains have been isolated from respiratory infections, most of the characterization of these viruses and the study of their diseases has been done on either HCV-229E or HCV-OC43. The typical morphology of a negatively-stained human coronavirus as seen by investigators in the earlier studies is provided by the electron micrograph in Figure 3.

Since their isolation, HCV-229E and HCV-OC43 have been grown in a variety of different cells, although very slowly. HCV-229E, however, has only been grown in cell lines of human origin, while HCV-OC43 has been adapted to suckling mouse brain (McIntosh et al., 1967) and has been grown by our laboratory in several mouse cell lines including Ltk- and NIH-3T3 cells and in baby hamster kidney cells. The human cell lines which will support HCV-229E replication are summarized in the Results section of this dissertation. It is assumed from the previous failure to recover HCV-229E from a clinical sample known to contain the virus by passage through WI38 cells (Hamre and Procknow, 1966) that organ cultures are necessary for the initial isolation of this virus from infected individuals. However, at least one strain of human respiratory coronavirus was reportedly isolated on the diploid intestinal cell line MA-177 (Kapikian et al., 1969).

Figure 3. Electron micrograph of negatively-stained human coronavirus particles. The glycoprotein spikes can be seen projecting from the viral envelope, providing the "corona" or halo around the virions (x180,000). Printed with permission. Electron microscopy and photograph by Dr. K. V. Holmes.



Human coronavirus 229E: Of the human coronaviruses, HCV-229E has received the most attention. While both HCV-229E and OC43 have been surveyed for prevalence and appear to cause equal morbidity, the characterization and molecular biology of HCV-OC43 has not advanced as far as that of HCV-229E. In the original isolation of HCV-229E, the virus was classically characterized as an enveloped RNA virus by ether sensitivity and resistance to 5-iododeoxyuridine, respectively. Earlier comparisons by electron microscopy of negative stains showed that HCV-229E exhibited typical coronavirus morphology and appeared identical to IBV and MHV (Almeida and Tyrrell, 1967). It was also stable during refrigeration and able to pass through a 170 nm filter but not a 110 nm filter (Hamre and Procknow, 1966). Other studies on the stability of HCV-229E indicate that the virion is also stable at 33°C and pH 6.0, but became less stable at temperatures above 4°C when pH was varied (Lamarre and Talbot, 1989). The same study showed that no infectivity was lost after 25 cycles of thawing and freezing.

All of the genes for the structural proteins of HCV-229E have been sequenced, as have several ORFs of the nonstructural proteins, some very recently (Schreiber *et al.*, 1989; Raabe and Siddell, 1989; Raabe *et al.*, 1990), however the entire genome has yet to be sequenced. The replication cycle of HCV-229E is assumed to be similar to

that of the previously described MHV. Several cell lines support HCV-229E infection and make it possible to propagate the virus and perform studies on infectivity and binding. Unlike HCV-OC43, HCV-229E does not express the HE glycoprotein, leaving only the S glycoprotein to function as a virus attachment protein. It was primarily for this reason that I chose to extend the coronavirus binding studies initiated by Dr. S. Compton on HCV-229E (Compton, 1988). My research goals were to characterize the HCV-229E-receptor interaction and identify the cellular receptor.

There are several important reasons to identify the HCV-229E receptor. The isolation of new HCV strains from clinical specimens has been difficult and most isolations have required the use human organ cultures. Identification of the HCV-229E receptor may facilitate the development of cell lines engineered for increased expression of the receptor to better support the replication of limited amounts of virus inoculum. The isolation of new and additional strains will allow for study of the epidemiology of HCV-229E and of the applicability of vaccines and/or anti-viral reagents. Cloning and sequencing of the receptor would provide the genetic basis for the synthesis of peptides which may serve as virus or receptor-targeted anti-HCV reagents. Receptor identification could also lead to the designation or the development of an animal model for the study of HCV-229E pathogenesis and for testing the

efficacy of anti-HCV vaccines or reagents. The animal model could be identified from among known animal coronavirus infections based on virus and/or receptor homologies or a transgenic mouse might be developed where expression of the human receptor in a normally resistant mouse results in acquired susceptibility to HCV-229E and natural infection.

## MATERIALS AND METHODS

Virus and Cell Propagation, Virus Purification: Human coronavirus 229E (HCV-229E) was obtained from Dr. M. Johnson-Lussenburg, University of Ottawa, Canada and grown in WI38 cells. Tissue culture infectious dose (TCID<sub>50</sub>) and plaque assays were performed to determine the titer of the batch of HCV-229E virus used throughout this project (see below). The titers by these methods were a TCID<sub>50</sub> of  $5 \times 10^6$  HCV-229E per milliliter (ml) and  $2 \times 10^6$  plaque forming units (PFU) per ml. WI38 cells (CCL 75) were obtained from American Type Culture Collection (ATCC, Rockville, Maryland), and propagated in Dulbecco's modified Eagle medium (DMEM, Gibco Laboratories, Grand Island, NY) with 10% fetal bovine serum (FBS, Gibco Laboratories) and 2% penicillin-streptomycin-fungizone (PSF, Gibco Laboratories) mixture. The virus stock used for all of the experiments described in this dissertation was of the same growth on WI38 cells. The virus was stored in 25 ml aliquots at  $-70^{\circ}\text{C}$ , which were subsequently thawed and further aliquoted as necessary for use. Porcine transmissible gastroenteritis virus (TGEV) was obtained from Dr. David Brian, University of Tennessee, Knoxville, TN. Rhabdomyosarcoma (RD) cells were obtained from Dr. Ortwin Schmidt (University of Washington, Seattle, WA), and were propagated in DMEM with 10% FBS, 2% PSF, and 1% gentamicin (Quality Biologicals



Inc., Gaithersburg, MD). HL60 cells were kindly provided by Mr. Monroe Vincent, USUHS, Bethesda, Md., and propagated in RPMI 1640 (Whittaker Bioproducts Inc., Walkersville, MD) with 20% FBS, 2% PSF, and L-glutamine (Gibco Laboratories). HRT-18 cells were obtained from Dr. D. Brian and grown in DMEM with 10% FBS and 2% PSF. U937 cells (CRL 1593) were purchased from ATCC and grown in DMEM with 10% FBS and 2% PSF. Baby hamster kidney (BHK) cells were provided by Dr. Iain Hay (USUHS, Bethesda, MD), and grown in DMEM with 10% FBS and 2% PSF.

Virus Purification: HCV-229E was purified by discontinuous and continuous sucrose density gradient ultracentrifugation. Supernatants from HCV-229E-infected WI38 cells were pooled and combined with 3.3% sodium chloride (weight/volume) on ice. A volume of 30% polyethylene glycol (Sigma Chemical Co., St. Louis, MO) equal to one half the original volume of supernatant was then added to precipitate virus from the supernatant on ice. The precipitate was pelleted by centrifugation in a Sorvall GS-3 rotor (Dupont Diagnostics, Wilmington, DE) for 30 minutes at 7,000 RPM at 4°C. The pellets were resuspended in 40 milliliters (ml) cold TMS buffer per 500 ml original precipitation solution. 20 ml of the suspension was then layered on top of discontinuous sucrose gradients consisting of 10 ml of 25% sucrose over 8 ml of 50% sucrose in Beckman Ultra-clear centrifuge tubes (Beckman Instruments,

Fullerton, CA). The gradients were centrifuged using an Beckman SW-28 rotor for 4 hours at 24,000 rpm at 4°C in a Beckman model L3-40 Ultracentrifuge. The band at the discontinuous interface was aspirated and 12 ml each were applied to the tops of a continuous 20-50% sucrose gradients and centrifuged overnight under the same conditions. The virus bands were illuminated by ultraviolet light and aspirated.

Plaque assay: The titer of the HCV-229E supernatants described above were determined by plaque assay on hAPN-3T3 cells and were  $2 \times 10^6$  PFU HCV-229E per milliliter. Briefly, HCV-229E was diluted in a 10 fold series in DMEM with 1% FBS. The medium was removed from subconfluent monolayers of hAPN-3T3 cells grown in 60 mm culture dishes and replaced with 0.5 ml of appropriate virus inoculum per plate in triplicate for each dilution. Dishes with virus challenge were incubated at 34°C for one hour with periodic rocking. The medium for overlay contained 2X MEM, 2% PSF, no FBS and 1.7% trypsin (Gibco Laboratories). This was combined with an equal volume of 1% agarose and 5 ml of agar overlay was added to each dish. The dishes were inverted and incubated for 48 hours at 34°C in 5% CO<sub>2</sub>. 5 ml of staining medium containing 0.5% agarose (Sigma Chemicals Co.), 4% FBS, 1% PSF and 1.7% neutral red (1:300 stock, MCOB Chemicals, Norwood, OH) was added to each plate, allowed to

solidify and returned to 34°C and 5% CO<sub>2</sub>. After 2-4 hours, plaques could be observed and counted.

Parental and transfected mouse and hamster cells: NIH-3T3, hAPN-3T3, hAPN<sub>mut</sub>-3T3 and hAPN-BHK cells were provided by Dr. A. Thomas Look, St. Jude Children's Research Hospital, Memphis, TN. All 3T3 cells were grown in DMEM with 10% FBS, 2% PSF and 25mM Hepes buffer (Gibco Laboratories). Cloning of the hAPN gene and transfection and expression of hAPN in NIH-3T3 cells were previously described (Look et al., 1989) and were performed similarly for the hAPN-BHK cells.

Generation of the hAPN expression vector bearing the 39 amino acid deletion and transfection and expression in the hAPN<sub>mut</sub>-3T3 cells was also previously described (NIH/CD13del, Ashmun et al., 1992). Parental and normal cross-reacting antigen (NCA)- and carcinoembryonic antigen (CEA)-expressing chinese hamster ovary (CHO) cells and parental and biliary glycoprotein 1 (BGP1)-expressing mouse SP2/0 cell lines were provided by the laboratory of Dr. Jack Shively, City of Hope, Duarte, CA. Parental, vector control, and CEA glycoprotein-expressing mouse LTK- cell lines were provided by the laboratory of Dr. Thomas Barnett, Molecular Diagnostics, Westhaven, CN.

Tissue Sources: Sources of animal intestine for brush border membrane preparations (BBM) were previously described

(Compton et. al., In preparation). Human adult small intestine (HAI) and upper respiratory epithelium (HRE) samples were obtained from the National Disease Research Interchange (NDRI, Philadelphia, Pa.) in the form of quick-frozen autopsy samples. Rat intestinal brush border membrane preparations were kindly provided by Sara Gagneten.

Brush border membrane (BBM) preparation: Animal intestinal BBMs were prepared by Dr. Susan R. Compton as previously described (Boyle et al., 1987). Human adult intestine (HAI) BBMs and human respiratory epithelium (HRE) were prepared using the same protocol. Briefly, human small intestine (HAI) or human trachea, bronchus, or larynx (HRE) samples were thawed and rinsed in cold phosphate-buffered saline (PBS). The epithelial layer was scraped and separated by a metal spatula or microscope slide and weighed. A Tekmar Tissumizer (Cincinnati, Ohio) was used to homogenize the scrapings in a 15 ml/gram homogenization buffer [300 mM mannitol, Sigma, 2 mM Tris hydrochloride, pH 7.4, containing 1% aprotinin, (Sigma)]. The homogenate was precipitated by 1% calcium chloride and centrifuged at 3,000xg for 15 minutes to remove extraneous material. The supernatant was ultracentrifuged at 15,000 RPM for 45 minutes in a Beckman SW28 rotor to pellet membranes, which were resuspended in Tris-ethylenediaminetetraacetic acid (EDTA) [10mM tris, pH7.4 and 1mM EDTA, (Sigma)] or phosphate-buffered saline

(PBS) containing 1% aprotinin. Protein concentrations were determined by the Bradford method (Bradford, 1976) using bovine serum albumin (BSA, Sigma) standards.

Cell membrane preparations: Cell membrane preparations (CMP) were prepared as follows. Individual cells types were grown as described under cell propagation above, in 150 cm<sup>2</sup> flasks or 850 cm<sup>2</sup> roller bottles to confluency. Monolayers of cells were rinsed twice in PBS and detached, if necessary, with PBS + 1mM EDTA (Sigma) and scraping. Detached or nonadherent cells were spun and cell pellets were washed twice in PBS and then resuspended in a hypotonic cell disruption buffer containing 10 mM potassium phosphate (KPi, Sigma) and 1% phenylmethyl-sulfonyl fluoride (PMSF, Sigma) and allowed to swell for 15 minutes on ice. Cells were then dounce homogenized in a 15 ml homogenizer (Bellco Glass Inc., Vineland, N.J.) using an 'A' pestle and spun at 3,000xg to pellet nuclei. Supernatants were ultracentrifuged at 25,000 RPM in an SW28 rotor for 1 hour to pellet membranes which were then resuspended in Tris-EDTA or PBS with 1% aprotinin and stored at -70°C until use. Protein concentrations were determined by the Bradford method using BSA standards.

Antisera, Antibodies: Preimmune and polyclonal goat anti-HCV-229E antisera were generated and donated by the

laboratory of Dr. Larry Sturman, State Department of Health, Albany, NY. The antisera were generated against density gradient-purified HCV-229E prepared by our laboratory. One pre-immune and a series of four immune serum samples were taken from one goat. The pre-immune serum and the serum collected from the first bleed were used exclusively for the experiments described in this dissertation. Rabbit anti-TGEV antiserum was obtained from Dr. D. Brian. Purified monoclonal antibodies specific for hAPN were donated by Dr. A. Thomas Look and have been recently described for their anti-hAPN properties (Ashmun et al., 1992).

Monoclonal antibody development and characterization: The monoclonal antibody development techniques and reagents used were as previously described with some minor modifications (Davis et al., 1986). Briefly, inbred female BALB/c mice were immunized intraperitoneally (IP) with 200  $\mu$ l of deoxycholate (DOC, Sigma)-solubilized HAI or CMP's of WI38, RD, or HL60 cells. Briefly, HAI or CMPs were pelleted by centrifugation at high speed in a microcentrifuge for 20 minutes at 4°C. Pellets were resuspended in 0.5% DOC in sterile distilled water at room temperature with shaking for 20 minutes. The suspension was again centrifuged to remove unsolubilized material and the supernatant was combined with an equal amount of Freund's complete (for initial immunizations) or incomplete (for subsequent immunizations)

adjuvant (Difco Laboratories, Detroit, MI). Approximately 200  $\mu$ g of membrane preparation per mouse was injected using a one ml Tuberculin syringe with a 26 gauge, 1/2 inch needle. The number of subsequent immunizations ranged from three to six, but were always of the same inoculum. The mice were eventually tail-bled and their polyclonal serum was assayed for the ability to protect WI38 cells from HCV-229E challenge. Those mice producing protective antibodies were chosen for fusion experiments. At 24 to 48 hours prior to the planned fusion time, mice to be used were given an intravenous tail boost of 50  $\mu$ l of untreated antigen (CMP) suspension. The procedures used for aseptic splenectomy, preparation of spleen and myeloma cells, cell ratios, fusion and plating of the fusion mixture were as described in Davis, et. al. (1986) with two exceptions. For the splenocyte-SP2/0 fusion, a volume of 0.5 ml of polyethylene glycol 1500 (50% [wt/vol] in RPMI 1640) was used and the medium used for the fusion was RPMI 1640 (as was used in the myeloma and hybridoma cell mediums). The initial plating medium, containing aminopterin, was used for two to three weeks with weekly refeeding, and replaced with aminopterin-free medium was used for all hybridoma growth thereafter. Plates of fused cells were kept in humid chambers at 5% CO<sub>2</sub> and 37°C and checked daily for hybridoma colony formation and acidic (yellowing) supernatants. All hybridoma screening was done similarly by testing 1:2 dilutions of



hybridoma supernatants for the ability to protect WI38 and/or RD cells from  $2 \times 10^4$  PFU HCV-229E or mock virus challenge per well. Screenings were read at 36 to 48 hours after challenge by the presence or absence of visible cytopathic effects. All supernatants were screened in duplicate and any cases of marginal protection or ambiguous results were re-screened. These protection assays were performed as described in the in vitro receptor-blocking assay paragraph below. After a total of five such fusion experiments by our laboratory and the screening of 1,624 hybridoma supernatants from these fusions, one hybridoma delayed HCV-229E CPE in WI38 and RD cells for up to 48 hours. This hybridoma was designated RBS. The successful fusion experiment utilized the spleens of a WI38-immunized mouse and an HL60-immunized mouse combined in a two spleen fusion experiment. RBS was subcloned by limiting dilution four times to monoclonal purity, with screening by the in vitro receptor-blocking assay. The typical subcloning procedure included dilution of the hybridoma cells to result in the plating of 2, 20 and 200 cells per 96 well plate with 2 to 4 plates at each dilution. The ideal plating dilution was 1 cell per 5 wells (or 20 cells per plate) with the additional plating of a 10-fold dilution of cells above and below this number to ensure success of the procedure against errors in counting, dilution and loss of cells due to poor growth. Conditioned hybridoma medium was added to the fresh

subcloning medium at a dilution of at least 1:4 to ensure the availability of growth factors for the singly plated cells. There are four current, protecting hybridomas maintained separately from the last subcloning. This monoclonal antibody has been named MAb-RBS. The isotype of MAb-RBS as an IgG1 was determined by using a Dynatech subisotyping kit (Dynatech Laboratories Inc., Chantilly, VA).

Monoclonal antibody ascites: Five female BALB/c mice were primed for induction of ascites by IP injection of 0.25 ml of 2,6,10,14-tetramethyl-decanoic acid (Pristane). On day 15 after priming,  $2 \times 10^6$  MAb-RBS hybridoma cells, suspended in 200  $\mu$ l of 5% (reduced) serum hybridoma medium, were injected IP into each mouse. After seven days, all mice had developed abdominal swelling of varying degrees and the ascites fluid was drained from each mouse under Metofane (Pitman-Moore) anesthesia using an 18 gauge needle. The ascites fluid from each mouse was maintained and processed separately rather than pooling to avoid dilution of concentrated antibodies until all were tested for their ability to protect WI38 cells from HCV-229E challenge. Three of the five mice were able to be drained a second time. Ascites fluid was processed after harvesting by incubating for one hour at 37°C, storing at 4°C overnight, and centrifuging at 3000xg for 10 minutes. After spinning,

the oil layer was removed and the clarified supernatant was collected. The ascites volume from each mouse varied from a total of 2 to 6 ml/animal. Metofane vapor anesthesia was used in all immunizations, priming and ascites collections. All ascites were found to provide comparable protection of WI38 cells in the in vitro receptor-blocking assay and were eventually pooled, aliquoted, and stored at -20°C.

Solid phase virus binding assay: Solid phase assays were performed as previously described (Boyle et al., 1987). Briefly, BBM's or CMP's were diluted in Tris-EDTA with 5% 2-mercaptoethanol (Bio-rad, Hercules, CA) to provide the proper concentration of material, boiled 5 minutes to reduce and denature endogenous antibodies, and applied to 0.45  $\mu$ m nitrocellulose (Bio-rad) using a Schleicher and Schuell Minifold transfer apparatus (Keene, NH). The nitrocellulose was treated for non-specific binding (blocked) in Tris-EDTA with 2-5% BSA or in sodium chloride-0.1% Brij 58 (Sigma Chemical Co.) blocking buffers. The blocked nitrocellulose was then cut into sections for subsequent virus blotting and immunoblotting steps. HCV-229E supernatants were used at 1:4 to 1:8 dilutions with WI38 medium similarly diluted as a non-virus control. Detection of bound virus was with a 1:1000 dilution of goat anti-HCV-229E or goat pre-immune antisera in separate incubation trays for 1 hour at room temperature with rocking. A similar incubation followed

using  $^{125}\text{I}$ -Staphylococcal protein A at  $1 \times 10^5\text{cpm}$  per milliliter and autoradiography. All dilutions and washes were in Tris-EDTA buffer with at least three five minute washes per incubation.

Virus overlay protein blot assay: Proteins from human intestinal BBMs (HAI) and from pig intestinal BBMs were separated by SDS-PAGE (Laemmli, 1970) and transferred to nitrocellulose filter in a Trans-blot transfer apparatus (Bio-rad) using transfer buffer containing 25 mM Tris, 0.192 M glycine and 20% methanol, pH 8.6 (Towbin et al., 1979). Blocking and detection of bound viruses were performed as described for the solid phase virus binding assay (Boyle et al., 1987) except for the following modification. In this experiment, after nitrocellulose was blocked and cut into strips from top to bottom of the gel, these strips were incubated in a 3-step renaturation protocol with Lubrol PX (Sigma Chemical Co.). Briefly, the strips were soaked for 20 minutes in each of the 3 steps which included: (1) Tris-EDTA buffer with 0.05% Lubrol and 0.05% Tween 20; (2) Tris-EDTA buffer with 0.05% Lubrol only; and (3) Tris-EDTA only. Strips were replaced in BSA block and the detection of virus binding was carried out as previously described.

In vitro virus challenge and receptor-blocking assays:  
Living monolayers of cells for HCV-229E challenge and

protection from challenge were prepared by plating cells in 96 well tissue culture plates (Corning, Inc., Corning, NY or Costar, Cambridge, MA) and allowing the monolayer to grow to approximately 80 to 90% confluency. For in vitro virus challenge assays for susceptibility to HCV-229E infection, medium was removed and replaced with 100  $\mu$ l fresh medium containing  $2 \times 10^5$  PFU/ml HCV-229E or conditioned WI38 medium (mock virus). After one hour at 37°C, virus or mock virus supernatants were removed and replaced with fresh medium and the plates were incubated until the development of viral cytopathic effect or obvious cessation of growth or over-growth of cells with a failure of virus to infect. In vitro receptor blocking (protection) assays were first incubated with 80  $\mu$ l of the appropriate antiserum, antibody, ascitic fluid, or hAPN inhibitor in fresh medium for one hour at 37°C followed by the addition of 20  $\mu$ l of  $1 \times 10^6$  PFU/ml HCV-229E or WI38 conditioned medium for a final dilution of 1:10 HCV-229E for one hour at 37°C. This supernatant was then removed and replaced with 0.1 ml fresh medium containing the appropriate dilution of antiserum, antibodies, ascitic fluid, or inhibitors and incubated under normal conditions for the development of viral cytopathic effect in control wells. Wells were read microscopically for cytopathic effect and fixed with 10% buffered-formalin and stained with crystal violet (Sigma Chemical Co.) when appropriate.

Immunofluorescence assays: Assays for the immunofluorescent detection of intracellular virus antigens were performed as follows. Cells were plated on coverslips in 60 mM dishes (Costar) and grown under normal conditions until monolayers were 80 to 90% confluent. Medium was removed and replaced with 2 ml fresh medium containing the appropriate concentration of antisera, ascites, or antibodies. After one hour occasional rocking at 37°C, HCV-229E virus or conditioned WI38 medium was added for a final dilution of  $2 \times 10^5$  PFU/ml for one hour at 37°C. The supernatant was then removed and replaced with fresh medium containing the appropriate concentration of antisera, ascites, or antibodies. For protection assays, MAb-RBS ascites was diluted 1:10 in cell medium for virus blocking before and during the application of virus challenge medium and replaced with fresh medium containing a 1:25 dilution of MAb-RBS ascites for the remainder of the experiment. After incubating for 8-10 hours or overnight, the cells were rinsed with PBS and fixed on the coverslips by -20°C acetone for 8 minutes and stored at -20°C until used. Coverslips for immunofluorescent staining were rehydrated for 30 minutes in PBS with 2% normal rabbit serum, which was also used for all subsequent washes and dilutions. Coverslips were then blotted and inverted in 50  $\mu$ l of 1:50 goat anti-HCV-229E or pre-immune antiserum for one hour at 37°C. Coverslips were then washed and soaked twice for 15 minutes,

followed by a similar incubation in 1:100 rhodamine-labeled rabbit anti-goat antibodies (Boehringer Mannheim, Indianapolis, IN). The coverslips were then washed and soaked for 15 and 30 minutes, blotted dry, and mounted on microscope slides. Cells were observed and photographed using a Zeiss immunofluorescent microscope (Carl Zeiss, Inc., Thornwood, NY). Pictures were taken with Kodak TMAX 400 speed film for black and white prints.

Enzyme-linked immunosorbant and virus binding assays:

Membrane preparations assayed for antibody or virus binding were appropriately diluted in carbonate buffer, (0.1 M sodium carbonate, pH 9.6) and 100  $\mu$ l was allowed to adhere to the wells of Dynatech Immulon 1 microtiter plates (Dynatech Laboratories, Chantilly, VA) overnight at 4°C. Except where protein concentrations varied within the experiment, 1  $\mu$ g of protein was normally applied to each well. Coated plates were blocked with 5% BSA in PBS for at least one hour at room temperature with rocking. For MAb-RBS detection of membrane proteins, 1:100 dilutions of MAb-RBS ascites or normal mouse ascites in PBS were applied and allowed to incubate at room temperature for 1 hour with rocking. Primary antibody solutions were removed and the plates were washed 3 times for 5 minutes with PBS. The bound mouse antibodies were detected by addition of horseradish peroxidase-labeled goat anti-mouse antibodies



[Kirkegard and Perry Laboratories (KPL), Gaithersburg, MD] diluted 1:1000 in PBS, followed by washing and addition of 3,3',5,5'-tetramethylbenzidine (TMB) substrate solution (KPL). The enzyme-substrate reaction was quenched with 0.5% SDS or 1 M phosphoric acid and read on a Dynatech M700 Elisa reader. For virus binding assays, HCV-229E or WI38 conditioned medium diluted 1:4 in DMEM with 25 mM Hepes buffer, was added for one hour at room temperature with rocking. Bound virus was detected with 1:1000 goat anti-229E or pre-immune antiserum followed by 1:1000 horseradish peroxidase-labeled rabbit anti-goat antibodies (KPL). Substrate reactions were conducted and read as described for MAb-RBS detection. For assays of competition between HCV-229E and MAb-RBS for binding to CMPs, MAb-RBS was diluted 1:10 in DMEM and allowed to incubate for one hour prior to during the addition of HCV-229E or WI38 conditioned medium. Bound virus detection and quantitation was as previously described.

Immunoprecipitation of hAPN: Subconfluent cultures of NIH-3T3 and hAPN-3T3 cells were incubated 15 minutes in starvation medium lacking methionine and glutamine and with 5% (reduced) FBS. This medium was removed and replaced with starvation medium containing 0.1 mCi/ml of L-[<sup>35</sup>S]methionine and incubated for pulse times of either 30 or 60 minutes for metabolic labeling of cellular proteins. After the

appropriate pulse, labeling medium was removed and the cells were washed once with normal 3T3 medium. Cells labeled for 60 minutes were incubated for an additional 60 minute chase in normal medium. Cells were lysed by adding 1 ml lysis buffer [50 mM Tris pH 7.4, 300 mM NaCl, 0.1% NP40, 5mM EDTA, 1mM PMSF, and 1mM dithiothreitol (DTT, Bio-Rad)] to each 75 cm<sup>2</sup> flask of 3T3 cells or an equivalent of HL60 cells. Lysates were transferred to Eppendorf tubes and spun 2 minutes at high speed to pellet nuclei and debris. Lysate samples were counted on an LKB Wallac 1219 Liquid Scintillation Counter (Turku, Finland) to equilibrate counts per immunoprecipitation mixture. Equal CPMs of labeled lysate were transferred to new tubes and 80 µl of either normal mouse or MAB-RBS ascites or 40 µl of 0.1 mg/ml anti-hAPN antibody MY7 were added as precipitating antibodies and these mixtures were rocked overnight at 4°C. Staphylococcal protein A-sepharose beads (Sigma) were conjugated with rabbit anti-mouse IgG (Cappel) and 60µl of the conjugated beads were added to each tube of lysate/primary antibody mixture. After an incubation of 1 hour with rocking at room temperature, the immunoprecipitated complexes were washed 3 times with lysis buffer, resuspended in 70 µl of sample treatment mix (62.5 mM Tris HCl pH6.8, 2.3% [wt/vol] SDS, 5% [vol/vol] BME, 10% [vol/vol] glycerol), boiled 5 minutes, and separated by SDS-PAGE using 8% acrylamide (Bio-rad). The gels were dried using a Bio-Rad Model 483 Slab Gel Dryer

and autoradiographed for a 10 day exposure.

Enzyme activity and enzyme inhibition assays: Assays for aminopeptidase activity were adapted from previously described methods (Ashmun and Look, 1989). Briefly, the presence of hAPN activity was detected spectrophotometrically by monitoring the increase in optical density of reaction mixtures at 405 nm in a Dynatech M700 Elisa Reader. The previously described reactions were carried out in tubes on suspensions of whole, living cells for cell surface APN activity. My assays modified the assay from testing whole cells in suspension to testing cell membrane preparations in microtiter plate wells for enzyme activity. Final reaction mixtures contained a 1:1 ratio of 100  $\mu$ l enzyme source and 100  $\mu$ l substrate in experiments to demonstrate enzyme activity only and a 1:2:1 ratio of 50  $\mu$ l enzyme source, 100  $\mu$ l enzyme activity blocking reagent, and 50  $\mu$ l substrate, respectively, in experiments testing for inhibition of enzyme activity. Enzyme sources included: bovine alanine aminopeptidase (bAAPN, Sigma), the positive control for aminopeptidase activity; NIH-3T3, hAPN-3T3, or HL60 cellular membrane preparations, each diluted appropriately in PBS; or PBS only, serving as a negative control. Typical amounts of enzyme source for comparable enzyme activity were 8 mU bAAPN per well and 10  $\mu$ g hAPN-3T3 or HL60 CMP per well. When MAb-RBS or normal mouse ascites were tested for their ability to

inhibit enzyme activity, the appropriate dilutions were made in PBS to 100  $\mu$ l per well. Positive and negative substrates were used for all tests and working concentrations were 6 mM/l in PBS. The positive control substrate for neutral exopeptidase activity was alanine-p-nitroanilide (Ala-PNA; Sigma), which is sensitive to aminopeptidase N cleavage, and the negative control substrate was proline-p-nitroanilide (Pro-PNA; Sigma), which is resistant to aminopeptidase N cleavage. If cleaved, either substrate produced a yellow-orange color which could be read optimally at 405 nm. For tests of enzyme activity, the enzyme sources were plated first, followed by the addition of substrate just prior to the first reading. A 12 channel pipetter was used to add the substrate as rapidly as possible to reduce inter-well variations within duplicates of the same condition. All reagents were kept at 4<sup>0</sup>C until the first reading was taken. For tests of enzyme inhibition, enzyme sources and blocking reagents were plated together and incubated for 1 hour at 37<sup>0</sup>C and then chilled to 4<sup>0</sup>C prior to addition of cold substrate. After the addition of substrate, an immediate reading was taken to serve as a background control and could be subtracted from later readings for net enzyme activity. Where stated, net enzyme activity was the net change in O.D. after this subtraction, as opposed to actual O.D.

## RESULTS

Growth of HCV-229E in WI38 cells and detection of HCV-229E antigens: Human coronavirus strain HCV-229E was isolated from throat washings from a patient suffering from common cold symptoms by two blind passages in secondary human kidney cells followed by growth in the WI38 line of human diploid lung fibroblast cells (Hamre and Procknow, 1966). WI38 cells have been used by our lab extensively to propagate HCV-229E. Goat anti-HCV-229E antiserum was raised against purified HCV-229E by the laboratory of Dr. L. Sturman. The pre-immune and 4 immune serum samples which resulted were used to detect SDS-PAGE separated proteins from WI38 cells which were infected or mock-infected with the same source of HCV-229E used in the preparation of the goat immunogen. After 48 hours of challenge, these cells were solubilized using an extraction buffer containing 1% Nonidet-P 40 and 0.5% deoxycholate and the solubilized proteins were separated and transferred to nitrocellulose filter. The serum samples detected the large 180kDa S glycoprotein and two forms of the 50-60kDa nucleocapsid (N) protein of HCV-229E only in infected cells and only by the post-immunization samples (data not shown). These results confirmed that these antisera could be used to detect the presence of HCV-229E antigens and one of the four immune sera was selected for use in all of the following

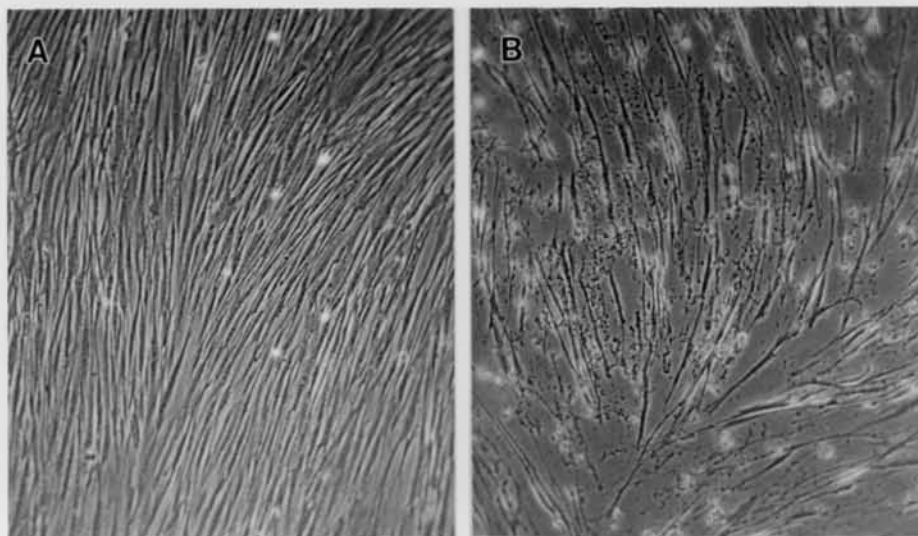
experiments.

Growth and cytopathic effects of HCV-229E in cell culture:

Previous attempts by C. Cardellichio to identify an anti-receptor monoclonal antibody which would protect susceptible cells from HCV-229E challenge employed the use of the WI38 human lung fibroblast cells previously mentioned. The rationale for this type of screening was based on the assumption that an anti-receptor antibody would recognize and bind to the receptor and block HCV-229E infection of the WI38 cells. HCV-229E has also been propagated by our laboratory and/or others in human intestinal fibroblasts M177 (Kapikian et al., 1969), other human lung fibroblasts including L132 (Chaloner-Larsson and Johnson-Lussenburg, 1981), IMR 90, MRCc (Kraaijeveld et al., 1980), MRC-5, MRC-9, human fetal tonsil (FT) cells (Schmidt et al., 1979), human rhabdomyosarcoma (RD) cells (Schmidt et al., 1979), and in human promyelocytic HL60 and U937 cells. Figures 4-6 illustrate HCV-229E cytopathic effects (CPE) in WI38, HL60, and RD cells. This CPE could be seen in WI38 monolayers in 36 to 48 hours with total destruction of the monolayer within 60 hours, whereas mock-infected cells remained in confluent monolayers. HCV-229E cytopathic effects included spindling of the cells with vacuolization, detachment of the cells from the substrate and cell lysis (Figure 4). HCV-229E also infected the nonadherent human promyelocytic HL60

Figure 4. HCV-229E growth and cytopathic effects in WI38 cells. Monolayers of human WI38 diploid lung fibroblast after 48 hours of challenge with either (A) mock-HCV-229E or (B)  $2 \times 10^5$  pfu HCV-229E virus per milliliter (multiplicity of infection of 0.5 pfu/cell). Cytopathic effects include spindling, vacuolization and lysis or detachment of infected cells.





cells, and caused agglutination of normal appearing cells within 8 hours post infection, probably due to the expression of HCV-229E S glycoprotein on the cell surface. Cytopathic effects were observed after 96 hours (Figure 5). The human rhabdomyosarcoma cell line (RD) was known to support the growth of not only HCV-229E, but also the serologically-unrelated human coronavirus strain, HCV-OC43 (Schmidt et al., 1979). RD cells challenged with HCV-229E rounded and detached from the substrate but remained adherent to the monolayer by 72 to 96 hours post infection (Figure 6). HCV-229E did not infect mouse L2 cells which are susceptible to murine coronavirus MHV-A59 (Sturman and Takemoto, 1972).

These results indicated that HCV-229E was able to infect several human cell lines derived from different tissues, but not mouse cells. The failure of virus to replicate in certain cells may be due to blockade at several different stages of the virus replication cycle, including: binding of the virus to its cellular receptor(s); fusion of the virus envelope with the cellular membrane and penetration of the virus nucleocapsid into the cytoplasm; viral RNA or protein synthesis; virus assembly or virus release.

Figure 5. HCV-229E growth and cytopathic effects in HL60 cells. Suspension cultures of human HL60 promyelocytic cells after 48 hours of challenge with either (A) mock-HCV-229E or (B)  $2 \times 10^5$  pfu HCV-229E virus per milliliter. Cytopathic effects include fusion or agglutination of cells with eventual death or lysis.

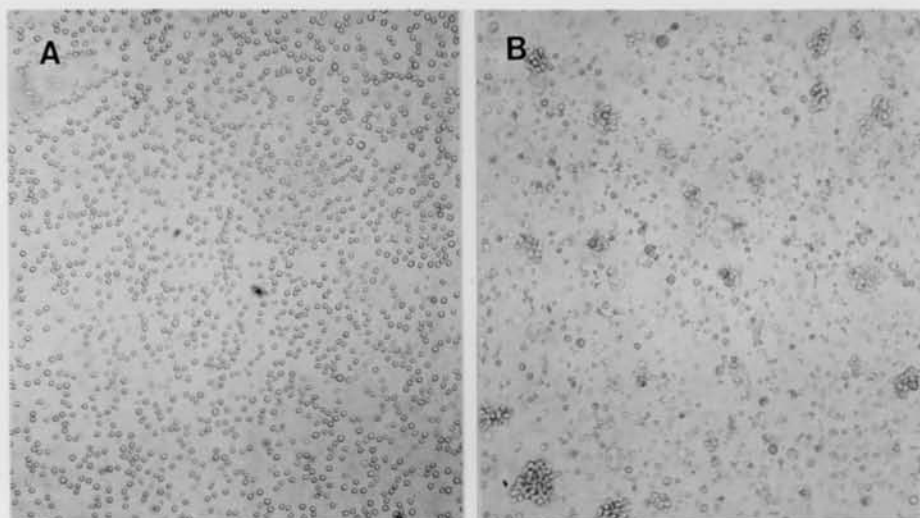
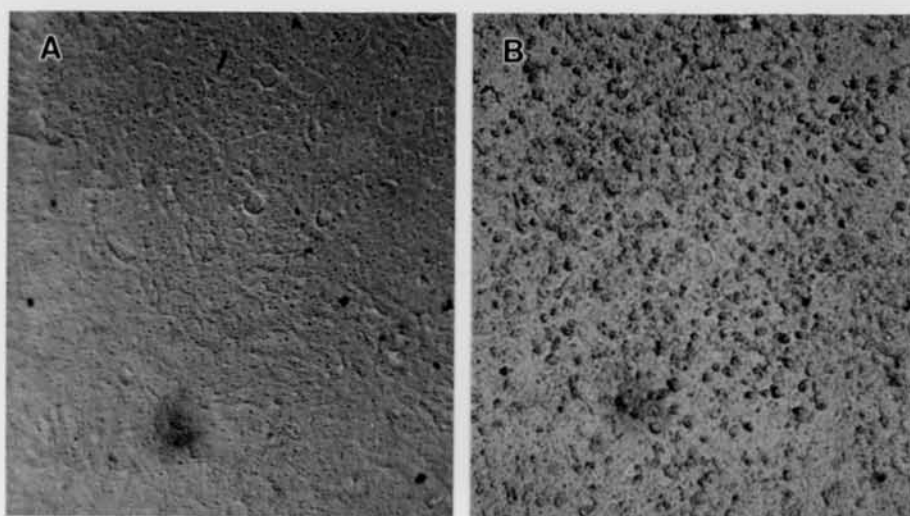


Figure 6. HCV-229E growth and cytopathic effects in human rhabdomyosarcoma (RD) cells. Monolayers of RD cells after 48 hours of challenge with either (A) mock-HCV-229E or (B)  $2 \times 10^5$  PFU HCV-229E virus per milliliter. Cytopathic effects included rounding of cells which remained adherent to the monolayer, but were detached from the substrate. It was necessary to focus the microscope slightly above the monolayer to see the rounded cells.





















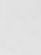
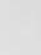
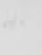
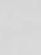

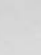

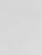




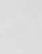
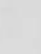
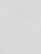
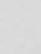






Species and tissue specificities of HCV-229E binding:

Binding of HCV-229E to human and animal intestinal brush border membranes: Preliminary studies of the specificity of the binding of HCV-229E to cell membranes were initiated by Dr. S. Compton in our laboratory (Compton, 1988). These studies showed that HCV-229E bound to human and animal intestinal brush border membrane preparations (BBMs). I repeated those experiments using the same solid phase virus binding assay, but modified it by using the recently-obtained goat anti-HCV-229E antiserum which had a lower level of nonspecific cross-reactivity than the rabbit anti-HCV-229E used in her assays. HCV-229E bound to brush border membrane (BBM) preparations of cat, dog, pig, cow, and cotton rat intestine at levels comparable to the binding seen to human BBM's (Figure 7). While the cat, dog and pig serve as natural hosts for the other coronavirus group 1 viruses, feline infectious peritonitis virus (FIPV), canine coronavirus (CCV), and transmissible gastroenteritis virus (TGEV), respectively, bovine coronavirus (BCV) and rat coronavirus (RCV) belong to other unrelated serogroups within the Coronaviridae. Therefore, the species tropism of HCV-229E infection appeared to be defined by a step in the virus replication cycle after adsorption to host membranes. A common receptor epitope or complete molecule recognized by HCV-229E may exist on the tissues of other species. Indeed,



Figure 7. HCV-229E binding to the intestinal brush border membranes of human and animal species. 10  $\mu$ g of BBMs pretreated with 5% BME from and the species shown were bound to nitrocellulose. Nitrocellulose sheets were incubated with HCV-229E (+) or (-) and virus binding was detected with 1:200 goat anti-HCV-229E, normal goat serum (NGS), or buffer only and  $^{125}$ I-SPA.

HCV-229E	SERUM	DOG	CAT	PIG	COW	MOUSE/BAI	RAT	COTTON RAT	RABBIT	CHICKEN	HUMAN
+	$\alpha$ 229E										
+	NGS										
+	BUFFER										
-	$\alpha$ 229E										

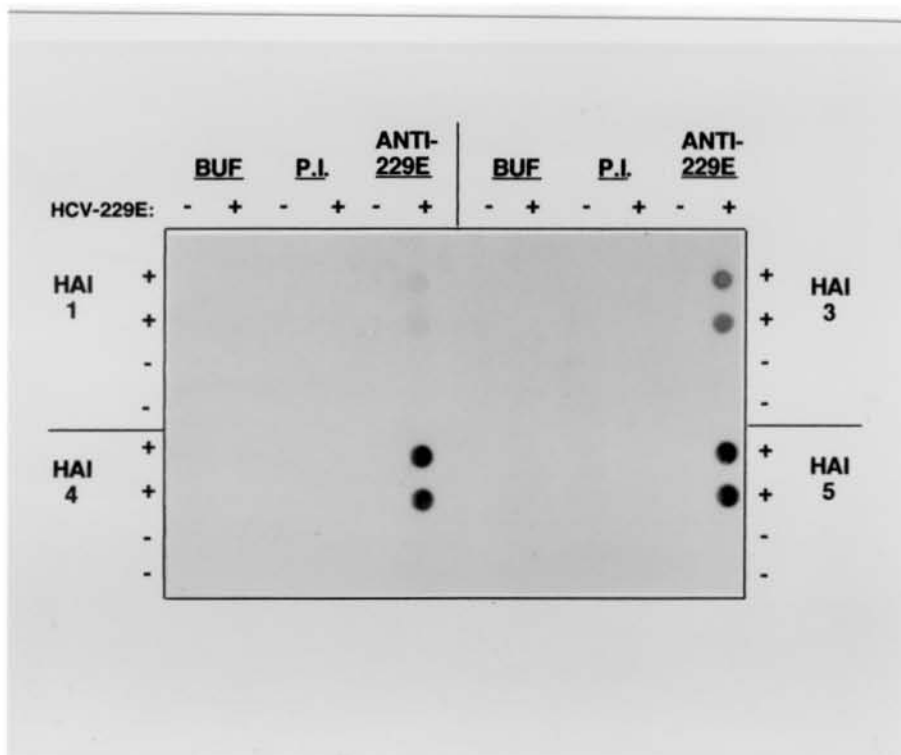
a glycoprotein sharing homology to a human cellular receptor for HCV-229E exists in the pig intestinal epithelium and HCV-229E's ability to bind to pig intestine was investigated in subsequent studies to be described in this dissertation.

Within the species, virus tropism may be further defined by the expression of the necessary receptor(s) among different individuals. In order to compare the binding of HCV-229E to preparations of adult intestinal (HAI) BBMs from 4 humans, a solid phase virus binding assay was performed using consistent amounts of BBM proteins from different individuals. Figure 8 shows that HCV-229E bound variably to all HAI preparations. Although the individuals from which these samples were derived differed in age, sex and race, all of the intestinal BBMs expressed the membrane component necessary for HCV-229E binding. The original HAI 1 preparation was several years old and bound a considerably lower amount of virus than the newer preparations, but was shown by Dr. S. Compton to bind HCV-229E specifically in her original studies (Compton, 1988).

#### Binding of HCV-229E to human respiratory epithelium:

The tropism of virus binding can be further defined among individuals of a species by differential expression of the receptor(s) among tissues types. While the binding of HCV-229E to human intestinal BBM's and the presence of a receptor in this tissue established a basis for studying the

Figure 8. HCV-229E binding to human adult intestinal (HAI) preparations from different individuals. 10  $\mu$ g of human adult BBMs from 4 different individuals pretreated with 5 % BME were bound to nitrocellulose. At this autoradiography exposure time, the signal resulting from HCV-229E binding to HAI 1 was low compared to the newer preparations, but this original preparation consistently bound HCV-229E in previous assays. HAI 2 bound HCV-229E comparable to HAI 1 (data not shown). Nitrocellulose sheets were incubated with HCV-229E (-) or (+), and virus binding was detected by a 1:200 dilution of goat anti-HCV-229E, goat pre-immune (P.I.) serum or buffer (BUF) only and  $^{125}$ I-SPA.

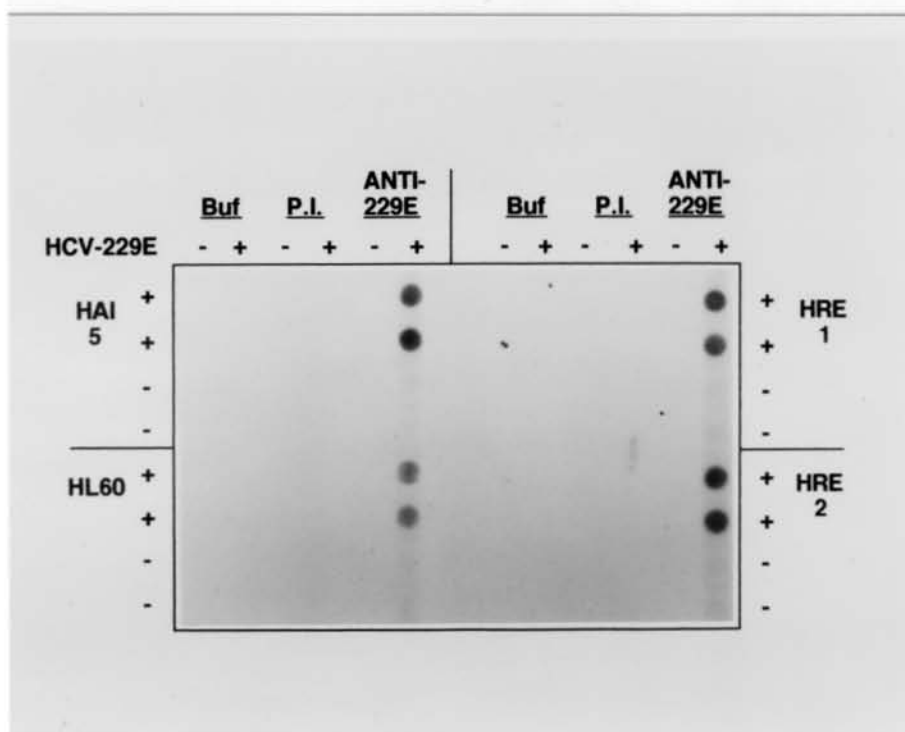


binding of HCV-229E to human tissues, it was important to determine whether virus binding could be detected on cells at the natural site of HCV-229E infection. Therefore, human trachea and bronchus samples were processed by the same method used to prepare BBMs from the intestinal samples. Figure 9 shows that 2 different preparations of human respiratory epithelium (HRE) membranes bound HCV-229E at levels comparable to those seen in HAI. Thus, HCV-229E bound to a biologically relevant tissue derived from the site of natural infection. While these experiments provided a way to study the HCV-229E-receptor interaction, the acquisition and preparation of actual human tissue for study was expensive and laborious. Additionally, the presence of endogenous human antibodies which would react with the  $^{125}\text{I}$ -labeled Staphylococcal protein A (SPA) used to detect bound virus-anti-virus antibody complexes required that the membrane preparations had to be boiled and reduced prior to use in solid phase assays (data not shown). Therefore, we sought to screen various human cell lines for the ability to bind HCV-229E.

Binding of HCV-229E to membranes of human and animal cell lines: With the ability to reliably detect HCV-229E binding to tissues bearing the receptor(s) for HCV-229E, our goals to characterize the virus-receptor interaction and to identify the receptor could be pursued. A thorough study of


















Figure 9. HCV-229E binding to membranes from human intestinal and respiratory epithelium and from a human cell line. 10  $\mu$ g of human intestinal BBMs (HAI 5), 2 different human respiratory epithelium (HRE 1,2) preparations and membranes from a human promyelocytic cell line (HL60) pre-treated with 5 % BME were bound to nitrocellulose. Nitrocellulose strips were incubated with HCV-229E (-) or (+), and virus binding was detected with a 1:200 dilution of goat anti-HCV-229E, goat pre-immune (P.I.) serum or buffer only (BUF) and  $^{125}$ I-SPA.





this interaction would, however, require better sources of membranes for HCV-229E binding and ample reagents for the detection of bound virus and for the various steps in biochemical analysis. A better source for this material might be one or more of the previously described human cell lines, which were susceptible to HCV-229E infection and therefore expressed a functional receptor for HCV-229E. A variety of HCV-229E-susceptible human cell lines were grown and processed to yield crude membrane preparations that were tested for the ability to bind HCV-229E. Membranes were prepared from the human HL60, WI38, RD, U937, and Human Rectal Tumor (HRT-18) cell lines. The first preparation was made from HL60 cells and its ability to bind HCV-229E was compared to HAI and HRE in Figure 9. When tested in the solid phase virus binding assay, other cell membrane preparations (CMP's) were found to bind HCV-229E at levels comparable to HAI and HRE (Figure 10). Specificity controls included CMPs prepared from mouse L2 cells that are nonpermissive to HCV-229E infection as well as BALB/c mouse, rat, and chicken adult intestinal membranes. At the level of sensitivity afforded by the solid phase assay and at this length of radiographic exposure, none of these animal membrane preparations demonstrated significant binding of HCV-229E, in agreement with the previous assay for HCV-229E binding to animal membranes (Figure 7). The ability to demonstrate HCV-229E binding to the membrane preparations

Figure 10. HCV-229E binding to human and animal tissue and cell membrane preparations with and without detergent extraction. 10  $\mu$ g of membrane preparations from human intestinal BBMs (HAI), human respiratory epithelium (HRE), the human cell lines WI38, HL60, RD, and HRT18, and from BALB/c intestinal (BAI), rat intestinal (RAI) and chicken intestinal (CAI) BBMs and from the mouse cell line L2 were pre-treated with (+) or without (-) 1 % NP-40 and 0.5 % DOC solubilization (Det. Extract.) and with 5 % BME were bound to nitrocellulose. Nitrocellulose strips were incubated with HCV-229E (-) or (+). Bound virus was detected with goat anti-HCV-229E or goat pre-immune (P.I.) serum and  $^{125}$ I-SPA.

	Membranes		Det. Extract	
HCV-229E	-	+	-	+
P.I.	+	+	+	+
ANTI-229E		+	+	+
HAI				
HRE				
WI38				
HL60				
RD				
HRT18				
L2				
BAI				
RAI				
CAI				

from cell cultures, both positive and negative for binding, established a ready source of receptor-bearing material for further study and characterization of the HCV-229E-receptor interaction.

#### Characterization of the HCV-229E-receptor interaction:

Sensitivity of HCV-229E binding activity to SDS-PAGE: Previous studies by our laboratory on the receptor for mouse coronavirus MHV-A59 resulted in the development of a virus overlay protein blot assay (VOPBA) (Boyle *et al.*, 1987). BALB/c mouse BBMs, separated by SDS-PAGE and transferred to nitrocellulose were incubated with MHV-A59 which bound to 2 proteins at 55kDa and 110kDa. For MHV-A59, the VOPBA provided not only molecular weights for the MHV-A59-binding proteins, but also a source of these recognized proteins for use in enzyme-linked assays to test for the binding of anti-receptor antibodies. VOPBAs with HCV-229E were attempted on HAI, HRE, and human RD, WI38 and U937 cellular proteins, but binding activity of HCV-229E in any of these experiments was very low with the most consistently seen bands at molecular weights below 35kDa. These results suggested that the component or epitope to which HCV-229E was binding may have been altered by the reduction and denaturation steps prior to and during SDS-PAGE.

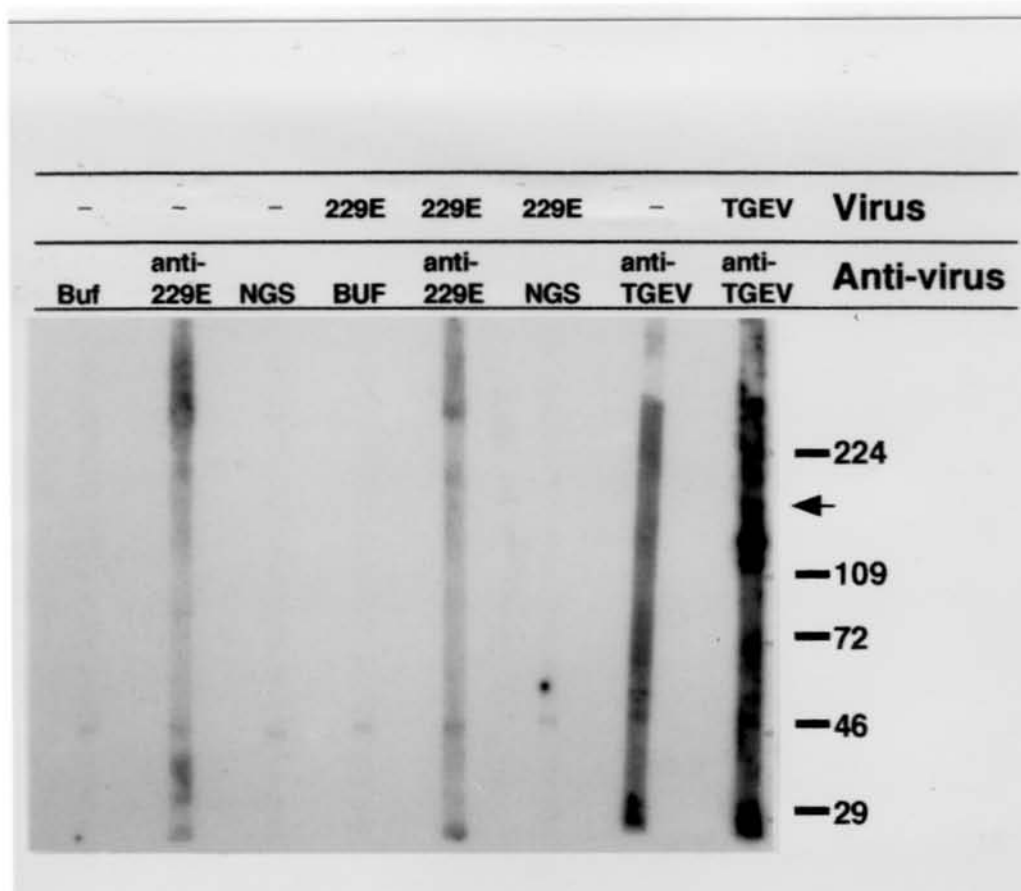
It was possible that recognition and binding of the

receptor(s) by the HCV-229E S glycoprotein depended upon the presence of a native conformation of the receptor(s). This conformation could either depend upon a multi-subunit structure of the receptor(s), or a conformation-dependent epitope lost by reduction of intrachain disulfide bonds or by linearization and coating with SDS during electrophoresis. One VOPBA was performed by C. Cardellicchio using both HCV-229E and the porcine TGEV for binding to SDS-PAGE-separated human intestinal membranes. In this assay, the separated and transferred proteins were treated with lubrol PX to enhance renaturation prior to incubation with virus. Figure 11 shows the typical weak binding of HCV-229 to HAI proteins, but a greater level of TGEV binding. We were therefore unable to ascertain any valuable information for HCV-229E using this assay.

Effects of detergents on the HCV-229E receptor: To determine the reason for the loss of HCV-229E binding during SDS-PAGE, solid phase virus binding assays were performed on several human membrane preparations in which membrane proteins were solubilized with several detergents prior to application to the nitrocellulose. When used for bioseparation or reconstitution of membrane proteins, different classes of detergents have different effects on proteins (reviewed in Neugebauer, 1988). The binding of some detergent molecules can be to the membrane-spanning





























Figure 11. Virus overlay protein blot assay of HCV-229E and TGEV binding to partially renatured human intestinal membrane proteins (HAI). 100  $\mu$ g of HAI was separated by SDS-PAGE and transferred to nitrocellulose. Nitrocellulose sheets were incubated in a series of increasing concentrations of Lubrol PX and blocked with BSA and cut into strips. Strips were incubated with (+) or without (-) HCV-229E or TGEV and bound virus was detected with goat anti-HCV-229E or goat anti-TGEV, normal goat serum (NGS), or buffer only (BUF), followed by  $^{125}$ I-SPA and radiography. The arrow indicates a band at approximately 150kDa which was later determined to be the molecular weight of the HCV-229E receptor. Photograph courtesy of C. Cardellicchio.





hydrophobic regions of integral membrane molecules allowing a native conformation for the rest of the protein while other detergents can coat part or all of the protein, as with SDS. Even where the detergent may not alter the native conformation of a single polypeptide, it may separate the subunits of multi-subunit molecules, abolishing inter-molecular associations and the overall conformation possibly required for recognition by a virus. Since our SDS-PAGE protocol included boiling of samples in the presence of 2-mercaptoethanol and SDS prior to electrophoresis in the presence of SDS, it was necessary to examine the effects of detergents and reducing agents for their effect on HCV-229E recognition of the receptor(s). HRE and WI38 and RD CMP's were solubilized with 0.4% Lubrol PX, 0.4% deoxycholate, 0.4% NP40 or 0.4% SDS and assayed for HCV-229E binding activity. Figure 12 shows that Lubrol PX, NP-40 or deoxycholate extraction caused little or no loss of HCV-229E binding, but that SDS caused a significant loss of virus binding activity. While the effects of NP-40 and deoxycholate confirmed preliminary findings by Dr. S. Compton (Compton, thesis) in experiments using intestinal BBMs, my results differed in that the cellular membrane preparations were found to be sensitive to SDS. Although our assays were performed in a similar manner, Dr. Compton's assay was with an earlier HAI preparation not included in my assay. Lubrol PX did cause a significant loss of HCV-229E

Figure 12. Detergent and trypsin sensitivity of HCV-229E binding. 10  $\mu$ g of membrane preparations from human respiratory epithelium (HRE), and human WI38 and RD cells were pre-treated with or without (Control) 0.4 % concentrations of Lubrol PX, deoxycholate (DOC) or SDS, or 0.05 or 0.005 % trypsin and bound to nitrocellulose. Nitrocellulose was cut into strips and blocked with BSA. Strips were incubated with HCV-229E and bound virus was detected with goat anti-HCV-229E or goat pre-immune (P.I.) serum and  $^{125}$ I-SPA.

	CONTROL	LUBROL	DOC	SDS	NP-40	TRYPSIN	
						0.05	0.005
<b>P.I.</b>	+	+	+	+	+		
<b>ANTI-229E</b>	+	+	+	+	+	+	+
<b>HRE</b>							
<b>WI38</b>							
<b>RD</b>							
<b>NO SAMPLE</b>							

binding activity from the HRE preparation in my experiment. Also shown in Figure 12 was treatment of the membrane preparations with 2 concentrations of the enzyme trypsin, which had a slight effect only on the HRE preparation. These results demonstrated that the HCV-229E binding activity of HRE, RD and WI38 membranes is destroyed by SDS, possibly accounting for the loss of binding observed after SDS-PAGE. Similarly, we determined the sensitivity of HCV-229E binding to the same membranes as well as those from HAI and HL60, HRT-18 and L2 cells to an extraction buffer containing 1% NP-40 and 0.5% deoxycholate. Figure 10 shows that HCV-229E binding activity to these membranes was not affected by solubilization with both NP-40 and DOC. As will be shown below, immunization of mice with DOC-solubilized HAI and HL60 membranes yielded polyclonal antiserum which protected WI38 cells from HCV-229E challenge.

Effects of heat and reduction on the HCV-229E receptor: Compton (1988) found that in the solid phase binding assay, membrane preparations derived from intestinal BBMs had to be boiled and reduced to eliminate background due to binding of  $^{125}\text{I}$ -labeled SPA to endogenous antibodies bound to the BBMs. Boiling and reductions are normal steps in the denaturation of proteins prior to SDS-PAGE. However, to test HCV-229E binding to CMP's devoid of endogenous antibodies such as the membranes of cultured cells, this

step should not be necessary. A solid phase assay was therefore performed on CMPs of RD cells to determine the effects of heat and reduction on HCV-229E binding. Figure 13 shows that boiled samples bound virus well, with or without reduction. A parallel experiment using dithiothreitol instead of BME as a reducing agent gave the same results (data not shown). Interestingly, boiling also seemed to enhance the level of HCV-229E binding. It is possible that (1) boiling could alter the conformation of the receptor for HCV-229E so that it binds virus better, (2) boiling could change a different membrane component so as to become recognizable by HCV-229E, or (3) boiling could dissociate the HCV-229E receptor from a membrane molecule normally associated with and masking the receptor. Because I was concerned that boiling might introduce such a complicating artifact, I avoided boiling of samples when possible, or boiled all samples within an experiment. A summary of the characteristics of the HCV-229E receptor(s) known at this point in my project is given in Table 4.

Alternative approaches to characterization of the HCV-229E-receptor interaction: One of the most straightforward ways to demonstrate specific virus binding is to inhibit that binding with a monoclonal antibody (MAb) directed against a cell membrane component. Therefore, we attempted to develop a monoclonal antibody directed against the HCV-229E

Figure 13. HCV-229E binding after treatment of membranes with heat and reduction. 10  $\mu$ g of human rhabdomyosarcoma (RD) cells were pre-treated with 5 %, 1 % or no BME and/or 100 or 60<sup>0</sup>C heat and bound to nitrocellulose. Nitrocellulose was incubated with HCV-229E (-) or (+) and bound virus was detected by goat anti-HCV-229E, goat pre-immune (P.I.) or buffer only (BUF) and <sup>125</sup>I-SPA.





TABLE 4

HCV-229E Binding Activity Of Membranes From Cell Cultures  
And Tissues

<u>Species and tissue Specificity</u>	<u>HCV-229E Binding</u>	<u>HCV-229E Infection</u>
<u>Human</u>		
<u>Cell Cultures</u>		
Embryonic kidney organ culture	+	+ <sup>1</sup>
Diploid Lung Fibroblast Cell Lines (W138, MRC-5, -9, IMR-90)	+	+
Promyelocytic cell lines (HL60, U937)	+	+
Rhabdomyosarcoma cell line (RD)	+	+
Diploid Intestinal Fibroblast Cell Lines (MA 177)	+	+ <sup>2</sup>
Rectal Tumor (HRT-18)	+	+
<u>Tissues</u>		
Respiratory epithilium (HRE)	+	+
Adult small intestine Epithelium (HAI)	+	+
<u>Animal</u>		
<u>Cell Cultures</u>		
Mouse L-2	+	-
<u>Tissues</u>		
Mouse intestinal epithelium (BAI)	+/-	-
Pig intestinal epithelium	+	?
Dog intestinal epithelium	+	?
Cat intestinal epithelium	+	?
Cow intestinal epithelium	+	?
<u>Sensitivity to Detergent</u>		
	<u>Sensitive</u>	
Lubrol Px	No	
Deoxycholate	No	
Nonidet P-40	No	
Sodium deodcyl sulfate	Yes	
<u>Sensitivity to Reduction</u>		
2-mecaptoethanol	No	
Dithiothreitol	No	
<u>Heat sensitivity</u>		
37° - Boiling	No	

<sup>1</sup>Hamre and Procknow, 1966.

<sup>2</sup>Kapikan, et al., 1969.

receptor. Serum from mice immunized with HAI protected WI38 cells from HCV-229E challenge, but many hybridomas derived from the spleens of these mice were screened for inhibition of HCV-229E infection and none was found to block infection.

Our screening method to identify hybridoma supernatants relied on the expectation that one MAb would protect WI38 cells from HCV-229E challenge if there were only one receptor for HCV-229E. The use of protecting anti-receptor MAbs allowed Hsu *et al.* (1988) to demonstrate that one group B Coxsackievirus could utilize distinct receptors on different cell types. Difficulty in isolating protecting MAb could be due to the expression of an additional or alternate HCV-229E receptors on WI38 cells. If there were 2 different types of receptors on a single host cell type, it might only be possible to demonstrate a partial reduction in HCV-229E binding to cells or to CMPs. The quantitation of such a partial reduction in binding would be essential. The most practical approach was to develop an assay to quantify HCV-229E binding and the reduction of that binding by antibodies to the CMP's.

#### Development of an enzyme-linked virus binding assay:

To quantify virus binding, an enzyme-linked virus binding assay was developed. This assay used lower concentrations of membranes, virus, goat anti-HCV-229E and secondary antibodies. Briefly, cell membranes were coated on Dynatech 96 well ELISA plates and then non-specific protein binding

sites were blocked with bovine serum albumin (BSA). The wells were then incubated sequentially with HCV-229E, goat anti-HCV-229E, and with peroxidase-linked anti-goat secondary antibody. Biotin-labeled secondary antibodies could also be used in conjunction with peroxidase-linked avidin for even greater sensitivity within the assay. This assay not only quantitated HCV-229E binding more precisely, but also significantly reduced the time and quantity of reagents required when compared to the previous radiologic solid phase assay on nitrocellulose. Table 5 summarizes the concentrations and dilutions of reagents and the advantages gained in using the enzyme-linked virus binding assay (ELVIRA) over the solid phase virus binding assay. Figure 14 provides typical results of assays of HCV-229E binding to CMPs of human and mouse cell lines. As can be seen in Figure 14, the increased sensitivity of the ELVIRA revealed some binding of HCV-229E to the mouse membranes which had been assumed to be negative for HCV-229E binding by previous solid phase assays. This was the first indication that HCV-229E would recognize and bind to some component on mouse cells and this activity will be discussed when it is seen with mouse 3T3 cells later.

One approach to analyzing the possible existence of alternate receptors for HCV-229E was to raise mouse antibodies to membranes of different HCV-229E-susceptible cells and use these antibodies to try to block HCV-229E

TABLE 5

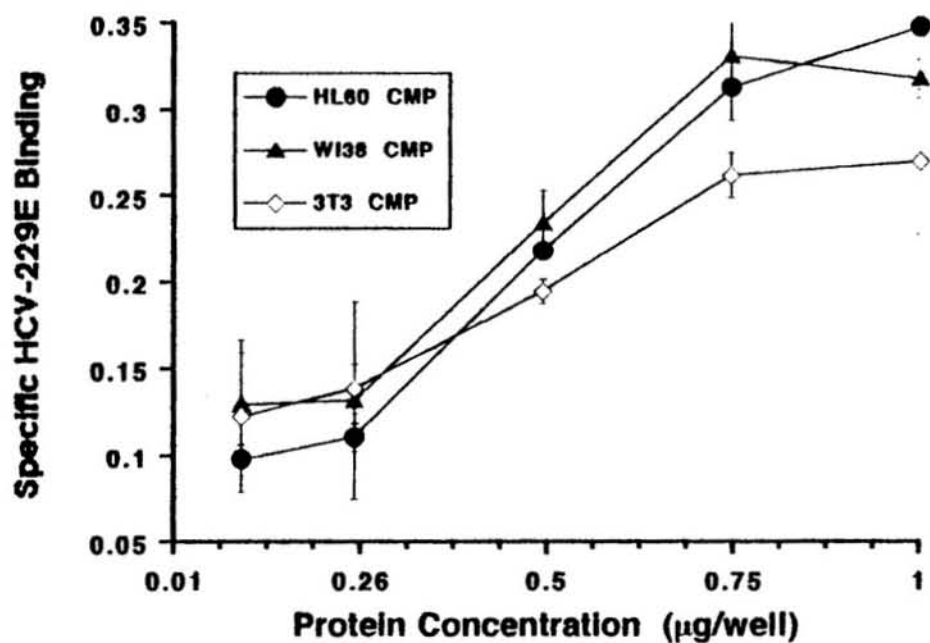
Comparison of Solid Phase and Enzyme-Linked  
Virus Binding Assays

	<u>Solid Phase</u>	<u>Enzyme-linked</u>
<u>Assay Component</u>		
Membrane preparation	10 mg/dot	0.1-1.0 mg/dot
Virus Concentration	$5 \times 10^5$ PFU/ml	$2.5 \times 10^4$ PFU/ml
Polyclonal anti-virus dilution required for detection	1:200	1:1000-1:5000
Reagents for detection of bound antibody	$^{125}\text{I}$ -SPA ( $1 \times 10^5$ CPM/ml)	enzyme linked anti-primary antibody $\geq 1:1000$ dilution
<u>Quantitation</u>		
Method	Autoradiography with optional scanning	Optical Density read by ELISA reader
Development/Results	Autoradiograph or scanned image	Changes in Optical Density of enzyme- substrate reaction
Time	17 hours to 7 days; or with Phosphoimager $\geq 2$ hours	5-30 minutes
<u>Other Consideration</u>		
Number of test Conditions	96	384
Radioisotope Handling	$^{125}\text{I}$ Iodine	None

\*The reasonable number of test conditions per assay manageable by one person in one day with all conditions performed in duplicate.

Figure 14. Enzyme-linked virus binding assay (ELVIRA) of HCV-229E binding to membranes of human and mouse cells. 1  $\mu$ g of mouse NIH-3T3 or human HL60 or WI38 membranes was adsorbed to each well of a 96 well plate and blocked with BSA.  $2.5 \times 10^4$  PFU of HCV-229E was added to each well and virus bound was detected by a 1:1000 dilution of goat anti-HCV-229E followed by biotinylated rabbit anti-goat antibodies and peroxidase-conjugated avidin. Optical density (O.D.) of the colorimetric TMB substrate cleavage reaction was read by ELISA reader. Specific HCV-229E binding is the net O.D. value after subtraction of nonspecific O.D. background in control wells. Blank values were not assigned to control wells prior to reading. The O.D. values of control wells (clear or empty wells) averaged about 0.125nm and this value was determined for each plate and subtracted from the values of each of the other wells on the same plate to yield the net specific binding.

**Binding of HCV-229E to Human and Mouse Cell Membranes  
(Enzyme-Linked Virus Binding Assay)**



binding to membranes of the same or other cell lines. This was attempted by immunizing different pools of 5 mice each with either HAI, HL60, WI38, or RD membrane preparations and testing these antisera as blocking reagents in the ELVIRA. Although more efficient blocking by certain anti-CMP antisera was observed, these initial results were inconclusive since partial blocking could have been due to differences in anti-receptor antibody concentrations among the different antisera (data not shown). Our plans to titer the antisera were preempted by the discovery of a protecting monoclonal antibody in our concurrent efforts to develop a monoclonal antibody as described below. The ELVIRA did, however, provide an increased level of sensitivity and the ability to quantify variability in HCV-229E binding and binding inhibition and would prove useful in subsequent studies.

#### Development of an anti-receptor monoclonal antibody:

The value of anti-receptor antibodies in receptor identification has been proven repeatedly, as demonstrated by the success of our laboratory with its use in identifying and purifying the MHV-A59 receptor and by others to study the receptors of human immunodeficiency virus (Landau et al. and Mizukami et al., 1988), poliovirus (Minor et al., 1984), and rhinovirus (Colonno et al., 1986). Using a different strategy, Kauffman et al. (1983) developed an



anti-idiotypic antibody with anti-receptor specificity by immunizing rabbits with a neutralizing monoclonal antibody directed against the virus attachment protein of reovirus type 3. Following the monoclonal antibody approach, our laboratory has attempted to develop antibodies against human cell membrane proteins that might serve as HCV-229E receptors. These experiments are summarized in Table 6 which shows the various human membrane preparations used as immunogens and the number of hybridoma supernatants from each fusion tested for the ability to protect WI38 or RD cells from HCV-229E infection. In addition to our concern for the possibility of alternate receptors for HCV-229E was a concern for the relative affinities of the HCV-229E S glycoprotein and anti-receptor antibodies for the same receptor. If the virus attachment protein possessed a greater affinity than an anti-receptor antibody for the receptor, the virus could displace the potentially protecting antibody rather than be blocked by it. Our screening protocol for the hybridoma supernatants was modeled after that used for development of the anti-MHV-A59 MAb (Williams et al., 1990). In this assay, antibody candidates were added and removed prior to addition of challenge virus. If HCV-229E possessed a greater affinity for the receptor than a competing anti-receptor antibody, the virus could displace it, infect the WI38 cells, and mask the presence of the anti-receptor antibody in this assay.

TABLE 6

**Screening of Hybridoma Supernatants for Antibody  
to the HCV-229E Receptor**

Experiment #	Immunogen(s) <sup>1</sup>	Hybridomas Screened <sup>2</sup>	Number Positive <sup>3</sup>
I	HAI;DOC-HAI	381	0
II	HAI;DOC-HAI	103	0
III*	HAI	619	0
IV*	DOC-HAI; DOC-RD CMP	169	0
V*	DOC-HL60 CMP, DOC-WI38 CMP	352	1
	<b>TOTAL</b>	<b>1624</b>	<b>1</b>

<sup>1</sup> CMP-Cell membrane preparation, DOC - 0.5% deoxycholate solubilized, HAI-human adult intestine BBM, RD-human rhabdomyosarcoma cells, HL-60-Human promyelocytic cells, WI38-Human diploid lung fibroblast.

<sup>2</sup> Method of Screening is described in detail in Materials and Methods. Briefly, subconfluent monolayers of WI38 and/or RD cells (both WI38 and RD were used for experiments II and III) were pretreated with a 1:23 dilution of hybridoma supernatant in medium for 1 hour at 37°C followed by addition of HCV-229E for one hour at 37°C. Virus was removed and replaced with fresh medium plus 1:2 hybridoma supernatant and incubated until the development of visible cytopathic effect in virus-infected control wells without blocking MAb, usually 36-48 hours after challenge.

<sup>3</sup> Positive-hybridoma supernatant protected cells from virus-induced cytopathic effect.

\* Fusion experiments performed by the author.

Also, membrane recycling during the 1 hour virus challenge could result in the expression of new receptor molecules, rendering the cells susceptible to infection even after incubation with blocking antibodies. In order to provide an opportunity for the blocking antibodies to compete with the virus for newly-expressed receptor, the assay was modified so as to add the challenge virus directly to the pre-incubation medium containing the hybridoma supernatants. We also refed the cells for the remainder of the assay with medium containing 50% hybridoma supernatant, providing the opportunity for continued competition between the virus and antibodies. It should also be mentioned that the protection provided by any of the polyclonal antisera could be more accurately described as a delay in the development of HCV-229E-induced CPE when compared to mock-virus controls. Regardless of the concentration of these and other protecting antibodies eventually tested, HCV-229E infection was always able to overcome the protection and destroy the monolayers within 60 to 72 hours after challenge. This ability of HCV-229E to overcome protection even in the presence of blocking antibodies suggests a higher affinity by this virus for its receptor than any of the antibodies found.

Identification of a monoclonal antibody that blocked HCV-229E infection of WI38 cells: Splenocytes from mice

immunized with deoxycholate-solubilized HL60 and WI38 CMP's were fused with mouse SP2/0 myeloma cells. One of the hybridomas supernatants from this fusion contained antibodies which protected WI38 cells from HCV-229E infection in the modified screening assay described above. The protecting hybridoma was subcloned 4 times by limiting dilution and designated MAb-RBS. The supernatant medium from the hybridoma cell culture protected WI38 and RD cells from HCV-229E infection as well as the polyclonal antiserum from the immunized mice. The immunoglobulin isotype of MAb-RBS was IgG1 by ELISA assay utilizing anti-mouse subisotype antibodies. To identify membrane proteins recognized by MAb-RBS, membranes from human tissues and cell cultures were separated by SDS-PAGE, transferred, and immunoblotted with MAb-RBS hybridoma supernatants, but no bands were detected. This result suggested that MAb-RBS, like the HCV-229E virus that it blocks, might also recognize a conformation-dependent epitope of a receptor protein that is destroyed by SDS-PAGE, or that the quantity of receptor was too low for detection by immunoblotting.

Generation of MAb-RBS mouse ascites: In order to obtain a higher concentration of MAb-RBS than that present in hybridoma supernatants, BALB/c mice were used to generate MAb-RBS ascitic fluid. When compared to the MAb-RBS hybridoma supernatants for their relative abilities to

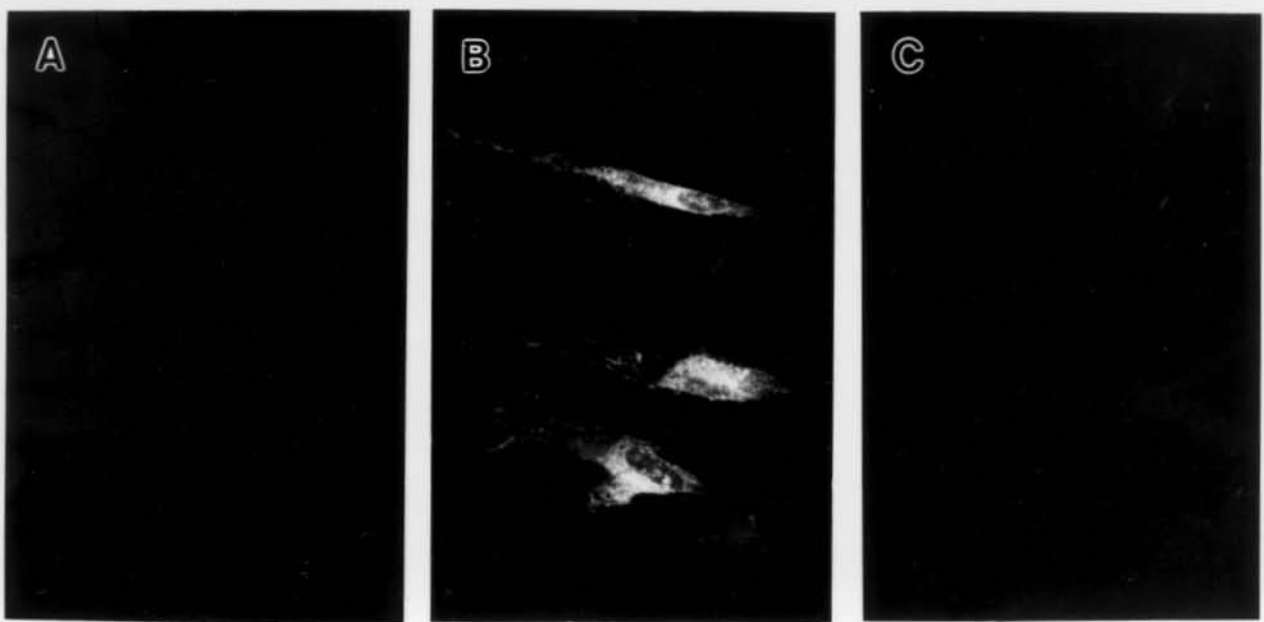
protect WI38 cells against HCV-229E challenge, the ascites protected at a dilution 20-fold greater than that of the supernatant. Figure 15 shows that pretreatment of WI38 cells with a 1:10 dilution of MAb-RBS ascites significantly reduced the number of HCV-229E-infected WI38 cells. Immunofluorescence assays in which infected and uninfected cells were counted demonstrated a 96% reduction in HCV-229E infected cells after an 8 hour challenge when MAb-RBS was used at a 1:10 dilution prior to and during HCV-229E challenge and maintained at a 1:25 dilution for the 8 hour incubation. This ascites was used for the remainder of experiments during this project.

#### Testing of Carcinoembryonic Antigen Family members as HCV-229E receptor candidates:

Several members of the immunoglobulin superfamily of molecules in their various roles on the surface of cells have proven to be attractive vehicles for virus binding and entry (reviewed in the Introduction). Their structure, function, and expression on a wide variety of cells appear to favor their use as receptors for several viruses.

The use of a murine CEA-related glycoprotein by the mouse coronavirus MHV-A59 led us to the test a variety of human CEA glycoproteins as candidates for use by HCV-229E as a cellular receptor. Commercially available anti-CEA glycoprotein antibodies were tested for their ability to

Figure 15. Protection of WI38 cells from HCV-229E challenge by MAb-RBS. Monolayers of human WI38 cells were challenged by (A) mock virus, (B)  $2 \times 10^5$  PFU HCV-229E and (C) treatment with a 1:10 dilution of MAb-RBS ascites before and during a  $2 \times 10^5$  PFU HCV-229E challenge for 10 hours and cold-acetone fixed. Cytoplasmic HCV-229E antigens were detected by a 1:50 dilution of goat anti-HCV-229E and rhodamine-labeled rabbit anti-goat antibodies. Intracellular HCV-229E antigens can be seen in the HCV-229E challenged WI38 cells only. No protection was seen in cells treated with control normal mouse ascites (data not shown).



block HCV-229E binding to HAI and WI38 CMPs in solid phase virus binding assays. Antibodies specific for the human carcinoembryonic antigen (CEA), pregnancy specific glycoprotein (PSG) and for both CEA and normal cross-reacting antigen (NCA) failed to inhibit HCV-229E binding whereas the positive control anti-HL60 antisera diminished virus binding (Table 7). Several human CEA-related glycoproteins have been cloned including CEA, NCA, PSG and biliary glycoprotein (BGP). These had been expressed in chinese hamster ovary (CHO) cells and mouse SP2/0 and LTK-cells and were obtained from the laboratories of Dr. Jack Shively (City of Hope, Duarte, CA) and Dr. Tom Barnett (Molecular Diagnostics, Westhaven, CN). These stable transfectants and the non-transfected parental cell lines were challenged with HCV-229E and none of these cell lines showed any viral CPE (Table 8). Additionally, C. Cardellicchio in our laboratory tested these cells for development of HCV-229E antigens by immunofluorescent labeling and found no intracellular viral antigens after HCV-229E challenge (data not shown). These experiments demonstrated that HCV-229E would not utilize any of the CEA-related glycoproteins tested as a cellular receptor.



TABLE 7

## Anti-CEA Antibodies Tested for Binding Inhibition HCV-229E

<u>Antibody</u>	<u>Inhibition of HCV-229E Binding<sup>1</sup></u>
Polyvalent anti-CEA/NCA	-
Specific: anti-CEA	-
anti-NCA	-
anti-PSG	-
Polyvalent anti-DOC-HL60 <sup>2</sup>	+

<sup>1</sup> Assays for inhibition of HCV-229E binding as described in Materials and Methods.

<sup>2</sup> Polyvalent anti-DOC-HL60 from mice immunized with deoxycholate-solubilized HL60 cell membrane proteins.

TABLE 8

**CEA Glycoprotein-expressing Rodent Cells  
Challenged by HCV-229E**

Transfected Cell Type	Glycoprotein Expressed	Viral <sup>1</sup> CPE	Virus Antigen <sup>2</sup> by IF
CHO (Chinese Hamster Ovary)	None	-	-
	CEA	-	-
	NCA	-	-
SP20 (Mouse Myelome)	None	-	-
	BGP1	-	-
L tk- (Mouse Fibroblast)	None	-	-
	Vector only	-	-
	CEA(GPI linked)	-	-
	NCA	-	-
	TM1(Integral CEA)	-	-
	TM2(Integral CEA)	-	-

<sup>1</sup> In vitro virus challenge assays were performed as described in materials and methods by C. Cardellicchio and R. Williams.

<sup>2</sup> As detected by Immunofluorescence assay for intracellular virus antigen as described in materials and methods.

Abbreviations: CEA - carcinoembryonic antigen; NCA - non-specific cross-reacting antigen; BFP1 - biliary glycoprotein I; TM1 - trans-membrane form 1; TM2 - transmembrane form 2.

Identification of human aminopeptidase N as a cellular receptor for HCV-229E:

Correlation of the genetic mapping of HCV-229E sensitivity with the discovery of a porcine coronavirus receptor: Previous studies utilizing somatic cell hybridization of HCV-229E-resistant mouse cells with HCV-229E-susceptible HL60 cells resulted in the assignment of HCV-229E sensitivity to the q arm of human chromosome 15 (Sakaguchi and Shows, 1982). Genes in this region could include possible receptor candidates for HCV-229E. Among genes mapped to this region were those of two cell membrane proteins that might be capable of serving as virus receptors. One was the  $\beta_2$ -microglobulin protein which is expressed on nearly all cell types, usually in association with, but also possibly independent of, the MHC class I glycoprotein (Maloy and Coligan, 1985). This molecule, in the immunoglobulin superfamily, facilitates the binding and entry of human cytomegalovirus (Grundy *et al.*, 1987). With a molecular weight of 11.9kDa, this protein would have run off the gels in VOPBAs. Anti- $\beta_2$ -microglobulin antibodies were tested for the ability to prevent HCV-229E binding to HAI in the solid phase assay or to protect WI38 cells in the in vitro receptor blocking assay. This antibody had no effect on virus binding or infection (data not shown), so  $\beta_2$ -microglobulin, like the CEA-related glycoproteins tested,

was dismissed as a receptor candidate for HCV-229E.

Another cell membrane glycoprotein mapped to the same region of human chromosome 15 was aminopeptidase N (hAPN) (Look et al., 1986). While its extracellular expression would permit its use as a site of virus binding, hAPN represented a class of membrane-bound proteases that have not previously been shown to serve as virus receptors. An interesting caveat to this was the demonstrated requirement for the proteolytic cleavage of the coronavirus MHV-A59 attachment glycoprotein (S) during the MHV-A59 replication cycle which is necessary for cell fusing activity of this virus (Sturman et al., 1985). While cleavage of the S glycoprotein of HCV-229E has not been observed, it was possible that an extracellular protease such as hAPN might perform this function.

At the time our work was in progress, Delmas and Laude (Unite de Virologie et Immunologie Moleculaires, NRA, France) reported at a public meeting that a MAb directed against pig intestinal membranes could protect swine testicular cells from infection with the porcine coronavirus TGEV. Immunoprecipitation of a protein with this MAb permitted N terminal amino acid sequencing that showed the protein to be porcine aminopeptidase N. Dr. S. Compton and I had established by solid phase assays that HCV-229E could bind to the intestinal BBMs of pig and that the serologically-related TGEV could bind to intestinal BBMs of

humans. These binding activities are demonstrated in Figure 16 and were previously seen in Figure 7. Although TGEV did not recognize the human BBMs as strongly as the porcine BBM, both viruses appeared to recognize some membrane component common to both host tissues. These data and the significant homology shared by the TGEV and HCV-229E S glycoproteins and by the published human and porcine APN glycoproteins led us to investigate hAPN as a cellular receptor for HCV-229E. Most of the known characteristics for hAPN are provided in Table 9.

Dr. A. Thomas Look (St. Jude Children's Research Hospital, Memphis, TN) supplied us with specific anti-hAPN antibodies and hAPN-transfected and untransfected control mouse NIH-3T3 cells. Our laboratory had shown previously that HCV-229E failed to infect mouse L2 cells, and it was likely that the mouse 3T3 cells would also be resistant to HCV-229E infection. Thus, the parental and hAPN-transfected NIH-3T3 cells provided a system with which to test for a correlation between the expression of hAPN and the acquisition of HCV-229E binding and susceptibility to infection. In the transfected NIH-3T3 (Swiss) cells, an hAPN cDNA was under the transcriptional control of a retroviral promotor. These cells over-expressed hAPN by approximately 30-fold when compared to HL60 cells (Ashmun and Look, 1990).

Figure 16. HCV-229E and TGEV binding to membranes of human and pig intestinal epithelium. 10  $\mu$ g of human intestinal (HAI) or pig intestinal (PIG INT) BBMs were treated with 5% BME and bound to nitrocellulose. The nitrocellulose was blocked with BSA and incubated with (+) or without (-) HCV-229E or TGEV. Bound virus was detected by a dilution of 1:200 goat anti-HCV-229E or goat anti-TGEV, pre-immune (P.I.) serum or buffer only (BUF) and  $^{125}$ I-SPA.

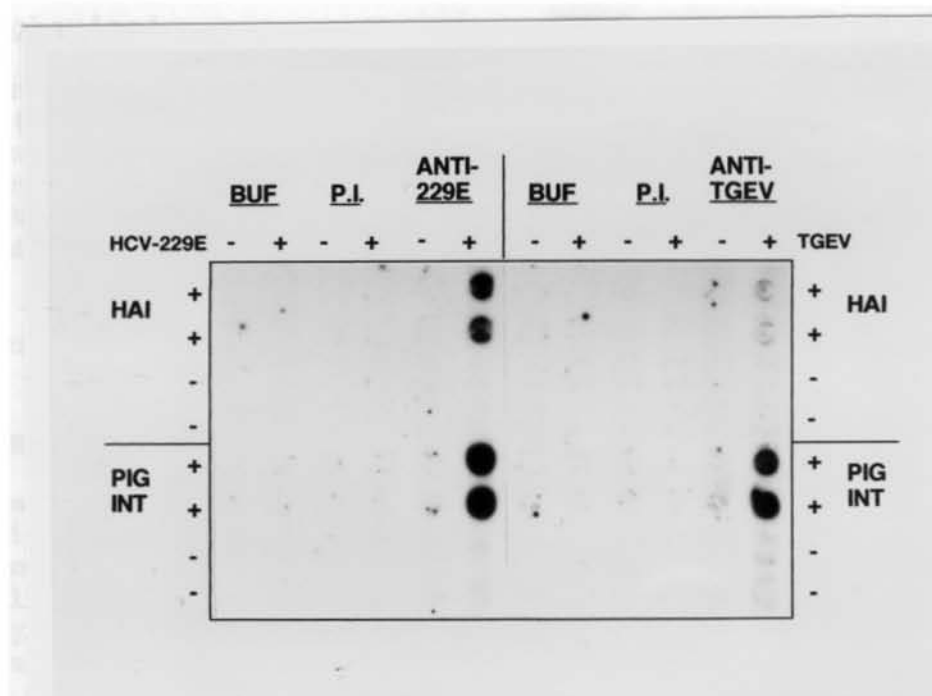


TABLE 9

Characteristics of Human Aminopeptidase N/CD13

---

Biochemical

Integral Type II membrane glycoprotein  
(cytoplasmic N-Terminus)  
Expressed as a homodimer on apical plasma membranes  
Molecular mass of 150 kilodaltons (also seen as a 130  
kilodaltons partially glycosylated form)  
967 amino acids with a 24 amino acid hydrophobic membrane  
on clear/leader sequence and a pentapeptide  $Zn^{++}$   
binding sequence.  
 $Zn^{++}$  binding metalloenzyme with neutral exopeptidase  
activity

Tissue Distribution

Respiratory and intestinal epithelium  
Fibroblasts and hepatocytes  
Renal proximal tubules  
Placenta  
Synaptic membranes of the central nervous system  
Macrophages, granulocytes

Genetics

Gene located on bands  $q^{25}-q^{26}$  of chromosome 15  
Level of expression regulated by different promoters in  
different tissues  
cDNA for cloning derived from HL60 promyelocytic cells

Proposed Functions

Breakdown of small peptides in the gut  
Biodegradation of neuroactive peptides

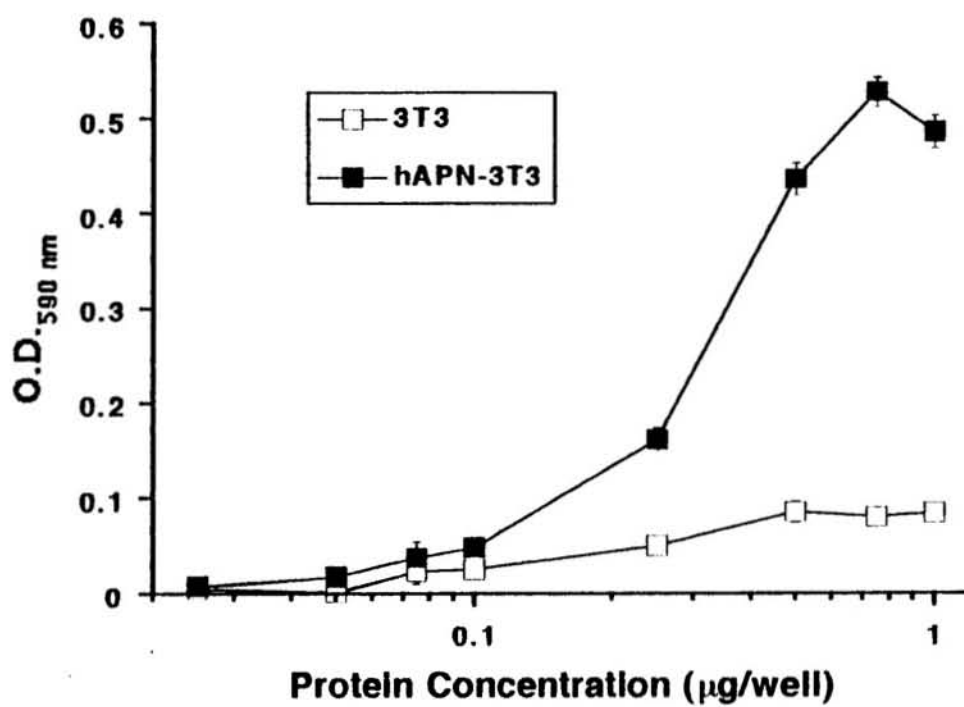
---



Binding of MAb-RBS to hAPN in hAPN-transfected mouse cell membranes: MAb-RBS prevented HCV-229E infection of WI38 cells presumably by preventing or interfering with the interaction of HCV-229E with its cellular receptor(s). If MAb-RBS recognized hAPN specifically, then hAPN could serve as the functional receptor for HCV-229E. As a result, MAb-RBS should bind specifically to membranes of cells which express the human APN only. To test the specificity of MAb-RBS, CMPs derived from human cell lines and from the parental and hAPN-expressing 3T3 cell lines were assayed for MAb-RBS recognition by a modified enzyme-linked immunosorbant assay with these CMPs applied to the wells of 96 well plates. Figure 17 shows that MAb-RBS recognized the hAPN present on the hAPN-3T3 CMPs, but did not bind to the parental NIH-3T3 CMPs. These results indicated that MAb-RBS recognized a component present only in cells that expressed the hAPN through genetic engineering. Additionally, Drs. R. Ashmun and A. Look showed that MAb-RBS bound to cells expressing the native hAPN on their surface by the use of fluorescein-activated cell sorting (FACS) (Yeager et al., 1992). Dr. Look's laboratory compared the recognition of hAPN by MAb-RBS with that of a commercially available anti-hAPN MAb designated MY7 in FACS experiments and found that our monoclonal antibody sorted hAPN-expressing cells in a manner similar to the previously-characterized anti-hAPN antibody.

Figure 17. MAb-RBS binding to hAPN-transfected mouse cells membranes. One  $\mu\text{g}$  of hAPN-transfected (hAPN-3T3) or parental NIH-3T3 (3T3) cell membranes was adsorbed to each well of a 96 well microtiter plate and blocked with BSA. Antibody preparations containing MAb-RBS or the control antibody, an irrelevant mouse IgG1 hybridoma supernatant, were applied to the coated wells. Bound mouse antibodies were detected by a 1:1000 dilution of peroxidase-labeled goat anti-mouse antibodies. Optical density (O.D.) of the colorimetric TMB substrate cleavage reaction was read by ELISA reader.

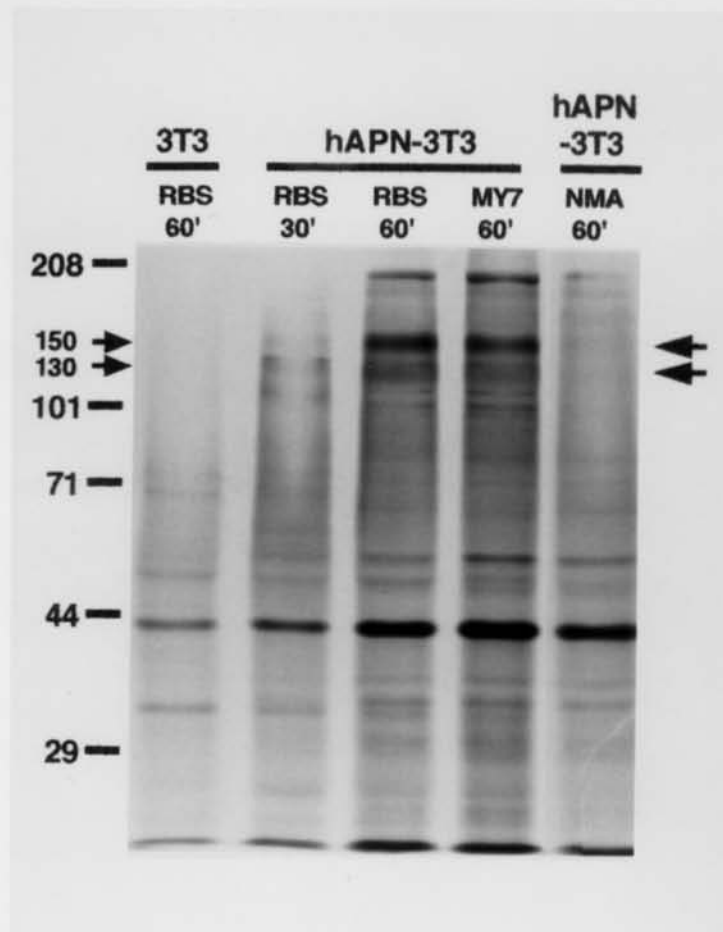
### MAB-RBS Binding to hAPN-transfected Mouse Cell Membranes



Immunoprecipitation of hAPN from hAPN-transfected cells by MAb-RBS: We found that MAb-RBS failed to recognize any proteins of human BBMs and CMPs after SDS-PAGE separation of the proteins (data not shown) which would bind HCV-229E in solid phase binding assays (Figure 10). We used immunoprecipitation to determine whether MAb-RBS would recognize and bind the native hAPN from hAPN-3T3 cells. These cells and the control NIH-3T3 cells were metabolically labeled with a 30 or 60 minute pulse of [<sup>35</sup>S]methionine and lysed. The lysates were immunoprecipitated using normal mouse ascites, MAb-RBS ascites and MAb-MY7 (Figure 18). While several molecular weight proteins were either immunoprecipitated non-specifically or not eliminated by repeated washings of the immunoprecipitated complexes, among those proteins recognized by only MAb-RBS and MAb-MY7 were the 130kDa and 150kDa hAPN molecules only from the hAPN-transfected cells. The 150kDa protein is the mature hAPN molecule while the 130kDa protein is a partially-processed precursor routinely seen in hAPN immunoprecipitations. These data indicate that MAb-RBS recognized and bound to the same hAPN molecules previously recognized and specifically immunoprecipitated by MAb-MY7 (Look et al., 1989).

Binding of HCV-229E to hAPN-transfected cell membrane preparations and blocking of virus binding by MAb-RBS: In previous solid phase virus binding assays, HCV-229E

Figure 18. Immunoprecipitation of hAPN by MAb-RBS and MAb-MY7. NIH-3T3 and hAPN-transfected mouse cells (hAPN-3T3) were metabolically labeled with [<sup>35</sup>S]-methionine for 30 or 60 minutes and lysed. Lysates were immunoprecipitated with normal mouse ascites (NMA), MAB-RBS or hAPN-specific MAb-MY7 and SPA-sepharose beads armed with rabbit anti-mouse antibodies. Immunoprecipitates were boiled in sample treatment mix containing 2-mercaptoethanol and sodium dodecyl sulfate and centrifuged to remove beads and antibodies. Supernatants were separated by SDS-PAGE in 8% acrylamide gels which were dried and autoradiographed. Arrows indicate the 130kDa and 150kDa forms of the human APN immunoprecipitated.

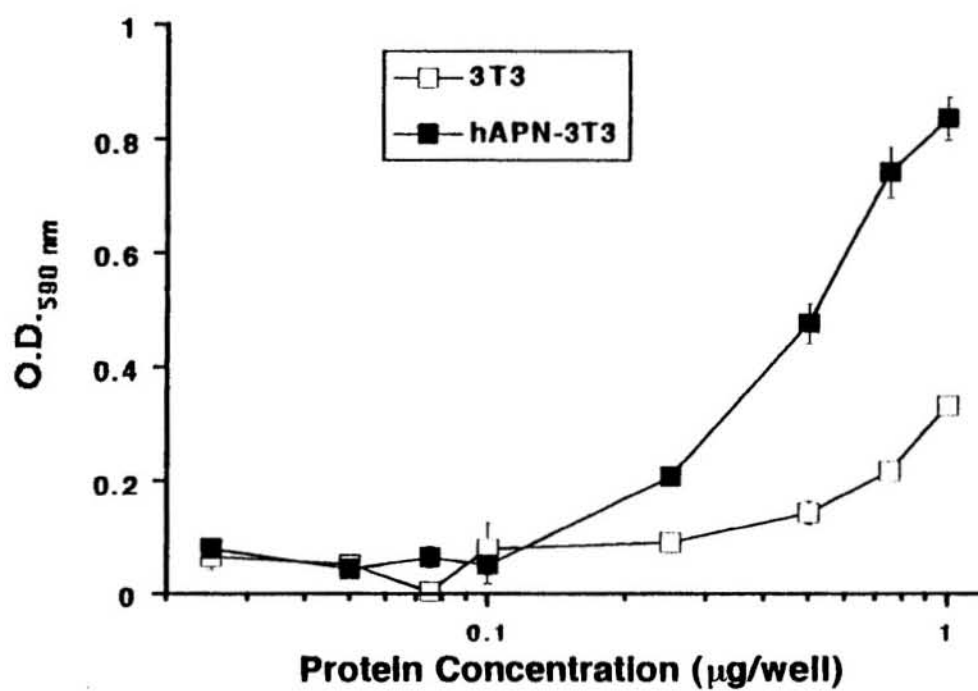


bound weakly or not at all to most membranes preparations of mouse origin. One interesting finding from the more sensitive and optimized enzyme-linked virus binding assay was that HCV-229E would consistently bind to BALB/c mouse BBMs and to CMPs of mouse L2 cells. Since these preparations are from HCV-229E-resistant cells or non-permissive tissues for HCV-229E infection, it was assumed that this low level of HCV-229E binding was due either to non-specific recognition of similar mouse epitopes or specific recognition of mouse molecules homologous to the human receptor without subsequent virus entry and replication. If hAPN were serving as the receptor for HCV-229E, the virus should bind to the hAPN-3T3 CMPs much more strongly than to the parental 3T3 CMPs. In enzyme-linked virus binding assays optimized for maximum detection of HCV-229E binding, rather than minimal background, HCV-229E bound to the hAPN-3T3 membrane preparations much more strongly than to the 3T3 parental CMPs (Figure 19). Interestingly, Dr. Look previously demonstrated a level of aminopeptidase activity on the mouse NIH-3T3 cells comparable to that seen in HL60 cells, though it was presumably due to the activity of a native mouse aminopeptidase (Ashmun and Look, 1990). The mouse aminopeptidase N gene has not yet been cloned, but those of rat and rabbit have been cloned and sequenced (see below) and found to be highly homologous at the amino acid level when compared to the human APN (Look *et al.*, 1986;

Figure 19. HCV-229E binding to hAPN-transfected mouse cell membranes. One  $\mu\text{g}$  of human hAPN-transfected 3T3 (hAPN-3T3) or parental (3T3) mouse cell membranes was adsorbed to the wells of a 96 well microtiter plate and blocked with BSA. Five  $\times 10^4$  PFU HCV-229E was added to each well and bound virus was detected by a dilution of 1:1000 goat anti-HCV-229E followed by biotinylated rabbit anti-goat antibodies and peroxidase-labeled avidin. Optical density (O.D.) of colorimetric TMB substrate reactions were read by ELISA reader.



**HCV-229E Binding to hAPN-transfected  
Mouse Cell Membranes**

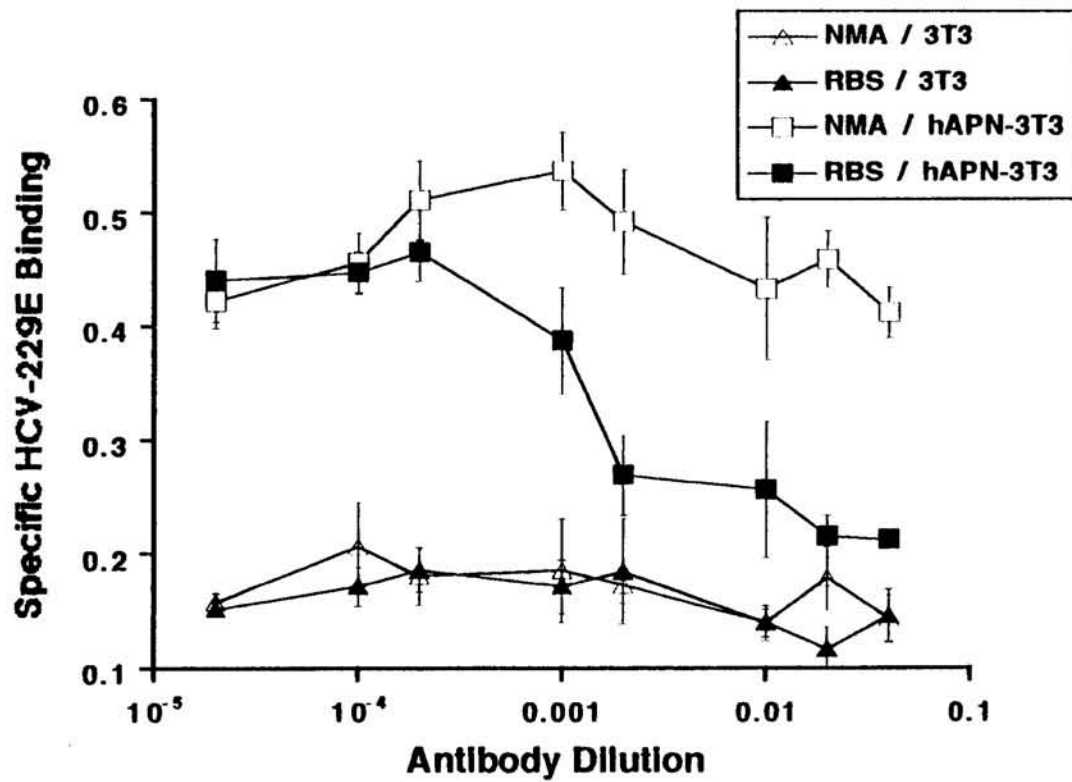


Watt and Yip, 1989; Norén et al., 1989). The partial sequence of porcine APN is also similar to human APN (Olsen et al., 1989).

The demonstration that MAb-RBS inhibited HCV-229E infection of WI38 cells and immunoprecipitated hAPN from hAPN-expressing 3T3 cells strongly suggested that MAb-RBS and HCV-229E both bound to the same membrane component. Also, because both MAb-RBS and HCV-229E recognized the hAPN-transfected 3T3 cells much more strongly than the parental 3T3 cells, it was then necessary to demonstrate whether MAb-RBS and HCV-229E would compete for binding this component and demonstrate that the HCV-229E receptor and hAPN were one in the same. In a competitive enzyme-linked assay of HCV-229E binding to the NIH-3T3 and hAPN-3T3 CMPs, MAb-RBS ascites was first applied to the CMP-coated wells and incubated for 1 hour prior to the addition of HCV-229E. As in the in vitro receptor blocking assay, HCV-229E was added directly to the MAb-RBS incubation to allow competition between the antibody and virus. As can be seen in Figure 20, HCV-229E binding increased in a concentration-dependent manner as the MAb-RBS concentration was decreased, indicating direct competition between antibody and virus for binding. These results demonstrated that MAb-RBS and HCV-229E competed for binding to the same component only in the hAPN-expressing cells and that HCV-229E must utilize hAPN as a cellular receptor for adsorption to cell membranes.

Figure 20. Concentration-dependent competition between HCV-229E and MAb-RBS for binding to parental and hAPN-transfected mouse cell membranes. One  $\mu\text{g}$  of NIH-3T3 (3T3) or hAPN-transfected 3T3 (hAPN-3T3) cell membranes was adsorbed to each well of a 96 well microtiter plate and blocked with BSA. A 1:10 dilution of normal mouse ascites (NMA) or MAB-RBS was added to each well before and during the addition of  $2 \times 10^5$  PFU HCV-229E per well. Bound virus was detected by the use of a 1:1000 dilution of goat anti-HCV-229E followed by biotinylated rabbit anti-goat antibodies and peroxidase labeled avidin. Optical density of the colorimetric TMB substrate cleavage reaction was read by ELISA reader and background readings of control wells (normally in the range of 0.050-0.150nm, depending on the initial optical density of the reaction mixtures and the length of reaction time allowed before quenching) were subtracted to yield specific HCV-229E binding. Error bars represent standard deviation of values of 4 identical wells for each condition.

### Competitive Binding of HCV-229E and MAb-RBS

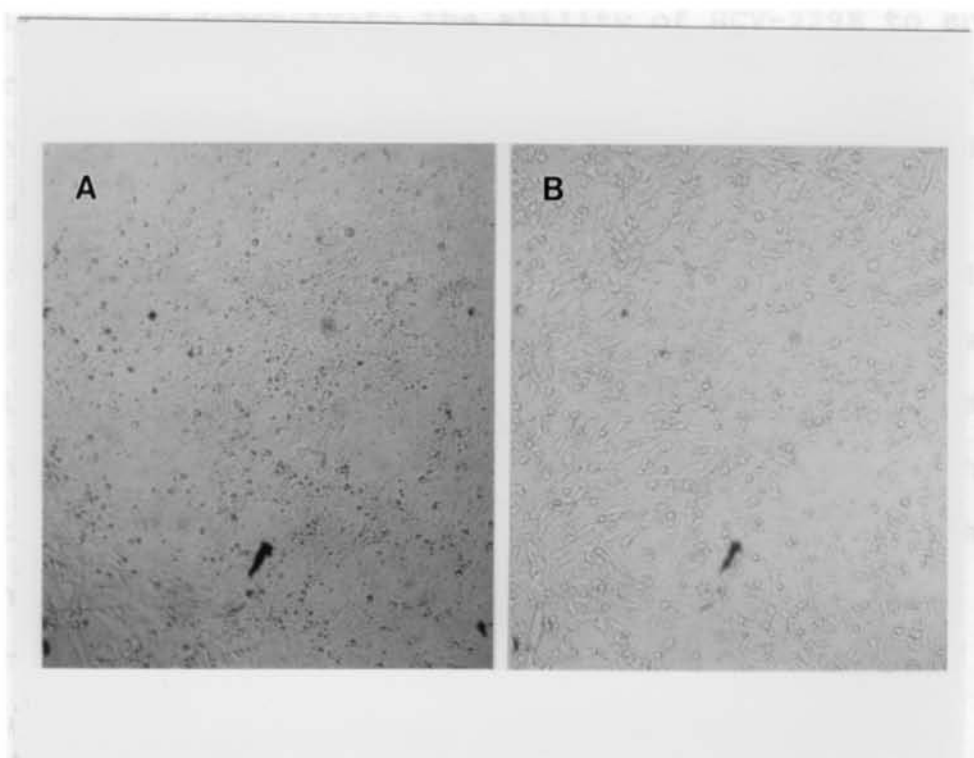


HCV-229E infection of hAPN-transfected mouse and hamster cells: While the previous data indicated that HCV-229E bound to hAPN and competed with the protecting antibody for this binding, the binding of a virus to a membrane protein does not always lead to successful fusion and entry of the virus into the cell. The hemagglutinin protein of influenza virus has been shown to bind to sialic acid components of host membrane-expressed glycoproteins (Paulson *et al.*, 1979), but this carbohydrate moiety exists on many membrane proteins as a consequence of complex glycosylation of proteins by the cell (reviewed in Alberts *et al.*, 1989). Although it has been demonstrated that both MAb-RBS and HCV-229E specifically bind hAPN, this molecule may not necessarily be the mediator of HCV-229E entry into the cell or the only receptor used by HCV-229E.

To learn whether the hAPN molecule alone could serve as the receptor for HCV-229E, the parental and hAPN-transfected 3T3 cells were challenged by HCV-229E and observed for virus-induced cytopathic effects. After 3 days of HCV-229E challenge, the hAPN-3T3 cells began to show CPE not seen in the parental 3T3 cells. By day 4, the CPE seen in Figure 21 had developed and was still not present in the parental 3T3 cells. These results suggested that HCV-229E could infect the hAPN-expressing cells, but not the parental cells.

To confirm that this CPE was due to the adsorption,

Figure 21. Growth and cytopathic effect of HCV-229E in hAPN-transfected mouse cells. Monolayers of parental (A) and hAPN-transfected (B) mouse 3T3 cells were challenged with  $2 \times 10^5$  PFU HCV-229E per milliliter for 96 hours. Cytopathic effects seen only in the hAPN-3T3 cells included spindling and rounding of cells by 96 hours and, eventually, detachment of cells from the substrate.



entry and replication of HCV-229E in the hAPN-3T3 cells, these and hAPN-transfected BHK cells, as well as their untransfected parental cells, were challenged by HCV-229E and assayed for the presence of intracellular virus antigens by immunofluorescent labeling. Figures 22 and 23 show the presence of cytoplasmic HCV-229E antigens after virus challenge and demonstrate the ability of HCV-229E to enter and replicate in both of the hAPN-transfected animal cells, but not in the untransfected cells. It should be noted that a lack of intracellular virus antigen would not have disproved the ability of HCV-229E to use hAPN as a cellular receptor since the mouse cells could have blocked virus replication at a step subsequent to the binding of this human virus. Such a finding would have necessitated the identification of an HCV-229E-resistant human cell line which would not support HCV-229E replication unless it were genetically engineered and shown to express hAPN. Fortunately, HCV-229E was able to utilize the cellular machinery available in both the mouse and hamster cells to synthesize virus antigens.

In addition to the parental and hAPN-transfected mouse cells, Dr. Look provided us with another 3T3 cell line stably transfected with a cDNA clone of hAPN bearing a 39 amino acid deletion including the zinc-binding motif and the catalytic site of hAPN activity (Ashmun et al., 1992). Human APN is a metalloprotease and its enzyme activity is



Figure 22. Intracellular virus antigens in hAPN-transfected mouse cells after HCV-229E challenge. Monolayers of parental (A), hAPN-transfected (B) or hAPN<sub>mut</sub>-transfected mouse 3T3 (C) cells were challenged with  $2 \times 10^5$  PFU HCV-229E for 22 hours and cold acetone-fixed. Intracellular HCV-229E antigens were detected with a 1:50 dilution of goat anti-HCV-229E and rhodamine-labeled rabbit anti-goat antibodies. Intracellular HCV-229E antigens can only be seen in the hAPN-transfected cells.

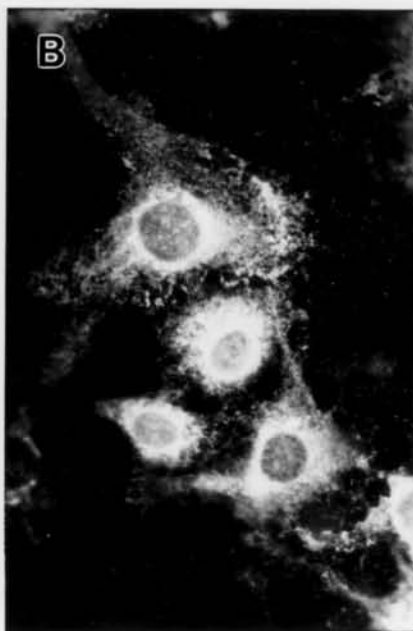
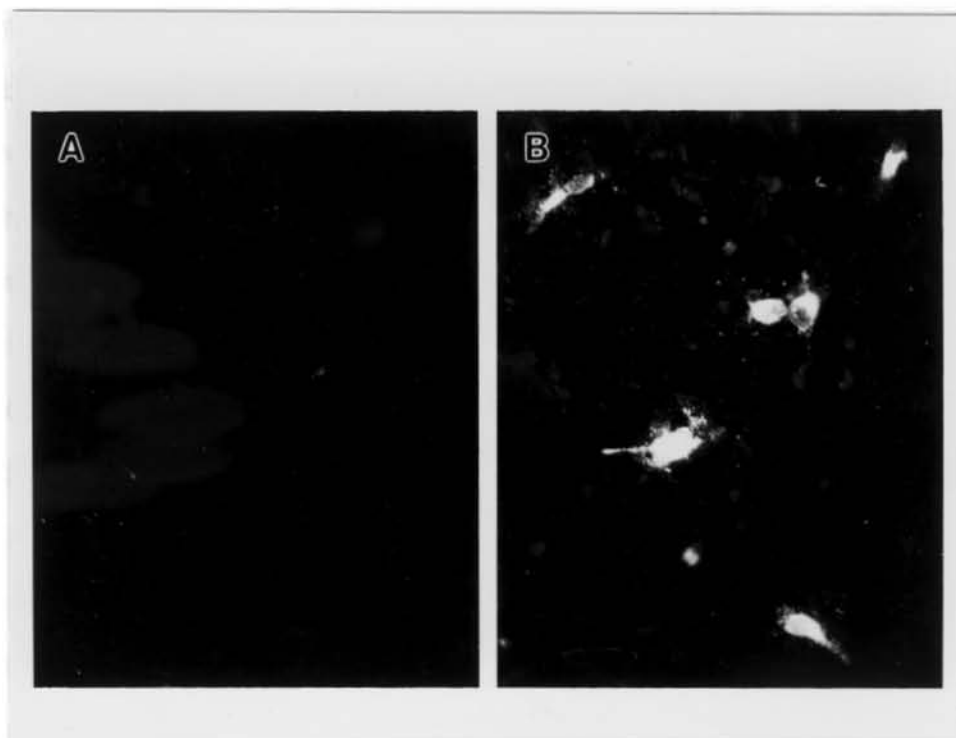


Figure 23. Intracellular virus antigens in hAPN-transfected BHK cells after HCV-229E challenge. Monolayers of untransfected (A) and hAPN-transfected (B) baby hamster kidney cells (BHK) were challenged with  $2 \times 10^5$  PFU HCV-229E for 22 hours and cold acetone-fixed. Intracellular HCV-229E antigens were detected with a 1:50 dilution of goat anti-HCV-229E or goat pre-immune serum and rhodamine-labeled rabbit anti-goat antibodies. Intracellular HCV-229E antigens can only be seen in the hAPN-transfected cells.

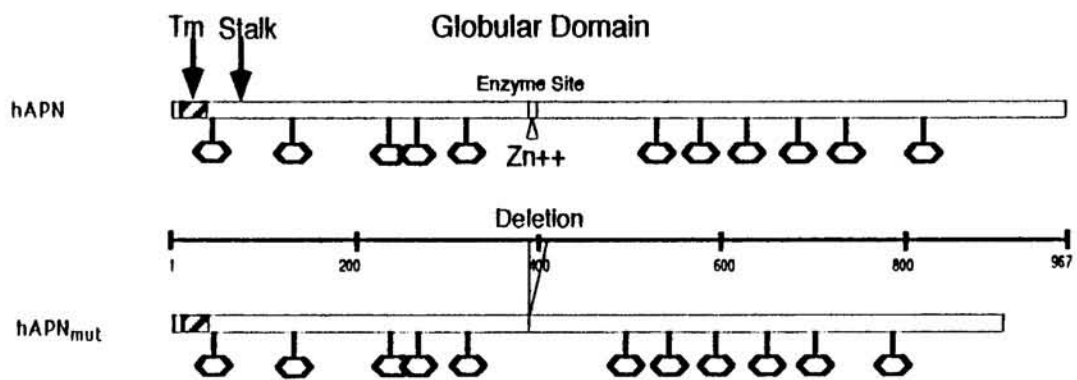


dependent upon the binding of one  $Zn^{++}$  ion per molecule of hAPN, probably contributing to the molecular structure of the enzyme catalytic pocket and allowing the necessary conformation for substrate recognition and catalytic activity (Ashmun *et al.*, 1992). A list of hAPN characteristics was presented in Table 9 and a schematic of the predicted structures of the hAPN and hAPN<sub>mut</sub> molecules can be seen in Figure 24. These cells were previously shown to express the mutant hAPN by FACS using the anti-hAPN antibody MY7 but to lack aminopeptidase enzyme activity (Ashmun *et al.*, 1992). In the same immunofluorescence assay for intracellular HCV-229E antigens, these cells which express the mutated hAPN (hAPN<sub>mut</sub>-3T3) were not infected with HCV-229E (Figure 22C). These results demonstrated the ability of HCV-229E to utilize a molecule expressed only on the mouse cells transfected with and expressing a non-mutated form of hAPN. The inability of HCV-229E to enter using the mutated hAPN could mean that either the virus did not recognize and bind to the deleted molecule or that the mutant molecule would not facilitate proper entry of the virus after binding.

The results of the two previous experiments where MAb-RBS (1) competed for binding with HCV-229E to hAPN-3T3 cells (Figure 20) and (2) protected 96% of WI38 cells from HCV-229E infection (Figure 15) suggested that MAb-RBS should also protect the hAPN-3T3 cells from HCV-229E

Figure 24. Native hAPN and hAPN<sub>mut</sub> molecules. This figure shows the predicted domain organization of the hAPN glycoprotein and the location of the 39 amino acid deletion (shaded) of the hAPN<sub>mut</sub> molecule including the pentapeptide (HELAH) zinc-binding motif. (○) indicate potential glycosylation sites. (Courtesy of Dr. Rick Williams).

## Human Aminopeptidase N (CD-13)



challenge. In the same immunofluorescence assay used to measure MAb-RBS protection of WI38 cells, a 1:10 dilution of MAb-RBS ascites provided 35% protection to the hAPN-3T3 cells (data not shown). While the number of infected hAPN-3T3 cells was decreased in the presence of MAb-RBS and demonstrated some inhibition of HCV-229E binding, this inhibition was partial compared to that seen for the WI38 cells. A possible explanation for the ability of MAb-RBS to only partially protect the hAPN-3T3 cells may be the 20-30-fold increase in hAPN expression by these cells as compared to the level of expression in WI38 and HL60 cells (Dr A.Thomas Look, personal communication). Also, as mentioned previously, the ability of HCV-229E to overcome MAb-RBS protection in susceptible cells after prolonged virus challenge in the presence of blocking antibodies suggests that HCV-229E may have a stronger affinity for hAPN than MAb-RBS.

With strong evidence to support the use of hAPN as a cellular receptor by HCV-229E, we proceeded to use available cells and reagents to locate the actual site of HCV-229E binding on the hAPN molecule.

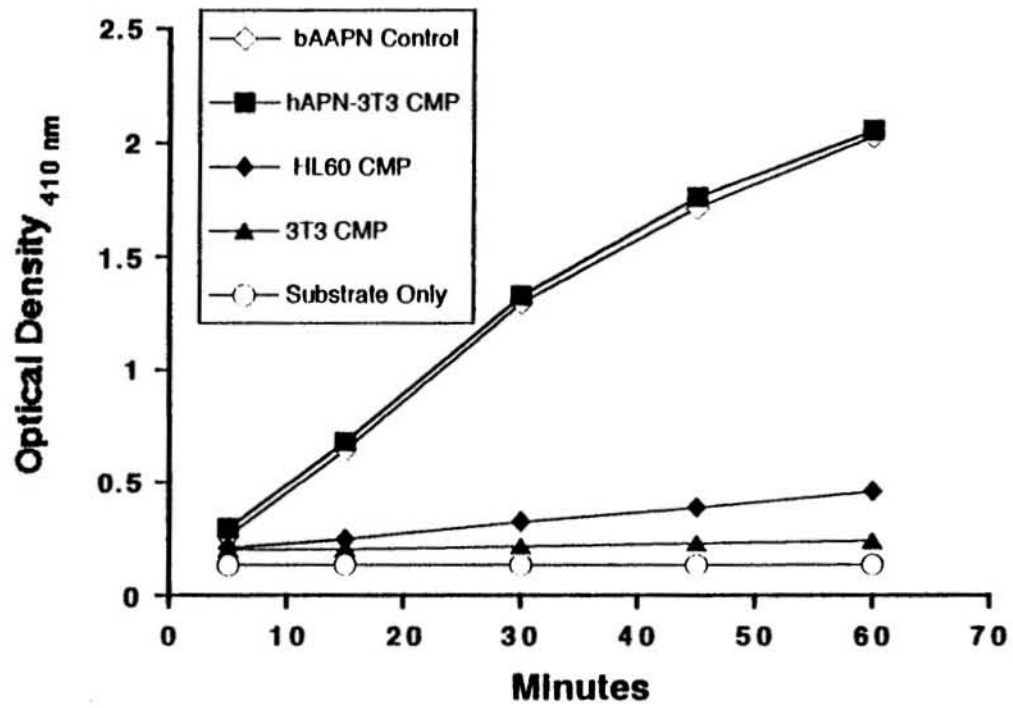
MAb-RBS inhibition of hAPN enzyme activity in hAPN-transfected mouse cells and HL60 cells: Several monoclonal anti-hAPN antibodies had been shown previously to inhibit the aminopeptidase activity of hAPN (Ashmun et al., 1992).



These MAbs possibly bound to hAPN at sites near or in the catalytic domain of the enzyme or, by binding elsewhere on the hAPN molecule or dimer, altered the conformation so as to inhibit enzyme activity. The specific binding site of MAb-RBS on hAPN could be defined further by analyzing the ability of MAb-RBS to inhibit this activity also. Enzyme assays of cell membrane preparations were done by a modification of a published protocol (Ashmun and Look, 1990). Briefly, colorimetric amino acid substrate-conjugates were incubated in the presence of CMPs and monitored for a change in optical density due to the cleavage of L-alanine from its paranitroanalide conjugate by hAPN. Figure 25 shows the aminopeptidase activity of 3T3, hAPN-3T3, and HL60 CMPs compared to the positive control bovine alanine aminopeptidase (bAAPN) for specific cleavage of the positive substrate L-alanine and a negative substrate L-proline. The final concentration of the bAAPN was adjusted to provide a level of hAPN activity comparable to that seen in 10  $\mu$ g of the hAPN-3T3 cells. The higher activity seen in the hAPN-3T3 CMP is most undoubtedly due to the over-expression of hAPN by the hAPN-3T3 cells and is consistent with higher activity of transfected CMPS in both MAb-RBS and HCV-229E binding assays (Figures 17 and 19). The same assay was performed in the presence of a 1:100 dilution of MAb-RBS ascites for one hour prior to and during the addition of cold substrate and the resulting

Figure 25. APN enzyme activity assay of control APN and membranes of parental and hAPN-transfected mouse cells and HL60 cells. Final reaction concentrations consisted of 8 mU of bovine alanine aminopeptidase (bAAPN) or 10  $\mu$ g of NIH-3T3, hAPN-3T3, HL60 or no membrane preparations combined with 6 mM of cold alanine-paranitroanalide substrate and were monitored for optical density at room temperature by ELISA reader at the time points indicated. Values are averages of 3 wells (reactions) for each condition from an assay representative of 3 or more experiments.

### APN Enzyme Activity



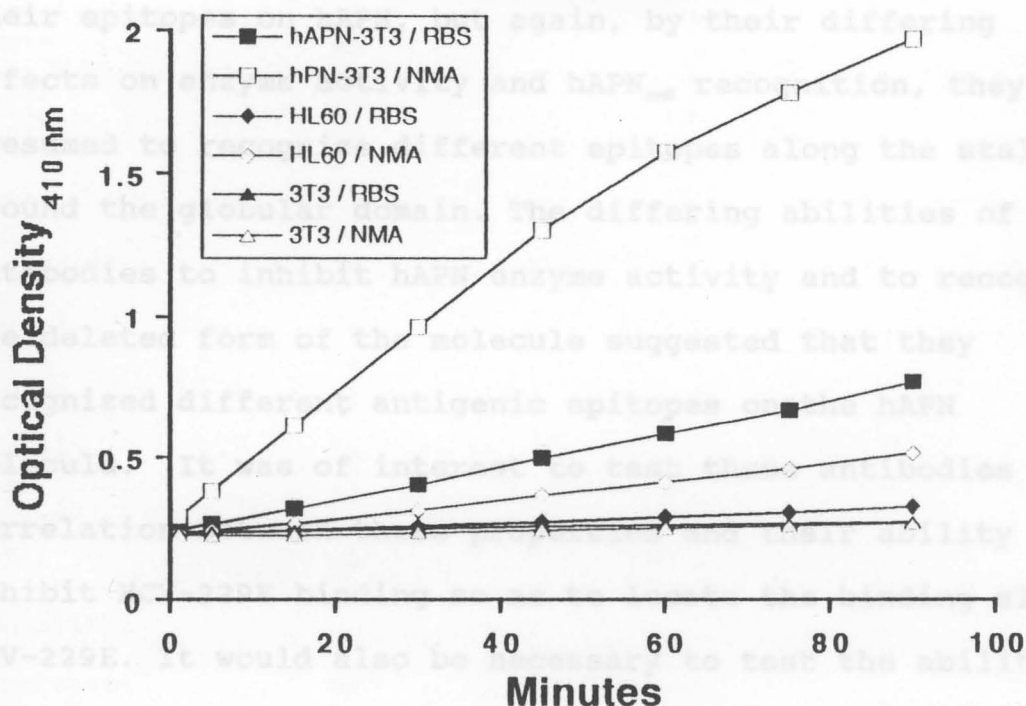
inhibition of hAPN activity by MAb-RBS can be seen in Figure 26. MAb-RBS inhibited the aminopeptidase activity of both the hAPN-3T3 and HL60 CMPs. The ability of MAb-RBS to block hAPN enzyme activity and to compete with HCV-229E for binding to hAPN suggests that both the antibody and the virus may bind to the same site and in the proximity of the catalytic enzyme site on the hAPN molecule.

These results suggested that HCV-229E binding to hAPN might also inhibit this hAPN activity. Preliminary studies using both unpurified and gradient-purified HCV-229E in the same enzyme inhibition assay demonstrated that the presence of HCV-229E did not reduce detectably the enzyme activity of hAPN on hAPN-3T3 cells (data not shown). Since the amount of virus present even in the purified HCV-229E preparation could have been limiting when compared to the number of hAPN molecules in the reaction mixtures, this result was inconclusive. This question will eventually require additional virus purification, titration of the CMPs, and virus and substrate concentrations to provide a more sensitive assay for this inhibition, if present.

Specific anti-hAPN antibodies and some hAPN enzyme activity inhibitors protected WI38 cells from HCV-229E challenge: The predicted structure of hAPN derived from its amino acid sequence revealed it to have a small cytoplasmic domain, a hydrophobic transmembrane region and

Figure 26. hAPN enzyme activity inhibition by MAb-RBS. Ten  $\mu$ g of 3T3, hAPN-3T3, or HL60 membranes were treated with a 1:100 dilution of MAb-RBS ascites or normal mouse ascites (NMA) for 1 hour prior to and during the addition of alanine paranitroanalide substrate. The optical density of the reaction mixtures was monitored at the times indicated by ELISA reader. MAb-RBS inhibited APN enzyme activity in both the hAPN-transfected mouse cell and HL60 cell membranes. Each value is the average of 3 wells (reactions) of the same condition from one assay representative of two assays performed.

### hAPN Enzyme Activity Inhibition by MAb-RBS



an extracellular stalked structure with a globular domain containing the zinc-binding motif and probably the site of catalytic enzyme activity (Ashmun et al., 1992). A variety of anti-hAPN antibodies which had been characterized for their ability to inhibit the aminopeptidase activity of hAPN and to recognize the hAPN<sub>mut</sub> form of hAPN (Ashmun et al., in press). These anti-hAPN antibodies have not been mapped to their epitopes on hAPN, but again, by their differing effects on enzyme activity and hAPN<sub>mut</sub> recognition, they are presumed to recognize different epitopes along the stalk or around the globular domain. The differing abilities of these antibodies to inhibit hAPN enzyme activity and to recognize the deleted form of the molecule suggested that they recognized different antigenic epitopes on the hAPN molecule. It was of interest to test these antibodies for a correlation between these properties and their ability to inhibit HCV-229E binding so as to locate the binding site of HCV-229E. It would also be necessary to test the ability of MAb-RBS for its ability to inhibit hAPN enzyme activity and to recognize the hAPN<sub>mut</sub> molecule. A battery of 14 anti-hAPN antibodies was tested for their ability to protect WI38 cells from HCV-229E challenge. The results of these tests are shown in Table 10. Based on these results, we were able to assign these antibodies to four different groups. The first group of five antibodies (RBS ascites, WM15, F23, U71, and U81), inhibited both HCV-229E infection and enzyme

TABLE 10  
PROPERTIES OF ANTI-APN MONOCLONAL ANTIBODIES AND INHIBITORS

	%Inhibition of Enzyme Activity <sup>1</sup>	Inhibition of HCV-229E Infection <sup>2</sup>	Binds hAPN <sub>mut</sub> -3T3 Cells <sup>1</sup>
<u>Monoclonal Antibodies</u>			
RBS Ascites	86	+	-
WM15	85	+	-
F23	85	+	-
U71 <sup>3</sup>	68	+	-
U81 <sup>3</sup>	73	+	-
3D8	64	+	+
MY7	45	+	+
CLB/M/G2	39	+	+
MCS2	0	+	+
MY32	4	+	+
RMAG6	1	+	+
22A5	0	-	+
72A	11	-	+
SJ1D1	4	-	+
WM47	1	-	+
<u>Inhibitors</u>			
Amastatin	ND <sup>4</sup>	-	ND
Actinonin	100	-	ND
Bestatin	100	-	ND
1,10-Phenanthroline	100	+	ND
2,2'-Dipyridyl	100	+	ND

<sup>1</sup> From Ashmun, *et al.*, 1992.

<sup>2</sup> Protecting dilutions of monoclonal antibodies varied, but all inhibited infection of WI38 cells at a dilution of 1:200 or less. Inhibitor dilutions and cytotoxicity varied, but protection was observed at non-cytotoxic dilutions. Method: Microtiter wells of confluent WI38 cells were preincubated with appropriate dilutions of antibodies or inhibitors in medium for 1 hour.  $1 \times 10^5$  PFU of HCV-229E was added for an additional hour. Medium was removed and replaced with fresh medium containing appropriate dilutions of antibodies or inhibitors. After 48 hours, monolayers were observed for viral cytopathic effect.

<sup>3</sup> These MAb preparations caused cytotoxicity at dilutions up to 1:100, but provided protection at 1:200.

<sup>4</sup> Not determined.



activity but did not recognize the mutated hAPN. This suggests that the HCV-229E recognition site and the active enzyme site are close together and that the site(s) recognized by both are eliminated or altered by the deletion. A second group of 3 antibodies (3D8, MY7, and CLB/M/G2) was able to inhibit enzyme activity only partially and to protect WI38 cells, but these antibodies also recognized the mutated hAPN. These antibodies probably recognized an epitope lying at or near the virus binding and catalytic enzyme sites and not affected by the deletion. A third group of 3 antibodies (MCS2, MY32, and RMAG6) did not inhibit enzyme activity significantly, but prevented HCV-229E infection and recognized the mutated hAPN molecule. The binding sites of these antibodies must lie near enough to the virus binding site to interfere with HCV-229E binding and/or entry but not close enough to the active enzyme site to exert an inhibitory effect. The last group of 4 antibodies inhibited neither HCV-229E infection nor enzyme activity, but recognized epitopes conserved after the deletion.

Taken together, the properties of these groups of antibodies suggest that HCV-229E binding and enzyme activity are closely situated on the topology of the hAPN molecule. At the same time, binding of any of these molecules to any region of the molecule can potentially alter the conformation of the molecule so as to interfere with either

virus binding or enzyme activity. To maintain a reference for the size of components involved in these interactions, it should be remembered that the S glycoprotein of HCV-229E has a 180-200kDa molecular mass, the hAPN dimer a combined mass of 300kDa, and the interfering antibodies a mass of at least 150kDa, with the additional space requirements of glycosylation. These proportions yield a variety of arrangements for these molecules where they might interfere with the binding of one another regardless of the location of the actual site of contact.

Human APN is a metalloprotease and its enzyme activity is dependent upon the binding of one  $Zn^{++}$  ion per molecule of hAPN, probably contributing to the molecular structure of the enzyme catalytic pocket and allowing the necessary conformation for substrate recognition and catalytic activity (Ashmun et al., 1992). This  $Zn^{++}$ -dependent peptidase activity can be inhibited by several commercially available inhibitors which function either by the chelation of available  $Zn^{++}$  ions or by mimicking the substrate and competitively inhibiting the binding and processing of natural substrates. Competitive inhibitors such as amastatin, actinonin or bestatin, are small molecules (bestatin has a mass of approximately 300 Da) and are thought to occupy the active enzyme site, effectively preventing the binding of polypeptides and cleavage of the terminal amino acid. Cationic chelators such as 1,10-

phenanthroline and 2,2'-dipyridyl sequester the  $Zn^{++}$  ions necessary for binding and proper conformation and function of the enzyme catalytic pocket. These inhibitors described above were tested for their ability to inhibit HCV-229E infection of WI38 cells in an in vitro antibody blocking/virus challenge assay where the inhibitors were applied prior to and during the HCV-229E virus challenge. Table 10 shows the results of these tests. While an adequate concentration of these inhibitors has been shown to completely inhibit detectable hAPN activity (Ashmun and Look, 1990), several dilutions of each inhibitor were tested in anticipation of possible cytotoxic effects which can be confused with virus-induced CPE and to determine minimum inhibitory concentrations. The  $Zn^{++}$ -chelating inhibitors phenanthroline and dipyridyl were found to delay HCV-229E infection much as had the protective anti-hAPN antibodies, whereas the specific inhibitors, amastatin, actinonin, and bestatin, did not inhibit or delay HCV-229E infection. This finding suggested that a conformational requirement might exist within the hAPN molecule for HCV-229E recognition that was dependent upon the bound  $Zn^{++}$  ions. The smaller pocket-occupying inhibitors did not interfere with HCV-229E binding and infection. Considering the relative sizes of the HCV-229E S glycoprotein and the globular catalytic domain of hAPN and the inhibitors, it was not surprising that the virus was able to bind in the presence of these small

competitive inhibitors. These results, taken together, suggest that HCV-229E might bind in the immediate vicinity of the catalytic domain of hAPN, but at a site not involving the actual pocket of the enzyme.

## Discussion

The study of human coronavirus (HCV) infections and the epidemiology of these infections has been limited because isolation of new and additional strains of HCVs often requires human tracheal and kidney organ cultures (Larson *et al.*, 1980; McIntosh *et al.*, 1967; Tyrrell and Bynoe, 1965; Hamre and Procknow, 1966). A possible limitation which has mandated the use of organ cultures in isolation may be that few receptor molecules are expressed by cells in continuous culture. While several HCV strains have been adapted to cell culture and much has been learned of the molecular biology of the intracellular steps in HCV replication, until our work, the biology of the HCV-receptor interaction had not been well-studied and the identity of the receptor molecule(s) had not been described.

The goal of my studies was to characterize HCV-229E-receptor interactions and to identify a cellular receptor for HCV-229E. Recognizing the importance of reliable reagents and methods with which to demonstrate and study the HCV-229E-receptor binding activity, I began by optimizing previous assays for virus binding and by developing new reagents and assays for extending these studies. Initially, my work on human coronavirus-receptor interactions and binding was modeled on that of the murine coronavirus, MHV-A59, where binding could be demonstrated to mouse intestinal and liver membrane preparations but not to the membranes of

cultured cells, probably because the amount of receptor(s) was too low to detect by this method. Therefore, our initial work on HCV binding was with membrane preparations from human tissues. Preliminary work by Dr. Susan Compton (Compton, 1988) had demonstrated that HCV-229E binds to intestinal BBMs from humans and from several animal species. This work suggested that HCV-229E binding was not species specific, since significant binding occurred to membranes of the host species of other animal coronaviruses within the same serological group as HCV-229E, including those of cat (FIPV), dog (CCV) and pig (TGEV). Though coronavirus-like particles have been observed in the feces of patients with diarrhea (Marshall *et al.*, 1989; Puel *et al.*, 1982), HCV-229E infection of human intestinal (HAI) membranes had not been demonstrated. Therefore, the binding activity of HCV-229E, which initially appeared as selective for certain species, but not specific for humans, could involve a receptor analog present in the membranes of human and animal intestinal epithelium which may not be a functional receptor.

HCV-229E can be propagated in WI38 human lung fibroblasts where it causes cytopathic effect and I found that polyclonal mouse serum raised against HAI membranes could protect these cells from HCV-229E infection. While the anti-HAI antiserum appeared to contain antibodies which were specific for the HCV-229E receptor(s) present on WI38

cells, several attempts to raise a monoclonal antibody using the spleens of mice producing anti-HAI antibodies failed to produce a single protective antibody. We therefore questioned the number and quantity of HCV-229E receptors present on the intestinal epithelium. To ensure that my characterization studies included the relevant HCV-229E receptor(s), I desired to demonstrate a similar virus-receptor interaction in the more biologically-relevant human respiratory epithelium, derived from the natural site of HCV-229E infection. I was able to demonstrate HCV-229E binding to membrane preparations from human tracheal, bronchus and larynx tissues at levels equal to or greater than that seen in intestinal membranes (Figure 9). Although these results demonstrated the presence of a recognized membrane component in respiratory epithelium, however, the availability of both the human intestinal and respiratory tissues was limited and the preparation of samples was both costly and time consuming. I therefore improved virus binding assays to the point where I could demonstrate HCV-229E binding to membranes from more readily available HCV-229E-sensitive human cell lines including WI38, HL60, U937, RD and HRT-18 cells. While virus adaptation to cell culture can sometimes involve changes in receptor specificity due to mutation of the virus attachment protein (Rogers et al., 1983), the use of WI38 cells in the initial isolation and purification of HCV-229E (Hamre and Procknow, 1966) suggests

that these cells provide an HCV-229E-receptor interaction closely resembling or actually representing that of a natural HCV-229E infection.

The assays for this HCV-229E binding interaction were improved from a solid phase virus binding assay, with reduced and boiled membranes on nitrocellulose, to an enzyme-linked virus binding assay (ELVIRA, Figure 14). The ELVIRA required much less reagents, was faster and more quantitative, and could include more samples per experiment. The ELVIRA procedure may prove useful for the study of receptor interactions of many different viruses and for testing the effectiveness of anti-viral reagents such as receptor-mimetic and virus attachment protein (VAP)-mimetic compounds designed to inhibit virus binding.

The virus-receptor interaction was partially characterized by demonstration that the HCV-229E binding activity of the membranes was diminished by sodium dodecyl sulfate (SDS) solubilization, but was relatively unaffected by NP-40, deoxycholate or Lubrol PX solubilization, or by the reducing agents, mercaptoethanol and dithiothreitol (Figures 12 and 13). The demonstrated sensitivity to SDS may help to explain HCV-229E's weak recognition of any SDS-PAGE-treated membrane proteins in the virus overlay protein blot assay (VOPBA). This assay, which demonstrated virus binding to separated and denatured proteins, was very helpful in the characterization and identification of the



MHV-A59 receptor (MHVR) allowing the assignment of a molecular weight of 110kDa to the MHVR and providing an initial source of semi-purified receptor material (Williams et al., 1990). Several attempts to perform this assay under non-denaturing conditions or to re-nature cellular proteins once separated by SDS-PAGE and transferred to nitrocellulose resulted in a very low amount of virus binding to several bands of low molecular weight.

After performing 5 separate fusion experiments, a monoclonal antibody, MAb-RBS, was developed using splenocytes from mice immunized with deoxycholate-solubilized WI38 and HL60 cell membranes that blocked HCV-229E infection of the susceptible human WI38, HL60 and RD cells. The final successful fusion resulted from mice immunized with human cell culture membrane preparations rather than human adult intestinal membrane preparations, as had been used in the previous 4 fusions. The MAb-RBS was discovered by screening the supernatants of the fusion products in a WI38 cell protection assay modified from a previously-used protocol to allow the incubation of hybridoma supernatants before and during challenge with HCV-229E. In ELISA's and FACS analysis, this MAb recognized the human cell lines but not a mouse 3T3 cell line. The monoclonal antibody and the development of the ELVIRA together permitted the rapid testing of molecules which might serve as an HCV-229E receptor. It was anticipated

that MAb-RBS would be used for immuno-affinity purification of the HCV-229E receptor as was done by with MAb-CC1 in the purification of the MHVR (Williams et al., 1990).

While my work was in progress, our group identified the MHV-A59 receptor as a member of the CEA family of molecules by computer alignment of a partial amino acid sequence of the N-terminus of the purified MHVR with other sequenced molecules (Williams et al., 1991). To test the hypothesis that all coronaviruses might bind to homologous receptors, I performed several HCV-229E binding assays. Antibodies specific for the human CEA, NCA, PSG and BGP molecules, which are related to the MHVR, were unable to block HCV-229E binding to WI38 and HAI membrane preparations. Also, when challenged with HCV-229E, naturally-resistant mouse and BHK cells, transfected with cDNAs of these and additional forms of the human CEA glycoprotein, were unable to support infection by HCV-229. While HCV-229E would not bind to the several well-characterized CEA family representatives tested, the human family of CEA molecules contains an ever-expanding group of different members, all of which could not be tested or ruled out as HCV-229E receptor candidates. Data which did not support the use of a CEA glycoprotein by HCV-229E included the chromosomal mapping of the human CEAs to chromosome 19 (Zimmermann et al., 1988), whereas HCV-229E sensitivity had been mapped to chromosome 15 (Sakaguchi and Shows, 1982).

Also, the lack of antigenic cross-reactivity between the viral components of MHV-A59 and HCV-229E (McIntosh et al., 1969) and the very limited homology between the S glycoproteins of MHV-A59 (Luytjes et al., 1987) and HCV-229E (Raabe et al., 1990) indicate that these viruses may have different VAP structures and receptor specificities.

At that point, the discovery of the ability of porcine aminopeptidase N molecule to serve as a receptor for the porcine coronavirus, TGEV (Delmas et al., 1992), which is closely related to HCV-229E, alerted us to the possibility that HCV-229E might utilize the homologous human aminopeptidase N (hAPN) as a receptor. This and the following interesting and correlative data on the human APN molecule supported the investigation of this molecule as an HCV-229E receptor candidate. The binding of HCV-229E to human respiratory and intestinal epithelium as well as to human lung fibroblasts and promyelocytic cell lines correlated with the previous findings of others on the tissue distribution of the hAPN molecule among these tissues as well as in kidney and nervous tissues (Norën et al., 1989; Semenza, 1986; Kenny and Maroux, 1982; Look et al., 1989). Secondary human kidney cultures had been used in the initial isolation of HCV-229E from an infected individual and the isolate was eventually grown and purified on WI38 cells (Hamre and Procknow, 1966). Also, previous somatic cell hybridization studies resulted in the mapping of HCV-

229E sensitivity (Sakaguchi and Shows, 1982) to the same region of human chromosome 15 to which the gene for hAPN had been mapped (Look et al., 1986). The cloning and expression of hAPN by our collaborators (Look et al., 1989) utilized an hAPN cDNA derived from the same human HL60 promyelocytic cell line (Look et al., 1989) we had used for demonstration of HCV-229E binding and infection as well for immunizing the mice for MAb-RBS development. Our collaboration resulted in the availability of parental and hAPN-transfected mouse 3T3 and BHK cell lines and a panel of specific anti-hAPN antibodies. Using enzyme-linked immunosorbant and virus binding assays, I was able to demonstrate greater binding of both MAb-RBS and HCV-229E to human cells and to hAPN-transfected 3T3 mouse cells than to parental mouse 3T3 cells. More importantly, MAb-RBS and HCV-229E competed in a concentration-dependent manner for this binding in both the hAPN-3T3 and HL60 cell membrane preparations. Flow cytometry studies performed by Dr. Look's laboratory using MAb-RBS to label cells for sorting also demonstrated the specific recognition of hAPN by MAb-RBS, which bound with equal or greater specificity than another specific anti-hAPN antibody, MY7. Finally, when challenged with HCV-229E, both mouse 3T3 and BHK cells were resistant to infection except when genetically engineered to express the human APN molecule as demonstrated in the immunofluorescent detection of intracellular HCV-229E antigens in only the hAPN-

transfected animal cells. Taken together, these results demonstrated the ability of HCV-229E to use the hAPN molecule as a portal of entry allowing us to publish the identification of hAPN as a cellular receptor for HCV-229E (Yeager et al., 1992). This also marks the first described use of an extracellular enzyme as a virus receptor.

Having demonstrated the use of hAPN as a cellular receptor, an additional 3T3 cell line expressing a mutated hAPN molecule and various anti-hAPN antibodies and enzyme inhibitors were used to define further the HCV-229E binding site on the hAPN molecule. The inability of HCV-229E to bind to or infect the hAPN<sub>mut</sub>-3T3 cells and the ability of some, but not all, of the panel of anti-hAPN antibodies to inhibit both APN enzyme activity and HCV-229E infection strongly suggested that the virus might bind the hAPN molecule at or near the active enzyme site. Also, some Zn<sup>++</sup>-chelating inhibitors of APN prevented HCV-229E binding while other small competitive inhibitors appeared to have no effect. The predicted structure of the enzymatically active domain of hAPN has described as having 3 subsites (Helene et al., 1991). The functions of substrate and inhibitor binding and catalytic activity of APN have been further characterized and assigned to the different subsites within the enzyme domain (Helene, et al., 1991). In a homologous hog kidney APN, the specific modification of amino acid constituents of the subsites and the effects of these

modifications on the binding and inhibition by APN-specific inhibitors showed that a specific aspartic acid residue in one subsite was necessary for substrate cleavage while the other subsites served to bind and position susceptible polypeptide substrates. The molecular interaction between the HCV-229E S glycoprotein and its binding site on hAPN was not inhibited by the binding of the small Bestatin and Actinonin inhibitors suggesting that the binding portions of the S glycoprotein must not interact directly with the subsites to which the small competitive inhibitors bind. While the small competitive inhibitors had no effect on HCV-229E infection, the  $Zn^{++}$ -chelating inhibitors, phenanthroline and dipyridyl, did protect WI38 cells from HCV-229E challenge and may deny the APN molecule its necessary conformation for HCV-229E recognition. The hAPN<sub>mut</sub> molecule with its 39 amino acid deletion lacked the  $Zn^{++}$ -binding motif and several surrounding amino acids and was not recognized by HCV-229E or MAb-RBS; however, the possible conformational changes within the overall hAPN molecule resulting from this deletion limits us in concluding anything about HCV-229E's need for the deleted region. Since the mutated form of the molecule was expressed on the surface of the transfected cells and some anti-hAPN antibodies did recognize the mutated form of the molecule, some epitopes of the native molecule must be conserved. Based on these studies, the exact binding site of HCV-229E

cannot be predicted. We do expect that HCV-229E must bind the large globular domain of hAPN very near or partially overlapping with the catalytic domain and it must depend on a conformation rendered by proper native expression and zinc coordination in this general region. Additional information about the site of HCV-229E binding may be obtained by comparing the expected HCV-229E binding region of hAPN to the binding sites of other coronaviruses to their receptor molecules as this information becomes available. The cloning and sequencing of human (Look et al., 1986), rat (Watt and Yip, 1989), rabbit (Nor  n et al., 1989), and pig (Olsen et al., 1989) APNs has shown that significant amino acid and predicted structural homologies exist between the APN molecules of different species and can be seen in Figure 27. When these sequences are aligned with and compared to the human CEA glycoproteins, there is also limited homology. Although several human CEA family members were tested and found not to facilitate HCV-229E infection of otherwise resistant cells, the evolution of the S glycoprotein of a coronavirus progenitor might have resulted in the use of a similar structural epitope on partially homologous, yet distinct classes of receptor molecules. A diagram based on the relative homology of these APN and the MHV receptor is presented in Figure 28. While the rabbit APN appears most homologous to the human APN, the available pig APN sequence is limited to about 200 amino acids. We suspect that when

Figure 27. Predicted amino acid sequences of human (APN), rabbit (Rabbitapn), rat (Ratapn), and pig (Pigapnfrag) aminopeptidase N molecules and the mouse MHV-A59 receptor (Mhvr). Alignment from top to bottom is by the extent of homology. Red symbols indicate identity with the human APN and brackets [] enclose the  $\text{Zn}^{++}$ -binding heptad motif among amino acids 388-392.



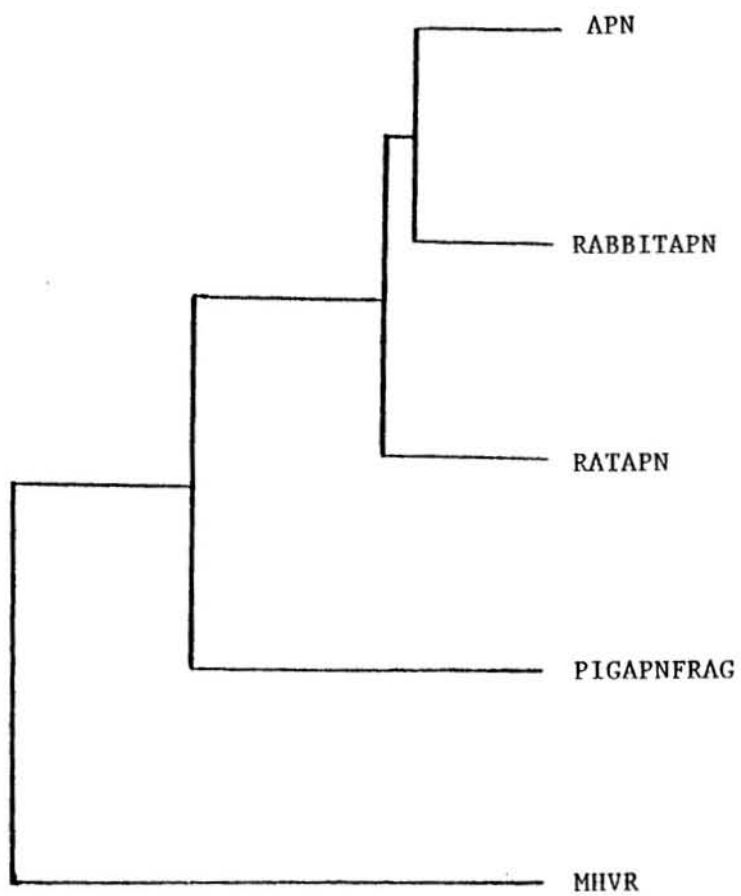
	1		50
Apn	MAKGFYISKS	LGILGILLGV	AAVCTIIALS VVYSOEKNKN ANSSPVASTT
Pigapnfrag	MAKGFYISKA	LGILGILLGV	AAVATIIALS VVYAOEKNKN AEHVPOAPTS
Rabbitapn	.....	.....	.....
Ratapn	MAKGFYISKT	LGILGILLGV	AAVCTIIALS VVYAOEKNRN AENSAIAPTL
Mhvr	.....	.....	.....
	51		100
Apn	PSASATTNPA	SATTLDO SKA	WNRRLPNTL KPDSYOVTLR PYLTPNDRGL
Pigapnfrag	P....TITTT	AAITLDQSKP	WNRRLPTTL LPDSYFVTLR PYLTPNADGL
Rabbitapn	.....	.....	.....
Ratapn	PGSTSATTST	TNPAIDESKP	WNOYRLPKTL IPDSYOVTLR PYLTPNEOGL
Mhvr	.....	.....	.....
	101		150
Apn	YVFKGSSTVR	FTCKEATDVI	IIHKKLNYT LSOGHRVVL R GVGGSQPPDI
Pigapnfrag	YIFKGKSIVR	LLCOEPTDVI	IIHKKLNYT .TOGHMVVL R GVGDSQVPEI
Rabbitapn	.....	.....	.....
Ratapn	YIFKGGSSTVR	FTCNETTNVI	IIHKKLNYT NKGHRVALR ALGDTPAPNI
Mhvr	.....	.....	.....
	151		200
Apn	DKTELVEPTE	YLVVHLKGSL	VKDSOYEMDS EFEGELADDL AGFYRSEYME
Pigapnfrag	DRTELVELTE	YLVVHLKGSL	OPGHMYEMES EFOGELADDL AGFYRSEYME
Rabbitapn	.....	.....	Q FOGELADDL AGFYRSEYME
Ratapn	DTTELVERTE	YLVVHLQSL	VKGHOYEMDS EFOGELADDL AGFYRSEYME
Mhvr	.....	.....	.....
	201		250
Apn	GNVRKVVATT	..OMQAADAR	KSFPCFDEPA MKAEFNITLI HPKDLTALSN
Pigapnfrag	GNV.....	.....	.....
Rabbitapn	GNVRKVVATT	OMOMQAADAR	KSFPCFDEPA SKATFNITLI HPRDYTALSN
Ratapn	GGNKVVATT	..OMQAADAR	KSFPCFDEPA MKA SFNITLI HPNNLTALSN
Mhvr	.....	.....	.....
	251		300
Apn	MLPKGPSTPL	PEDPNWNVTE	FHTTPKMSTY LLA FIVSEFD YVEKOASNGV
Pigapnfrag	.....	.....	.....
Rabbitapn	MLPRS .STAL	PEDPNWTVTE	FHTTPKMSTY LLAYIVSEFT NIEAOSPNNV
Ratapn	MLPKDSRT .L	QEDPSWNVTE	FHTTPKMSTY LLAYIVSEFK YVEAVSPNRV
Mhvr	.....	.....	.....
	301		350
Apn	LIRIWARPSA	IAAGHG DYAL	NVTGPILNFF AGHYDTPYPL PKSDOIGLPD
Pigapnfrag	.....	.....	.....
Rabbitapn	QIRIWARPSA	ISEGHGOYAL	NVTGPILNFF ANHYNTPYPL EKSDOIGLPD
Ratapn	QIRIWARPSA	IDEGHG DYAL	QVTGPILNFF AQHYNTAYPL EKSDOIALPD
Mhvr	.....	.....	.....
	351		400
Apn	FNAGAMENWG	LVTYRENSLL	FDPLSSSSSN KERVVTVIAH ELAHOWFGNL
Pigapnfrag	.....	.....	.....
Rabbitapn	FNAGAMENWG	LVTYRESALL	FDPLVSSISN KERVVTVVAH ELAHOWFGNL
Ratapn	FNAGAMENWG	LVTYRESALV	FDPOSSSISN KERVVTVIAH ELAHOWFGNL
Mhvr	.....	.....	MELASAH L H KGOVPWGGLL



	401		450
Apn	VTIEWWNDLW	LNEGFASYVE	YLGADYAEPT WNLKDL MVLN DVYRVMAYDA
Pigapnfrag	.....	.....	.....
Rabbitapn	VTVDWWNDLW	LNEGFASYVE	YLGADYAEPT WNLKDLIVLN ELHSVMAVDA
Ratapn	VTVDWWNDLW	LNEGFASYVE	FLGADYAEPT WNLKDLIVLN DVYRVMAYDA
Mhvr	LTASLLASWS	PATTAEVTI E	AVPPQV AE . DNNV LLLVH NLPLALGAF A
	451		500
Apn	LASSHPLSTP	ASEINTPAQI	SELFDAISYS KGASVLRMLS SFLSEDVFKO
Pigapnfrag	.....	.....	.....
Rabbitapn	LASSHPLSSP	ADEVNTPAQI	SELFDSITYS KGASVLRMLS SFLTEDLFKE
Ratapn	LASSHPLSSP	ANEVNTPAQI	SELFDSITYS KGASVLRMLS SFLTEDLFKK
Mhvr	WYKGNTTAID	KEIARFVPNS	NMN FTGOAYS .GREIIYSNG SLLFOMITMK
	501		550
Apn	GLASYLHTFA	YONTIYLNW	DHLOEAVNNR S .IQLPTTVR DIMNRWTLOM
Pigapnfrag	.....	.....	.....
Rabbitapn	GLASYLHTFA	YONTIYLDLW	EHLOQAVNSO SAIOLPASVR DIMDRWILQM
Ratapn	GLSSYLHTFO	YSNTIYLDLW	EHLOQAVDSO TAIKLPASVS TIMDRWILQM
Mhvr	DMGVYTLDMT	DEN.....	.....YR R TOATVRFHVH PILLK.....
	551		600
Apn	GFPVITVDT	TGTLSEHF	LDPDSNVTRP SEFNWVWIVP ITSIRDGROO
Pigapnfrag	.....	.....	.....
Rabbitapn	GFPVTVNTT	NGIISOHF	LDPTSNVTRP SDFNYLWIVP VSSMRNGVQO
Ratapn	GFPVITVNTS	TGEIYOEHF	LDPTSKPTRP SDFNYLWIVP IPYLKNG .K
Mhvr	..PNITSNN S	NPVEGDDSVS	LTCDSY .TDP DNINYLWSRN GESLSEGDRL
	601		650
Apn	ODYWLIDV .R	AQNDFSTSG	.NEWVLLNLN VTGYRVNYD EENWRKIOTO
Pigapnfrag	.....	.....	.....
Rabbitapn	OEFWLEGVEO	TQNSLFRVEG	DNNWILANLN VTGYOVNYD EGNWKKLOTO
Ratapn	EDHYWLETEK	NOSAE FOTSS	.NEWLLLNLN VTGYOVNYD ENNWRKIQNO
Mhvr	K.....	.....LS	EGNRT LTLN VTRNDTGPYV CETRNPV...
	651		700
Apn	LORDHSAIPV	INRAQIINDA	FNLASAHKVP VTLALNNTLF LIEEROYMPW
Pigapnfrag	.....	.....	.....
Rabbitapn	LOTNPSVIPV	INRAQIIHDA	FNLASAKVP VTLALDNTLF LIRETEYMPW
Ratapn	LOTDLVIPV	INRAQIIHDS	FNLASAGKLS ITLPLSNTLF LASETEYMPW
Mhvr	.....S V	NRSDFP .S	LNIIYGPDTP IISPSDIYLH PGSNLNLSCH
	701		750
Apn	E AALSSLSYF	KLMFDRSEVY	GPMKNYLKKO VTPLFIHFRN NTNNWREIPE
Pigapnfrag	.....	.....	.....
Rabbitapn	Q AALSSLNYF	KLMFDRSEVY	GPMKNYLSKO VRPLFEHFKN ITNDWTRRPD
Ratapn	E AALSSLNYF	KLMFDRSEVY	GPMKRYLKKO VTPLFAYFKI KTNWLDLDRPP
Mhvr	AASNPPAOYF	WLINEKPHA	SSOELFIPNI TTNSGTYTC FV NNSV .TG
	751		800
Apn	N LMDQYSEVN	AISTACSNV	PECEEMVSGL FKOWMENPNN NPIHPNLRST
Pigapnfrag	.....	.....	.....
Rabbitapn	T LMDQYNEIN	AISTACSNV	OECE TLVSDL FKOWMDPSN NPIHPNLRST
Ratapn	T LMEQYNEIN	AISTACSSGL	ECCRDLVGL YSQWMNSDN NPIHPNLRST
Mhvr	LSRTTVKNIT	VLEPVTOPFL	OVTNTT VKEL DSVTLTCLS N D .IGANIOWL

	801		850
Apn	VYCNAIA	OGG EEEWDFAWEO FRNATLVNE. ADKLR	AALAC SKELWILNRY
Pigapnfrag	.....	.....	.....
Rabbitapn	VYCNAIAL	GG EREWDFAWEO FRNATLVNE. ADKLR	SALAC SNEVWILNRY
Ratapn	VYCNAIA	FGG EEWNFAWEO FRKATLVNE. ADKLR	SALAC SNEVWILNRY
Mhvr	FNSQSLOL	TE RMTLSONNSI LRIDPIKR ED AGEYQCEISN	PVSRRS N..
	851		900
Apn	LSYTLNPD	LI RKODATSTII SITNNVIGOG LVWDFVOSNW	KKLFNDYGGG
Pigapnfrag	.....	.....	.....
Rabbitapn	LSYTLNPD	YI RRODATSTIN SIASNVIGOT LVWDFVOSNW	KKLFEDFGGG
Ratapn	LSYTLNPD	YI RKODATSTIV SIANNVVGOT LVWDFVRSNW	KKLFEDYGGG
Mhvr	. SIKLDIIFD	PTOGGLSD.G AIAGIVIGVV AGVALIAGLA	YF LYSRKS GG
	901		950
Apn	SFSFSNLIOA	VTRRFSTEYE LOOLEOFKKD NEETGFGSGT	RALEOALEKT
Pigapnfrag	.....	.....	.....
Rabbitapn	SFSFANLIRA	VTRRFSTEYE LOOLEOF RLN NLDTGFGSGT	RALEOALEQT
Ratapn	SFSFANLIQG	VTRRESSEFE LOOLEOFKED NSATGFGSGT	RALEOALEKT
Mhvr	SGSF*	.....	.....
	951		974
Apn	KANIKWVKEN	KEVVLQWTE	NSK.
Pigapnfrag	.....	.....	.....
Rabbitapn	RANIKWVOEN	KEAVLAWFTA	NSA*
Ratapn	KANIKWVKEN	KDVVLKWFTE	NS..
Mhvr	.....	.....	.....

Figure 28. Diagram of the relative homologies of the human (APN), rabbit (RABBITAPN), rat (RATAPN), and pig (PIGAPNFRAG) APNs and the mouse MHV-A59 receptor (MHVR). Human and rabbit are most homologous, while the MHVR shares the least homology.



the complete pig sequence is published, there will be a close and interesting homology in a region likely to be the specific site of HCV-229E binding. Ongoing studies in our laboratory to determine the exact MHV-A59 binding site on the CEA molecule are being accomplished by deletion and expression of various combinations of the 4 extracellular domains of the MHVR molecule. These studies have recently identified the most distal domain as the binding site for MAb-CC1 and MHV-A59 (personal communication). Alignment and comparison of the expected binding sites of HCV-229E and MHV-A59 on their respective receptor molecules may reveal region of similar structure and amino acid composition important in coronavirus binding. The same CEA molecules tested as HCV-229E receptors were tested by our laboratory for use as receptors by the other human coronavirus, HCV-OC43, and did not facilitate the entry of this virus either. While HCV-OC43 is unrelated to HCV-229E, it was expected that this MHV-A59-related virus might also use a CEA glycoprotein for its receptor. Similar binding and virus challenge assays revealed that the CEA molecules available would not facilitate HCV-OC43 infection. The study and identification of the HCV-OC43 receptor is complicated by the presence on this virus of the additional hemagglutinin esterase (HE) glycoprotein on this virus which can bind to 9-0-acetylated neuraminic acid residues of glycoproteins and glycolipids on cell membranes (Vlasak et al., 1988). The



presence of this alternative virus attachment protein and its undescribed role in HCV-OC43 binding and replication has and will present problems in determining the role and specificity of the HCV-OC43 S glycoprotein in receptor binding.

The identification of APNs as the receptors for the 2 serologically-related coronaviruses, TGEV (Delmas, et al, 1992) and HCV-229E (Yeager et al., 1992), and the identification of a murine CEA-related glycoprotein as the receptor (MHVR) for the serologically-unrelated MHV-A59 (Williams et al., 1991) suggests that coronaviruses of different antigenic groups have evolved to use different classes of membrane molecules as receptors. However, among coronaviruses within the same serological group such as TGEV and HCV-229E, host-specificities may have evolved by minor adaptation of the S glycoproteins to a homologous membrane component of the new host. The homology between the human and porcine APNs and between the HCV-229E and TGEV S glycoproteins suggests that one of these viruses may have preceded the other in host adaptation. In solid phase binding assays, both viruses bound to the intestinal BBMs of their own and each others hosts, but greater binding of HCV-229E to pig than TGEV to human was usually seen. Studies are under way to challenge TGEV-susceptible swine testicle cells with HCV-229E and the hAPN-transfected 3T3 cells with TGEV to test the ability of each virus to use the APN of the

other's host as a receptor. The higher degree of homology between the human and the rat and rabbit APN molecules would have predicted HCV-229E might recognize the BBMs of these animals, but solid phase virus binding experiments performed by both Dr. S. Compton and myself showed little, if any, recognition of these by HCV-229E. In trying to assess the binding site of HCV-229E, the conserved regions of these molecules when compared to the human APN might be eliminated as possible binding sites while close attention should be paid to homologous sites between pig and human APNs that are not present in the rat and rabbit APNs. Unfortunately, while the nearly complete sequences of the human, rat and rabbit APNs are published, the available sequence of the pig APN is limited to its first 209 amino acids starting at the cytoplasmic NH<sub>2</sub>-terminus which does not include the 5 amino acid zinc-binding motif located among amino acids 388-392 of the human sequence. While a significant homology exists between all of the sequences available up to the zinc-binding motif, there is a nearly identical homology among the human, rat, and rabbit sequences from position 315 to 540, a 225 amino acid region where only 23 positions differ between the three species and where we suspect HCV-229E might bind based on the previously mentioned data. The homology of the pig sequence in this same area will be important for comparing and targeting deletion studies. Another important contribution of studying these sequences



will be the development and testing of subunit anti-viral compounds. Peptides based on these possible virus-binding sequences which could be used to bind and saturate potential hAPN binding sites on the S glycoproteins of incoming HCV-229E virions, inhibiting virus attachment to cellular forms of the receptor and HCV-229E infection.

An interesting question arising from the apparent binding of HCV-229E to the vicinity of the enzyme site was whether APN activity might cleave or modify the S glycoprotein of HCV-229E as has been shown necessary for the cell fusion activity of the MHV-A59 S glycoprotein (Sturman et al., 1985) and for infectivity and hemagglutination by the S glycoprotein of the chicken coronavirus, Infectious Bronchitis Virus (IBV) (Cavanagh and Davis, 1986) . The 180kDa S glycoproteins of these viruses are cleaved at an internal site by a host enzyme yielding two 90kDa fragments which remain associated by intrachain disulfide binding. With the results of our antibody and inhibitor studies indicating probable binding of HCV-229E in the vicinity of the enzymatically active domain, the S glycoprotein of HCV-229E could undergo a similar processing through the exopeptidase activity of hAPN. To date, no such event has been described as necessary for HCV-229E infectivity or replication. A necessary difference between this model and that of the MHV-A59 S glycoprotein processing is the site at which the S glycoproteins would be cleaved. The internal

cleavage of the MHV-A59 protein by a host enzyme or other endopeptidase such as trypsin could not be duplicated by the exopeptidase activity of hAPN. The difference in the substrate specificities of these 2 peptidases would change the cleavage site of the S glycoprotein from one in the middle region of the MHV-A59 protein to the NH<sub>2</sub>-terminus of the HCV-229E S glycoprotein. While peptide degradation by hAPN could proceed from the exposed N-terminus of the HCV-229E S protein until a non-susceptible amino acid substrate is encountered, the ability of HCV-229E to infect WI38 cells in the presence of inhibitory concentrations of 3 different competitive inhibitors provides additional evidence that this modification may not be necessary for HCV-229E.

We plan to investigate further the specific site of HCV-229E binding to hAPN by several methods. The numerous available anti-hAPN antibodies have yet to be mapped to their respective epitopes by competitive binding and once their binding sites are determined, their ability to interfere with HCV-229E binding and infection should help to define the region of the HCV-229E binding. A more specific analysis of the hAPN amino acids involved in binding the HCV-229E S glycoprotein will be conducted by developing and testing specific deletions or mutations in the hAPN molecule for their affect on HCV-229E binding. Initial targeting of these mutations will be based on likely areas of homology seen between the human and pig APNs which

lie near the catalytic site and are not present in the rat and rabbit APNs. While similar mutational studies have proven helpful in determining which domain of the CEA receptor for MHV is necessary for virus recognition, the resultant conformational changes throughout the molecule are difficult to assess and could have downstream conformational effects on the virus binding site.

Another interesting finding in our studies was the inhibitory effect of the  $Zn^{++}$ -chelating APN inhibitors on HCV-229E infection. These results indicated a loss of recognition by HCV-229E when the  $Zn^{++}$  ions are not bound to the enzyme. Zinc has been shown to be integral component of nearly 300 enzymes including this class of metalloexopeptidases where it is essential for catalytic activity (Vallee and Auld, 1990). The  $Zn^{++}$  atom is coordinated to a short segment of the catalytic domain which contains 2 histidines and a glutamic acid in a linear arrangement. The aforementioned subsites are defined by these amino acid residues and the binding of zinc and formation of the cluster by its binding is thought to alter the conformation of the molecule so as to allow catalytic activity (Helene et al., 1991). Without the zinc-dependent conformation, the epitope recognized by HCV-229E is altered or removed. A recent approach in our laboratory to determine the role of zinc-binding in HCV-229E recognition has been to attempt the VOPBA under various conditions which

will allow renaturation, and possibly dimerization, of the separated hAPN molecules in the presence of supplemented zinc. Dimerization of the hAPN molecules may also be necessary for virus recognition. The dimerization of hAPN has been shown to occur prior to translocation from the rough endoplasmic reticulum to the golgi and may be necessary for this translocation prior to golgi modification and expression (Danielson, 1990). The hAPN<sub>mut</sub>-3T3 cells were not susceptible to HCV-229E and were not recognized by MAb-RBS, but were expressing the mutated form of the molecule in spite of the loss of the putative zinc-binding motif eliminated by the 39 amino acid deletion. Taken together, these findings suggest that although zinc may not be required for dimerization and surface expression of the hAPN glycoprotein, the conformation it provides is necessary for both enzyme activity and HCV-229E recognition.

A significant contribution of our findings may be to the study of the epidemiology of human coronavirus infections by enabling further isolation of HCV strains and comparison of their S glycoproteins. As mentioned, a limitation to HCV isolation has been the need for human tracheal or kidney organ cultures, possibly due to the scarcity of receptor molecules on differentiated human cell lines compared to tissue cultures. The increased expression of hAPN in the hAPN-transfected 3T3 cells provides approximately 30 times the hAPN found on HL60 and WI38 cells

as determined by FACS studies performed by Dr. T. Look. While the hAPN-3T3 cells supported HCV-229E infection, even a fairly homogeneous population of these cells, purified by cell sorting, resulted in only 35 to 50% of cells infected. While this may have been due to low virus titer in the inoculum, it may also have been due to inefficient virus replication using the mouse cell machinery. Human cells engineered to over-express hAPN may provide the necessary level of receptor expression for isolating limited quantities of virus from patient specimens.

Studying virus strain differences as they occur in natural infections is important in the development of effective anti-viral reagents and vaccines. Receptor-mimetic peptides designed to saturate incoming HCV attachment proteins and thereby block virus attachment and entry would be based on receptor epitopes recognized by the virus. If many strains of HCVs existed with variations in their S glycoproteins, such an anti-viral might be limited in its effectiveness in blocking the different strains. On the other hand, if the binding regions of the S glycoproteins of various HCV strains could be compared and were conserved so as to bind to the same region of the hAPN receptor, one anti-viral reagent might have a wide spectrum of applicability. Also, subunit vaccines based on the S glycoprotein region used in virus binding would need to represent a worthwhile proportion of HCV-229E strains in

order to be effective. In these respects, the development of cell lines for human coronavirus isolation would be quite valuable.

Recently, the development of transgenic mice to serve as models for the study of human diseases and has been adapted to study virus infections such as poliovirus by expressing the human receptor for the virus in the mouse tissues. Since the cloning of human APN (Look et al., 1986), the regulation of its expression has been studied and found to be different in myeloid and intestinal epithelial cells (Shapiro et al., 1991). Transcripts of two different sizes, but yielding the same polypeptide, were extracted from human cells from these tissues and shown to be controlled by different upstream promoters. This tissue-dependent regulation of expression may account for the differing levels of APN expressed in different tissues. Knowing the promoter sequences for tissue-specific expression and the sequence of hAPN will allow the engineering of an hAPN gene for oocyte microinjection which would increase the likelihood of proper expression of the receptor by a transgenic mouse. Therefore, the development of a transgenic mouse with acquired susceptibility to HCV-229E infection is possible. This mouse model of natural HCV-229E infection and could provide an excellent vehicle for studying the natural pathology of HCV infections and for evaluating the efficacy of anti-viral

reagents and vaccines.

## BIBLIOGRAPHY

Alberts, B., Lewis, J., Raff, M., Roberts, K., and Watson, J. D. (1989). *Molecular Biology of the Cell*, 2nd Ed. New York: Garland Pub.

Almeida, J. D. and Tyrrell, D. A. (1967). The morphology of three previously uncharacterized human respiratory viruses that grow in organ culture. *J. Gen. Virol.* **1**, 175-178.

Ashmun, R. A., Shapiro, L. H., and Look, A. T. (1992). Deletion of the zinc-binding motif of CD13/aminopeptidase N molecules results in loss of epitopes that mediate binding of inhibitory antibodies. *Blood*, in the press.

Ashmun, R. A. and Look, A. T. (1990). Metalloprotease activity of CD13/aminopeptidase N on the surface of human myeloid cells. *Blood* **75**, 462-469.

Baker, S. J., Mathan, M., Mathan, V. I., Jesudoss, S., and Swaminathan, S. P. (1982). Chronic enterocyte infection with coronavirus. One possible cause of the syndrome of tropical sprue? *Dig. Dis. Sci.* **27**, 1039-1043.



Beaudette, F. R. and Hudson, C. B. (1937). Cultivation of the virus of infectious bronchitis. *J. Am. Vet. Med. Assoc.* **90**, 51-60.

Bende, M., Barrow, I., Heptonstall, J., Higgins, P. G., al-Nakib, W., Tyrrell, D. A., and Akerlund, A. (1989). Changes in human nasal mucosa during experimental coronavirus common colds. *Acta Otolaryngol. (Stockh. )* **107**, 262-269.

Berry, D. M., Cruickshank, J. G., Chu, H. P., and Wells, R. J. H. (1964). The structure of infectious bronchitis virus. *Virology* **23**, 403-407.

Bhatt, P. N. and Jacoby, R. O. (1977). Experimental infection of adult axenic rats with Parker's rat coronavirus. *Arch. Virol.* **54**, 345-352.

Bournsnell, M. E., Brown, T. D., Foulds, I. J., Green, P. F., Tomley, F. M., and Binns, M. M. (1987). Completion of the sequence of the genome of the coronavirus avian infectious bronchitis virus. *J. Gen. Virol.* **68**, 57-77.

Boyle, J. F., Weismiller, D. G., and Holmes, K. V. (1987). Genetic resistance to mouse hepatitis virus correlates with absence of virus-binding activity on target tissues. *J. Virol* **61**, 185-189.

Bradburne, A. F., Bynoe, M. L., and Tyrrell, D. A. (1967). Effects of a "new": human respiratory virus in volunteers. *Brit. Med. J.* **3**, 767-769.

Bradford, M. M. (1976). A rapid and sensitive method for the quantitation of protein utilizing the principle of protein dye binding. *Anal. Biochem.* **72**, 248-254.

Brenner, S. and Horne, R. W. (1959). A negative staining method for high resolution electron microscopy of viruses. *Biochim. Biophys. Acta* **34**, 103-110.

Burks, J. S., DeVald, B. L., Jankovsky, L. D., and Gerdes, J. C. (1980). Two coronaviruses isolated from central nervous system tissue of two multiple sclerosis patients. *Science* **209**, 933-934.

Burness, A. T. H. and Pardoe, I. U. (1981). Effect of enzymes on the attachment of influenza and encephalomyocarditis viruses to erythrocytes. *J. Gen. Virol.* **55**, 275-288.

Buscho, R. O., Saxtan, D., Shultz, P. S., Finch, E., and Mufson, M. A. (1978). Infections with viruses and *Mycoplasma pneumoniae* during exacerbations of chronic bronchitis. *J. Infect. Dis.* **137**, 377-383.

Callebaut, P. and Pensaert, M. (1980). Characterization and isolation of structural polypeptides in hemagglutinating encephalomyelitis virus. *J. Gen. Virol.* **48**, 193-204.

Caul, E. O., Ashley, C. R., Ferguson, M., and Egglestone, S. I. (1979). Preliminary studies on the isolation of coronavirus 229E nucleocapsids. *FEMS microbiol. lett.* **5**, 101-105.

Caul, E. O. and Egglestone, S. I. (1977). Further studies on human enteric coronaviruses. *Arch. Virol.* **54**, 107-117.

Cavanagh, D. and Davis, P. J. (1986). Coronavirus IBV: removal of spike glycopolypeptide S1 by urea abolishes infectivity and haemagglutination but not attachment to cells. *J. Gen. Virol.* **67**, 1443-1448.

Chaloner-Larsson, G. and Johnson-Lussenburg, C. M. (1981). Establishment and maintenance of a persistent infection of L132 cells by human coronavirus strain 229E. *Arch. Virol.* **69**, 117-129.

Chany, C., Moscovici, O., Lebon, P., and Rousset, S. (1982). Association of coronavirus infection with neonatal necrotizing enterocolitis. *Pediatrics* **69**, 209-214.

Chatterjee, D. and Maizel, J. V., Jr. (1984). Homology of adenovirus E3 glycoprotein with HLA-DR heavy chain. *Proc. Natl. Acad. Sci. U. S. A.* **81**, 6039-6043.

Cheever, F. S., Daniels, J. B., Pappenheimer, A. M., and Bailey, O. T. (1949). A murine virus (JHM) causing disseminated encephalomyelitis with extensive destruction of myelin I. Isolation and biological properties of the virus. *J. Exp. Med.* **90**, 181-194.

Clarke, M. F., Gelmann, E. P., and Reitz, M. S., Jr. (1983). Homology of human T-cell leukaemia virus envelope gene with class I HLA gene. *Nature* **305**, 60-62.

Co, M. S., Gaulton, G. N., Tominaga, A., Homcy, C. J., Fields, B. N., and Greene, M. I. (1985). Structural similarities between the mammalian beta-adrenergic and reovirus type 3 receptors. *Proc. Natl. Acad. Sci. U. S. A.* **82**, 5315-5318.

Compton, S. R. (1988). *Coronavirus Attachment and Replication*, Thesis, The Uniformed Services University of the Health Sciences, Bethesda, MD.

Compton, S. R., Stephensen, C. B., Snyder, S. W., Weismiller, D. G., and Holmes, K. V. (1992). Coronavirus Species Specificity: Murine Coronavirus Binds to a Mouse-Specific Epitope on its CEA-Related Receptor Glycoprotein. *J. Virol* (in the press).

Dales, S. (1973). Early events in cell-animal virus interactions. *Bacteriol. Rev.* **37**, 103-135.

Dalgleish, A. G., Beverly, P. C. L., Clapham, P. R., Crawford, D. H., Greaves, M. F., and Weiss, R. A. (1984). The CD4 (T4) antigen is an essential component of the receptor for the AIDS retrovirus. *Nature* **312**, 763-767.

Dalgleish, A. G., Beverley, P. C. L., Clapham, P. R., Crawford, D. H., Greaves, M. F., and Weiss, R. A. (1984). The CD4 (T4) antigen is an essential component of the receptor for the AIDS retrovirus. *Nature* **312**, 763.

Danielson, E. M. (1990). Biosynthesis of Intestinal Microvillar Proteins. Dimerization of Aminopeptidase N and Lactase-Phlorizin Hydrolase. *Biochemistry* **29**, 305-308.

Davis, L.G., Dibner, M.D., and Battey, J. F. (1986). *Methods in Molecular Biology*, New York: Elsevier Publishing.

Dea, S., Garzon, S., and Tijssen, P. (1989). Isolation and trypsin-enhanced propagation of turkey enteric (bluecomb) coronaviruses in a continuous human rectal adenocarcinoma cell line. *Am. J. Vet. Res.* **50**, 1310-1318.

Dea, S. and Tijssen, P. (1988). Identification of the structural proteins of turkey enteric coronavirus. *Arch. Virol.* **99**, 173-186.

Delmas, B., Gelfi, J., Haridon, R. L., Vogel, L. K., Sjostrom, H., Noren, O., and Laude, H. (1992). Aminopeptidase N is a major receptor for the enteropathogenic coronavirus TGEV. Nature (in press).

Denison, M. and Perlman, S. (1987). Identification of putative polymerase gene product in cells infected with murine coronavirus A59. *Virology* **157**, 565-568.

Deregt, D., Sabara, M., and Babiuk, L. A. (1987). Structural proteins of bovine coronavirus and their intracellular processing. *J. Gen. Virol.* **68**, 2863-2877.

Dimmock, N. J. (1982). Review article initial stages in infection with animal viruses. *J. Gen. Virol.* **59**, 1-22.

Doughri, A. M. and Storz, J. (1977). Light and ultrastructural pathologic changes in intestinal coronavirus infection of newborn calves. *Zentralbl. Veterinaarmed.* **29**, 367-385.

Doyle, L. P. and Hutchings, L. M. (1946). A transmissible gastroenteritis in pigs. *J. Am. Vet. Assoc.* **108**, 257-259.

Eppstein, D. A., Marsh, Y. V., Schreiber, A. B., Newman, S. R., Todaro, G. J., and Nestor, J. J., Jr. (1985). Epidermal growth factor receptor occupancy inhibits vaccinia virus infection. *Nature* **318**, 663-665.

Fox, G., Parry, N. R., Barnett, P. V., McGinn, B., Rowlands, D. J., and Brown, F. (1989). The cell attachment site on foot-and-mouth disease virus includes the amino acid sequence RGD (arginine-glycine-aspartic acid). *J. Gen. Virol.* **70**, 625-637.

Fried, H., Cahan, L. D., and Paulson, J. C. (1981). Polyoma virus recognizes specific sialyligosaccharide receptors on host cells. *Virology* **109**, 188-192.

Gerdes, J. C., Klein, I., DeVald, B. L., and Burks, J. S. (1981). Coronavirus isolates SK and SD from multiple sclerosis patients are serologically related to murine coronaviruses A59 and JHM and human coronavirus OC43, but not to human coronavirus 229E. *J. Virol* **38**, 231-238.

Gerna, G., Passarani, N., Battaglia, M., and Rondanelli, E. G. (1985). Human enteric coronaviruses antigenic relatedness to human coronavirus OC43 and its possible etiologic role in viral gastroenteritis. *J. Infect. Dis.* **151**, 796-803.

Gledhill, A. W. and Andrewes, C. H. (1951). A hepatitis virus of mice. *Brit. J. Exp. Path.* **32**, 559.

Greig, A. S., Johnson, C. M, and Bouillant, A. M. P. (1971). Encephalomyelitis of swine caused by a hemagglutinating virus. VI. Morphology of the virus. *Res. Vet. Sci.* **12**, 305-307.

Greve, J. G., Davis, G., Meyer, A. M., Forte, C. P., Yost, S. C., Marlov, C. W., Kamarck, M. E., and Mc Clelland, A. (1989). The major human rhinovirus receptor is ICAM-1. *Cell* **56**, 839-847.



Grundy, J. E., McKeating, J. A., Ward, P. J., Sanderson, A. R., and Griffiths, P. D. (1987). Beta 2 microglobulin enhances the infectivity of cytomegalovirus and when bound to the virus enables class I HLA molecules to be used as a virus receptor. *J. Gen. Virol.* **68**, 793-803.

Guadagni, F., Witt, P. L., Robbins, P. F., Schlom, J., and Greiner, J. W. (1990). Regulation of Carcinoembryonic Antigen Expression in Different Human Colorectal Tumor Cells by Interferon  $\gamma$ . *Cancer Res.* **50**, 6248-6255.

Gump, D. W., Phillips, C. A., Forsyth, B. R., McIntosh, K., Lamborn, K. R., and Stouch, W. H. (1976). Role of infection in chronic bronchitis. *Am. Rev. Respir. Dis.* **113**, 465-474.

Guyander, M., Emerman, M., Sonigo, P., Clavel, F., Montagnier, L., and Alizon, M. (1987). Genome organization and transactivation of the human immunodeficiency virus type 2. *Nature* **326**, 662-669.

Gwaltney, J. M., Jr., Moskalski, P. B., and Hendley, J. O. (1978). Hand-to-Hand transmission of rhinovirus colds. *Ann. Intern. Med.* **88**, 463-467.

Gwaltney, J. M., Jr. (1982). Transmission of experimental rhinovirus infection by contaminated surfaces. *Am. J. Epidemiol.* **116**, 828-833.

Hamre, D. and Beem, M. (1972). Virologic studies of acute respiratory disease in young adults. V. Coronavirus 229E infections during six years of surveillance. *Am. J. Epidemiol.* **96**, 94-106.

Hamre, D. and Procknow, J. J. (1966). A new virus isolated from the human respiratory tract. *Proc. Soc. Exp. Biol. Med.* **121**, 191-193.

Hasonry, H. J. and Macnaughton, M. R. (1982). Prevalence of human coronavirus antibody in the population of southern Iraq. *J. Med. Virol.* **9**, 209-216.

Helene, A., Beaumont, A., and Roques, B. P. (1991). Functional residues at the active site of aminopeptidase N. *Eur. J. Biochem* **196**, 385-393.

Helenius, A., Marsh, M., and White, J. (1980). The entry of viruses into animal cells. *Trends. Biochem. Sci.* **5**, 104-106.

Hendley, J. O., Wenzel, R. P., and Gwaltney, J. M., Jr. (1973). Transmission of rhinovirus colds by self-inoculation. *N. Engl. J. Med.* **288**, 1361-1363.

Hirano, N., Goto, N., Ogawa, T., Ono, K., Murakami, T., and Fujiwara, K. (1980). Hydrocephalus in suckling rats infected intracerebrally with mouse hepatitis virus, MHV-A59.

*Microbiol. Immunol.* **24**, 825-834.

Hogue, B. G. and Brian, D. A. (1986). Structural proteins of human respiratory coronavirus OC43. *Virus. Res.* **5**, 131-144.

Holmes, K. V., Frana, M. F., Robbins, S. G., and Sturman, L. S. (1984). Coronavirus maturation. *Adv. Exp. Med. Biol.* **173**, 37-52.

Holmes, K. V. (1989). *Virology* (Fields, B. N., Ed.) 2nd edition. Raven Press, New York.

Hoxie, J. A., Haggarty, B. S., Bonser, S. E., Rackowski, J. L., Shan, H., and Kanki, P. J. (1988). Biological characterization of a simian immunodeficiency virus-like retrovirus (HTLV-IV): evidence for CD4-associated molecules required for infection. *J. Virol.* **62**, 2557-2568.

Hoyle, L. (1968). *Virology Monographs* 4 (Gard, S., Hallauer, C., and Meyer, K. F., Eds.) Springer-Verlag, New York. 1-375.

Hsu, K. H., Lonberg-Holm, K., Alstein, B., and Crowell, R. L. (1988). A monoclonal antibody specific for the cellular receptor for the group B coxsackieviruses. *J. Virol.* **62**, 1647-1652.

Ijaz, M. K., Brunner, A. H., Sattar, S. A., Nair, R. C., and Johnson-Lussenburg, C. M. (1985). Survival characteristics of airborne human coronavirus 229E. *J. Gen. Virol.* **66**, 2743-2748.

Inada, T. and Mims, A. (1984). Mouse Ia antigens are receptors for lactate dehydrogenase virus. *Nature* **309**, 59-61.

Jacoby, R. O., Bhatt, P. N., and Jonas, A. M. (1975). Pathogenesis of sialodacryoadenitis in gnotobiotic rats. *Vet. Pathol.* **12**, 196-209.

Kapikian, A. Z., James, H. D., Jr., Kelly, S. J., Dees, J. H., Turner, H. C., McIntosh, K., Kim, H. W., Parrott, R. H., Vincent, M. M., and Chanock, R. M. (1969). Isolation from man of "avian infectious bronchitis virus-like: viruses (coronaviruses) similar to 229E virus, with some epidemiological observations. *J. Infect. Dis.* **119**, 282-290.

Kenny, A. J. and Maroux, S. (1982). Topology of microvillar membrane hydrolases of kidney and intestine. *Physiol. Rev.* **62**, 91-128.

Kern, P., Müller, G., Schmitz, H., Racz, P., Meigel, W., Riethmüller, G., and Dietrich, M. (1985). Detection of coronavirus-like particles in homosexual men with acquired immunodeficiency and related lymphadenopathy syndrome. *Klin. Wochenschr.* **63**, 68-72.

Klatzmann, D., Champagne, E., Chamaret, S., Gruest, J., Guetard, D., Hercend, T., Gluckman, J. C., and Montagnier, L. (1984). T-lymphocyte T4 molecule behaves as the receptor for human retrovirus LAV. *Nature* **312**, 767-768.

Komai, K., Kaplan, M., and Peeples, M. E. (1988). The Vero cell receptor for the hepatitis B virus small S protein is a sialoglycoprotein. *Virology* **163**, 629-634.

Kraaijeveld, C. A., Reed, S. E., and Macnaughton, M. R. (1980). Enzyme-linked immunosorbent assay for detection of antibody in volunteers experimentally infected with human coronavirus strain 229 E. *J. Clin. Microbiol.* **12**, 493-497.

Laemmli, U. K. (1970). Cleavage of structural proteins during the assembly of the head of bacteriophage T4. *Nature* **227**, 680-685.

Lamarre, A. and Talbot, P. J. (1989). Effect of pH and temperature on the infectivity of human coronavirus 229E. *Can. J. Microbiol.* **35**, 972-974.

Larson, H. E., Reed, S. E., and Tyrrell, D. A. (1980). Isolation of rhinoviruses and coronaviruses from 38 colds in adults. *J. Med. Virol* **5**, 221-229.

Leibowitz, J. L., Weiss, S. R., Paavola, E., and Bond, C. W. (1982). Cell-free translation of murine coronavirus RNA. *J. Virol.* **43**, 905-913.

Lomniczi, B. (1977). Biological properties of avian coronavirus RNA. *J. Gen. Virol.* **36**, 531-533.

Longerg-Holm, K. and Philipson, L. (1974). *Monographs in Virology* (Melnick, J. L., Ed.) Karger, S., Basel.

Look, A. T., Peiper, S. C., Rebentisch, M. B., Ashmun, R. A., Roussel, M. F., Lemons, R. S., Le Beau, M. M., Rubin, C. M., and Sherr, C. J. (1986). Molecular cloning, expression, and chromosomal localization of the gene encoding a human myeloid membrane antigen (gp150). *J. Clin. Invest.* **78**, 914-921.

Look, A. T., Ashmun, R. A., Shapiro, L. H., and Peiper, S. C. (1989). Human myeloid plasma membrane glycoprotein CD13 (gp150) is identical to aminopeptidase N. *J. Clin. Invest.* **83**, 1299-1307.

Luytjes, W., Sturman, L. S., Bredenbeek, P. J., Charite, J., van der Zeijst, B. A. M., Horzinek, M. C., and Spaan, W. J. (1987). Primary structure of the glycoprotein E2 of coronavirus MHV-A59 and identification of the trypsin cleavage site. *Virology* **161**, 479-487.

Macnaughton, M. R., Hasony, H. J., Madge, M. H., and Reed, S. E. (1981). Antibody to virus components in volunteers experimentally infected with human coronavirus 229E group viruses. *Infect. Immun.* **31**, 845-849.

Macnaughton, M. R. and Davies, H. A. (1981). Human enteric coronaviruses: Brief review. *Arch. Virol.* **70**, 301-313.

Maloy, W. L. and Coligan, J. E. (1985). Is  $\beta$ -2-microglobulin required for MHC class I heavy chain expression? *Immunol. Today* **6**, 263-264.

Mapoles, J. E., Krah, D. L., and Crowell, R. L. (1985). Purification of a HeLa cell receptor protein for group B coxsackieviruses. *J. Virol.* **55**, 560-566.

Marsh, M. and Helenius, A. (1989). Virus entry into animal cells. *Adv. Virus Res.* **36**, 107-151.

P., Kennedy, M. S., and Howle, A. C. (1986b). Binding of the

Marshall, J. A., Birch, C. J., Williamson, H. G., Bowden, D. K., Boveington, C. M., Kubenski, T., Bennett, P. H., and Gust, I. D. (1982). Coronavirus-like particles and other agents in the faeces of children in Efate, Vanuata. *J. Trop. Med. Hyg.* **85**, 213-215.

McIntosh, K., Dees, J. R., Becker, W. B., Kapikian, A. S.,

Marshall, J. A., Thompson, W. L., and Gust, I. D. (1989). Coronavirus-like particles in adults in Melbourne, Australia. *J. Med. Virol* **29**, 238-243.

Mastromarino, P., Conti, C., Goldoni, P., Hauttecoeur, B., and Orsi, N. (1987). Characterization of membrane components of the erythrocyte involved in vesicular stomatitis virus attachment and fusion at acidic pH. *J. Gen. Virol.* **68**, 2359-2369.



Mathan, M., Mathan, V. I., Swaminathan, S. P., Yesudoss, S., and Baker, S. J. (1975). Pleomorphic virus-like particles in human faeces. *Lancet* **1**, 1068-1069.

McDougal, J. S., Kennedy, M. S., Sligh, J. M., Cort, S. P., Mawle, A., and Nicholson, J. K. (1986a). Binding of HTLV-III/LAV to T4+ T cells by a complex of the 110K viral protein and the T4 molecule. *Science* **231**, 382-385.

McDougal, J. S., Nicholson, J. K., Cross, G. D., Cort, S. P., Kennedy, M. S., and Mawle, A. C. (1986b). Binding of the human retrovirus HTLV-III/LAV/ARV/HIV to the CD4 (T4) molecule: conformation dependence, epitope mapping, antibody inhibition, and potential for idiotypic mimicry. *J. Immunol.* **137**, 2937-2944.

McIntosh, K., Dees, J. H., Becker, W. B., Kapikian, A. Z., and Chanock, R. M. (1967b). Recovery in tracheal organ cultures of novel viruses from patients with respiratory disease. *Proc. Natl. Acad. Sci. USA* **57**, 933-940.

McIntosh, K., Kapikian, A. Z., Hardison, K. A., Hartley, J. W., and Chanock, R. M. (1969). Antigenic relationships among the coronaviruses of man between human and animal coronaviruses. *J. Immunol.* **102**, 1109-1118.

McIntosh, K., Kapikian, A. Z., Turner, H. C., Hartley, J. W., Parrot, R. H., and Chanock, R. M. (1970).

Seroepidemiologic studies of coronavirus infection in adults and children. *Am. J. Epidemiol.* **91**, 585-592.

McIntosh, K., Ellis, E. F., Hoffman, L. S., Lybass, T. G., Eller, J. J., and Fulginiti, V. A. (1973). The association of viral and bacterial respiratory infections with exacerbations of wheezing in young asthmatic children. *J. Pediatr.* **82**, 578-593.

McIntosh, K. (1974). Coronaviruses. A comparative review. *Curr. Top. Microbiol. Immunol.* **63**, 85-129.

McIntosh, K., Chao, R. K., Krause, H. E., Wasil, R., Mocega, H. E., and Mufson, M. A. (1974). Coronavirus infection in acute lower tract disease of infants. *J. Infect. Dis.* **139**, 502-510.

Mebus, C. A., Stair, E. L., Rhodes, M. B., and Twiehaus, M. J. (1973). Pathology of neonatal calf diarrhea induced by a coronavirus-like agent. *Vet. Path.* **10**, 45-64.

Mendelsohn, C. L., Wimmer, E., and Racaniello, V. R. (1989). Cellular receptor for poliovirus: molecular cloning, nucleotide sequence, and expression of a new member of the immunoglobulin superfamily. *Cell* **56**, 855-865.

Mishra, N. K., Ryan, W. L., and Chaudhuri, S. N. (1973). Elevation of the intracellular levels of cyclic adenosine monophosphate during in vitro infection of transmissible gastroenteritis virus. Brief report. *Arch. Gesamte. Virusforsch.* **41**, 280-283.

Montali, R. J. and Strandberg, J. D. (1972). Extrapерitoneal lesions in feline infectious peritonitis. *Vet. Pathol.* **9**, 109-121.

Monto, A. S. (1974). Medical reviews. Coronaviruses. *Yale J. Biol. Med.* **47**, 234-251.

Monto, A. S. and Lim, S. K. (1974). The Tecumseh study of respiratory illness. VI. Frequency of and relationship between outbreaks of coronavirus infection. *J. Infect. Dis.* **129**, 271-276.

Mortensen, M. L., Ray, C. G., Payne, C. M., Friedman, A. D., Minnich, L. L., and Rousseau, C. (1985). Coronaviruslike particles in human gastrointestinal disease. Epidemiologic, clinical, and laboratory observations. *Am. J. Dis. Child.* **139**, 928-934.

Norén, O., Dabelsteen, E., Hoyer, P. E., Olsen, J., Sjöström, H., and Hansen, G. H. (1989). Onset of transcription of the aminopeptidase N (leukemia antigen CD 13) gene at the crypt/villus transition zone during rabbit enterocyte differentiation. *FEBS Lett.* **259**, 107-112.

Olsen, J., Sjöström, H., and Norén, O. (1989). Cloning of the pig aminopeptidase N gene. Identification of possible regulatory elements and the exon distribution in relation to the membrane-spanning region. *FEBS Lett.* **251**, 275-281.

Paul, R. W. and Lee, P. W. (1987). Glycophorin is the reovirus receptor on human erythrocytes. *Virology* **159**, 94-101.

Paulson, J. C., Sadler, J. E., and Hill, R. L. (1979). Restoration of specific myxovirus receptors to asialoerythrocytes by incorporation of sialic acid with pure sialyltransferases. *J. Biol. Chem.* **254**, 2120-2124.

Paulson, J. C. (1985). *The Receptors* (Conn, P. M., Ed.) Academic Press, Orlando. 131-219.

Puel, J. M., Orillac, M. S., Bauriaud, R. M., Boughermouh, R., Akacem, O., and Lefevre-Witier, P. (1982). Occurrence of viruses in human stools in the Ahaggar (Alberia). *J. Hyg. (Lond)* **89**, 171-174.

Raabe, T., Schelle-Prinz, B., and Siddell, S. G. (1990). Nucleotide sequence of the gene encoding the spike glycoprotein of human coronavirus HCV 229E. *J. Gen. Virol* **71**, 1065-1073.

Raabe, T. and Siddell, S. (1989). Nucleotide sequence of the human coronavirus HCV 229E mRNA 4 and mRNA 5 unique regions. *Nucleic. Acids. Res.* **17**, 6387.

Raabe, T. and Siddell, S. G. (1989). Nucleotide sequence of the gene encoding the membrane protein of human coronavirus 229 E. *Arch. Virol* **107**, 323-328.

Ren, R. B., Costantini, F., Gorgacz, E. J., Lee, J. J., and Racaniello, V. R. (1990). Transgenic mice expressing a human poliovirus receptor: a new model for poliomyelitis. *Cell* **63**, 353-362.

Resta, S., Luby, J. P., Rosenfeld, C. R., and Siegel, J. D. (1985). Isolation and propagation of a human enteric coronavirus. *Science* **229**, 978-981.

Rettig, P. J. and Altshuler, G. P. (1985). Fatal gastroenteritis associated with coronaviruslike particles. *Am. J. Dis. Child.* **139**, 245-248.

Rogers, G. N., Paulson, J. C., Daniels, R. S., Skehel, J. J., Wilson, I. A., and Wiley, D. C. (1983). Single amino acid substitutions in influenza haemagglutinin change receptor binding specificity. *Nature* **304**, 76-78.

Sakaguchi, A. Y. and Shows, T. B. (1982). Coronavirus 229E susceptibility in man-mouse hybrids is located on human chromosome 15. *Somatic. Cell Genet.* **8**, 83-94.

Sawicki, S. G. and Sawicki, D. L. (1990). Coronavirus transcription: subgenomic mouse hepatitis virus replicative intermediates function in RNA synthesis. *J. Virol.* **64**, 1050-1056.

Schalk, A. F. and Hawn, M. C. (1931). An apparently new respiratory disease of baby chicks. *J. Am. Vet. Med. Assoc.* **78**, 413-422.

Schmidt, O. W., Cooney, M. K., and Kenny, G. E. (1979).  
Plaque assay and improved yield of human coronaviruses in a  
human rhabdomyosarcoma cell line. *J. Clin. Microbiol.* **9**,  
722-728.

Schreiber, S. S., Kamahora, T., and Lai, M. M. (1989).  
Sequence analysis of the nucleocapsid protein gene of human  
coronavirus 229E. *Virology*. **169**, 142-151.

Schultze, B. and Herrler, G. (1992). Bovine coronavirus uses  
N-acetyl-9-0-acetylneuraminic acid as a receptor determinant  
to initiate the infection of cultured cells. *J. Gen. Virol.*  
**73**, 901-906.

Semenza, G. (1986). Anchoring and biosynthesis of stalked  
brush border membrane proteins: glycosidases and peptidases  
of enterocytes and renal tubuli. *Annu. Rev. Cell Biol.* **2**,  
255-313.

Shapiro, L. H., Ashmun, R. A., Roberts, W. M., and Look, A.  
T. (1991). Separate promoters control transcription of the  
human aminopeptidase N gene in myeloid and intestinal  
epithelial cells. *J. Biol. Chem.* **266**, 11999-12007.

Siddell, S., Wege, H., and ter Meulen, V. (1983). The  
biology of coronaviruses. *J. Gen. Virol.* **64**, 761-776.

Siddell, S. G., Wege, H., Barthel, A., and ter Meulen, V. (1980). Coronavirus JHM: cell-free synthesis of structural protein p60. *J. Virol.* **33**, 10-17.

Smith, C. B., Golden, C. A., Kanner, R. E., and Renzetti, A. D., Jr. (1980). Association of viral and Mycoplasma pneumoniae infections with acute respiratory illness in patients with chronic obstructive pulmonary diseases. *Am. Rev. Respir. Dis.* **121**, 225-232.

Sorensen, O., Perry, D., and Dales, S. (1980). In vivo and in vitro models of demyelinating diseases. III. JHM virus infection of rats. *Arch. Neurol.* **37**, 478-484.

Spaan, W., Cavanagh, D., and Horzinek, M. C. (1988a). Review Article Coronaviruses: Structure and Genome Expression. *J. Gen. Virol.* **69**, 2939-2952.

Spaan, W., Cavanagh, D., and Horzinek, M. C. (1988b). Coronaviruses: structure and genome expression. *J. Gen. Virol* **69**, 2939-2952.

Staunton, D. E., Merluzzi, V. J., Rothlein, R., Barton, R., Marlin, S. D., and Springer, T. A. (1989). A cell adhesion molecule, ICAM-1, is the major surface receptor for rhinoviruses. *Cell* **56**, 849-853.



Strauss, E. G. and Strauss, J. H. (1983). Replication strategies of the single strand RNA viruses of eukaryotes. *105*, 1-98.

Sturman, L. S., Ricard, C. S., and Holmes, K. V. (1985). Proteolytic cleavage of the E2 glycoprotein of murine coronavirus: Activation of cell-fusing activity of virions by trypsin and separation of two different 90K cleavage fragments. *J. Virol.* **56**, 904-911.

Sturman, L. S. and Holmes, K. V. (1983). The molecular biology of coronaviruses. *Adv. Virus. Res.* **28**, 35-112.

Sturman, L. S. and Takemoto, K. K. (1972). Enhanced growth of a murine coronavirus in transformed mouse cells. *Infect. Immun.* **6**, 501-507.

Superti, F. and Donelli, G. (1991). Gangliosides as binding sites in SA-11 rotavirus infection of LLC-MK2 cells. *J. Gen. Virol.* **72**, 2467-2474.

Tanaka, R., Iwaskai, Y., and Koprowski, H. (1976). Intracisternal virus-like particles in brain of multiple sclerosis patient. *J. Neurol. Sci.* **28**, 121-126.

- Tardieu, M., Epstein, R. L., and Weiner, H. L. (1982). Interaction of viruses with cell surface receptors. *Int. Rev. Cytol.* **80**, 27-61.
- Tomassini, J. E., Maxson, T. R., and Colonno, R. J. (1989). Biochemical characterization of a glycoprotein required for rhinovirus attachment. *J. Biol. Chem.* **264**, 1656-1662.
- Towbin, H., Staehelin, T., and Gordon, J. (1979). Electrophoretic transfer of proteins from polyacrylamide gels to nitrocellulose sheets: Procedure and some applications. *Proc. Natl. Acad. Sci. USA* **76**, 4350-4354.
- Tyrrell, D. A., Almeida, J. D., Berry, D. M., Cunningham, C. H., Hamre, D., Hofstad, M. S., Mallucci, L., and McIntosh, K. (1968). Coronaviruses. *Nature* **220**, 650.
- Tyrrell, D. A., Almeida, J. D., Cunningham, C. H., Dowdle, W. R., Hofstad, M. S., McIntosh, K., Tejima, M., Zakstelskaya, L. Y. A., Easterday, B. C., Kapikian, A. Z., and Bingham, R. W. (1975). Coronaviridae. *Intervirology* **5**, 76-82.
- Tyrrell, D. A. and Bynoe, M. L. (1965). Cultivation of a novel type of common-cold virus in organ culture. *Br. Med. J.* **1**, 1467-1470.

Vallee, B. L. and Auld, D. S. (1990). Zinc Coordination, Function and Structure of Zinc Enzymes and Other Proteins. *Biochemistry* **29**(24), 5647-5659.

Vaucher, Y. E., Ray, C. G., Minnich, L. L., Payne, C. M., Beck, D., and Lowe, P. (1982). Pleomorphic, enveloped virus-like particles associated with gastrointestinal illness in neonates. *J. Infect. Dis.* **145**, 27-36.

Vlasak, R., Luytjes, W., Spaan, W., and Palese, P. (1988). Human and bovine coronaviruses recognize sialic acid-containing receptors similar to those of influenza C viruses. *Proc. Natl. Acad. Sci. U. S. A.* **85**, 4526-4529.

Watanabe, R., Wege, H., and ter Meulen, V. (1987). Comparative analysis of coronavirus JHM-induced demyelinating encephalomyelitis in Lewis and Brown Norway rats. *Lab. Invest.* **57**, 375-384.

Watt, V. M. and Yip, C. C. (1989). Amino acid sequence deduced from a rat kidney cDNA suggests it encodes the Zn-peptidase aminopeptidase N. *J. Biol. Chem.* **264**, 5480-5487.

Wege, H., Siddell, S., and ter Meulen, V. (1982). The biology and pathogenesis of coronaviruses. **99**, 165-200.

Wenzel, R. P., Hendley, J. O., Davies, J. A., and Gwaltney, J. M., Jr. (1974). Coronavirus infections in military recruits. *Am. Rev. Respir. Dis.* **109**, 621-624.

Williams, R. K., Jiang, G.-S., Snyder, S.W., Frana, M.F., and Holmes, K.V. (1990). Purification of the 110-Kilodalton Glycoprotein Receptor for Mouse Hepatitis Virus (MHV)-A59 from Mouse Liver and Identification of a Nonfunctional, Homologous Protein in MHV-Resistant SJL/J Mice. *J. Virol.* **64**, 3817-3823.

Williams, R. K., Jiang, G. S., and Holmes, K. V. (1991). Receptor for mouse hepatitis virus is a member of the carcinoembryonic antigen family of glycoproteins. *Proc. Natl. Acad. Sci. U. S. A.* **88**, 5533-5536.

Yeager, C. L., Ashmun, R., Williams, R. K., Cardellicchio, C. B., Shapiro, L. H., Look, A. T., and Holmes, K. V. (1992). Human Aminopeptidase N is a Receptor for Human Coronavirus 229E. *Nature* (in press).

Zimmermann, W., Weber, B., Ortlieb, B., Rudert, F., Schempp, W., Fiebig, H. H., Shively, J. E., von Kleist, S., and Thompson, J. A. (1988). Chromosomal localization of the carcinoembryonic antigen gene family and differential expression in various tumors. *Cancer Res.* **48**, 2550-2554.